Infrared Optical Properties of Thin CO, NO, CH_4, HCl, N_2O, O_2, N_2, Ar, and Air Cryofilms

J. A. Roux, B. E. Wood, A. M. Smith, and R. R. Plyler
ARO, Inc.

August 1980

Final Report for Period October 1, 1978 – September 1, 1979

ARNOLD ENGINEERING DEVELOPMENT CENTER
ARNOLD AIR FORCE STATION, TENNESSEE
AIR FORCE SYSTEMS COMMAND
UNITED STATES AIR FORCE

NOTICES
When U. S. Government drawings, specifications, or other data are used for any purpose other than a definitely related Government procurement operation, the Government thereby incurs no responsibility nor any obligation whatsoever, and the fact that the Government may have formulated, furnished, or in any way supplied the said drawings, specifications, or other data, is not to be regarded by implication or otherwise, or in any manner licensing the holder or any other person or corporation, or conveying any rights or permission to manufacture, use, or sell any patented invention that may in any way be related thereto.
Qualified users may obtain copies of this report from the Defense Technical Information Center.
References to named commerical products in this report are not to be considered in any sense as an indorsement of the product by the United States Air Force or the Government.

This report has been reviewed by the Office of Public Affairs (PA) and is releasable to the National Technical Information Service (NTIS). At NTIS, it will be available to the general public, including foreign nations.

APPROVAL STATEMENT

This report has been reviewed and approved.

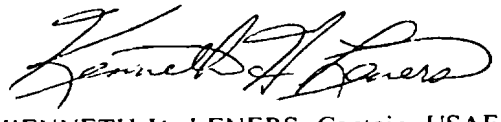

KENNETH H. LENERS, Captain, USAF
Project Manager
Directorate of Technology

Approved for publication:

FOR THE COMMANDER

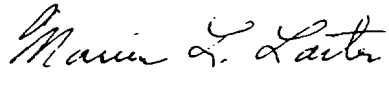

MARION L. LASTER
Director of Technology
Deputy for Operations

REPORT DOCUMENTATION PAGE

READ INSTRUCTIONS BEFORE COMPLETING FORM

1 REPORT NUMBER: AEDC-TR-79-81	2. GOVT ACCESSION NO.
3 RECIPIENT'S CATALOG NUMBER	
4. TITLE (and Subtitle): INFRARED OPTICAL PROPERTIES OF THIN CO, NO, CH_4, HCl, N_2O, O_2, N_2, Ar, AND AIR CRYOFILMS	5 TYPE OF REPORT & PERIOD COVERED: Final Report - October 1978 September 1979
	6. PERFORMING ORG. REPORT NUMBER
7. AUTHOR(s): J. A. Roux, B. E. Wood, A. M. Smith, and R. R. Plyler, ARO, Inc., a Sverdrup Corporation Company	8. CONTRACT OR GRANT NUMBER(s)
9 PERFORMING ORGANIZATION NAME AND ADDRESS: Arnold Engineering Development Center/DOT Air Force Systems Command Arnold Air Force Station, Tennessee 37389	10. PROGRAM ELEMENT, PROJECT, TASK AREA & WORK UNIT NUMBERS: Program Element 65807F
11. CONTROLLING OFFICE NAME AND ADDRESS: Arnold Engineering Development Center/DOS Air Force Systems Command Arnold Air Force Station, Tennessee 37389	12. REPORT DATE: August 1980
	13. NUMBER OF PAGES: 86
14. MONITORING AGENCY NAME & ADDRESS(if different from Controlling Office)	15. SECURITY CLASS. (of this report): UNCLASSIFIED
	15a. DECLASSIFICATION DOWNGRADING SCHEDULE: N/A

16. DISTRIBUTION STATEMENT (of this Report)

Approved for public release; distribution unlimited.

17 DISTRIBUTION STATEMENT (of the abstract entered in Block 20, if different from Report)

18 SUPPLEMENTARY NOTES

Available in Defense Technical Information Center (DTIC)

19 KEY WORDS (Continue on reverse side if necessary and identify by block number)

thin films
optical properties
optical equipment
cryogenics
condensation
rocket exhaust
infrared equipment

20 ABSTRACT (Continue on reverse side if necessary and identify by block number)

The infrared spectral transmittance of cryofilms formed by CO, NO, CH_4, HCl, N_2O, O_2, N_2, Ar, and air were measured. These films were condensed on a 20 K germanium substrate and ranged in thickness from 0.25 to 15 μm; the deposition pressure for the films was 2×10^{-7} torr. Transmission spectra were obtained for the 500- to 3700-cm^{-1} wavenumber range using a Fourier transform spectrometer. Values of the complex index of refraction ($\bar{n} = n - ik$) for the cryodeposits were derived from the experimental data using an analytical model and the

DD FORM 1 JAN 73 1473 EDITION OF 1 NOV 65 IS OBSOLETE

20. ABSTRACT (Continued)

nonlinear least-squares method. The analytical model treats the germanium as a thick noninterfering film and the deposit as a thin film. Results from the least-squares method are also compared with a Kramers-Kronig determination of the real part of the index of refraction. The optical properties (n,k) of such cryofilms are required for predicting the degradation of contaminated, cryogenically cooled optical surfaces.

AFSC
Arnold AFS Tenn

PREFACE

The research reported herein was performed by the Arnold Engineering Development Center (AEDC), Air Force Systems Command (AFSC). Work and analysis for this research was done by personnel of ARO, Inc. (a Sverdrup Corporation Company), operating contractor of AEDC, AFSC, Arnold Air Force Station, Tennessee. The work covered the period from October 1, 1978 to September 1, 1979 and was done under ARO Project Numbers V32S-R1A, V32K-13A, and P32K-13A. Dr. H. E. Scott was the Air Force project manager. The manuscript was submitted for publication on September 25, 1979.

CONTENTS

ILLUSTRATIONS

Figure Page

Page

TABLES

1.0 INTRODUCTION

Requirements to observe radiation sources at long ranges and infrared wavelengths has created severe design problems for infrared optical systems. These systems are often required to function at cryogenic temperatures that cause contamination of optical surfaces by atmospheric and rocket exhaust plume gases. These gases condense upon contact with cold optical surfaces and degrade system performance through thin-film interference and vibrational band absorption.

To identify and account for the effects from possible contamination by bipropellant [monomethyl hydrazine/nitrogen tetroxide (MMH/N_2O_4)] and monopropellant [hydrazine (N_2H_4)] engines in the infrared (IR), spectra of MMH, N_2O_4, N_2H_4, water (H_2O), carbon dioxide (CO_2), ammonia (NH_3), and mixtures of these constituents in a nitrogen (N_2) matrix were previously measured (Refs. 1 and 2). In this report the IR spectra and optical properties of minor contaminating species such as carbon monoxide (CO), nitric oxide (NO), methane (CH_4), hydrogen chloride (HCl), nitrous oxide (N_2O), oxygen (O_2), N_2, argon (Ar), and air are reported. The normal transmittance spectra were measured using 20 K germanium as a substrate material. Germanium is one of the most commonly employed substrates for cryocooled optical components because of its higher thermal conductivity as compared to pure dielectrics, the Irtran®, or polycrystals. Also, germanium has a flat transmittance of 45 percent between 2 and 10 μm.

Complete experimental details are given in Ref. 3; thus, only a basic outline of the chamber and apparatus is presented here. The absolute transmittance of thin solid films ranging in thickness up to 15 μm is presented. Finally, a theoretical model of window plus film transmission is derived and is subsequently employed with the experimental results to determine the complex refractive index ($\bar{n} = n - ik$) of each of the above-mentioned species. The subtractive Kramers-Kronig treatment for calculation of the film refractive index has also been employed, and results are compared to those of the nonlinear least-squares determination.

2.0 INSTRUMENTATION

A plan view schematic of the experimental apparatus, showing the IR interferometer (Digilab Model FTS-14), the high-vacuum chamber containing the cryocooled substrate, and the IR source location is given in Fig. 1. The chamber is an all-stainless-steel cell equipped with a liquid-nitrogen (LN_2)-cooled liner. A water-vapor-free vacuum of 10^{-8} torr can be routinely obtained. The substrate holder can be actively cooled with either LN_2 (80 K) or gaseous helium (GHe) (20 K). Three platinum resistors located on the window holder yielded temperature measurements accurate to 0.5 K.

The 4-mm-thick germanium window was mounted for cryogenic cooling as shown in Fig. 2. To ensure that the germanium windows did not act as an optical stop in any manner, a stop was located in the "back-of-window" gas baffle. This stop was 1.5 in. in diameter, and the clear aperture of the germanium was 2.0 in. in diameter.

The spectral resolution of the interferometer system could be selected between 16 and 0.5 cm^{-1}, but 4-cm^{-1} resolution was found to be sufficient for all work reported herein. The wavelength accuracy of the interferometer is near 0.02 cm^{-1} since the interferogram sampling interval is governed by an auxiliary helium-neon (He-Ne) laser interferometer. Transmittance data were recorded in the 500- to 3700-cm^{-1} wavenumber region. Transmittance measurements were performed by rotating the germanium out of the beam and recording and storing a reference power spectrum. Up to 16 interferograms were generally co-added before execution of the Fourier transform, thereby improving the signal-to-noise ratio. Next the window was rotated into the beam and the process repeated. The reference file was then divided into the sample file and plotted by a digital incremental plotter, producing the final data record on a linear ordinate scale of 0 to 100-percent transmittance.

Controlled contamination of the crycooled germanium window was accomplished with the gas induction system shown schematically in Fig. 3. A toroidal-shaped header with thirty-six 1/16-in.-diam orifices spaced 10 deg apart directed the gas toward the germanium window. The upstream pressure was determined from the vapor pressure of the liquid, and the gas flow rate was regulated by the variable leak valve. The chamber pressure would rise from 1×10^{-8} up to only 2×10^{-6} torr during deposition at 20 K, indicating good cryopumping by the liner and window. Gas was prevented from condensing on the back of the germanium window by a gas baffle positioned close to the back of the window holder. This baffle also held the optical stop mentioned earlier. The gas induction system, although quite simple, worked well in that the deposition rate could be easily controlled and the final thin-film thickness was very uniform across the 2-in.-diam exposed window area. Film uniformity and absolute thickness are two important parameters since the ultimate objective of the experiment was to determine the complex refractive index of the thin film, a quantity derived by comparison of experimental transmittance versus thickness data with a theoretical model. Any error in absolute film thickness is directly introduced into the film complex refractive index results. A dual-angle laser interference technique (Ref. 4) was employed to monitor the film thickness and also the film refractive index at $\lambda = 0.6328\ \mu m$. Basically, two He-Ne laser beams are specularly reflected off the germanium window for two different and accurately measured incidence angles. As the gas is condensed two interference patterns of different periods are monitored in the reflected laser light. If the ratio of pattern periods is termed β, then the refractive index of the film is given by

$$n = \frac{\left(\sin^2\theta_b - \beta^2 \sin^2\theta_a\right)^{1/2}}{\left(1-\beta^2\right)^{1/2}} \qquad (1)$$

where θ_a and θ_b (typically 18 and 68 deg) are the two laser beam incidence angles. Once n has been established the thickness, d_l, of the film is readily calculated from $m_a\lambda = 2nd_l\,[1 - (\sin^2\theta_a/n^2]^{1/2}$, where m_a is the order of the interference maxima for incidence angle θ_a. The dual-laser-beam thickness monitor yielded thin-film refractive index values accurate to within two percent. A quartz crystal microbalance (QCM) was used in conjunction with the dual-laser-beam interference technique to determine the density of each contaminant. The QCM was located adjacent to and just above the germanium window (see Fig. 3) so that the mass deposition rate would be the same as on the germanium window. The surface density (in gm/cm^2) was determined from the QCM and the film thickness from the interference patterns. From these two values the film density was calculated. The QCM operates on the principle of the crystal vibration frequency changing linearly with a change in mass deposited on the crystal.

3.0 PROCEDURE

The chamber was initially pumped down to approximately 1.0×10^{-7} torr using the diffusion pump and the LN_2 liner. Chamber pressures in the low 10^{-8} torr range were obtained when the germanium substrate, holder, and transfer lines were cooled to approximately 20 K with the cryostat (2-kw capacity).

Samples of research grade test gas were obtained in lecture bottles for sample gases to be introduced into the chamber. Deposition of the gas on the cold germanium window was monitored using the two He-Ne laser beams with the two-angle interference technique. Generally, transmittance measurements were made upon reaching each interference maxima, at which point the gas flow was shut off. Upon completion of the transmittance measurements, the gas flow was again started and deposition occurred until a film thickness corresponding to the next interference maxima was reached, etc. In some instances in which very strong absorption bands were observed, transmittance measurements were alternately made for each interference minima and maxima. This was done since determination of n's and k's required the use of as many thicknesses as possible to increase the accuracy of the values determined.

After completion of a series of transmittance measurements for all the thicknesses, the cryogenic flow rate to the germanium substrate was turned off and the substrate and deposited film allowed to warm up. Transmittance measurements were made at intervals

during warmup. The time required for the interferometer to scan the sample (16 scans) was two to three minutes with a similar time required for the reference beam. With the time required for obtaining the Fourier transform and the plotting of the data, this resulted in a time interval of about 10 minutes between measurements. The temperature given on each warmup data plot is the temperature at the end of the sample interferometer scan.

The main intent was to obtain transmittance measurements for as many thicknesses as possible during an experiment on each gas. The number of thicknesses actually obtained depended considerably on the particular gas. For "well-behaved" deposits, 16 to 25 thicknesses (interference maxima or minima) were obtained, whereas in some cases only a few thicknesses were possible because of scattering in the film (at $\lambda = 0.6328\ \mu m$).

4.0 RESULTS

Transmittance measurements were made on the cryogenically cooled germanium window with condensed thin films of the gases being investigated for thicknesses that were multiples of the thickness determined from the film interference equation for maxima, which is

$$\tau = \frac{m\lambda}{2n\sqrt{1 - \frac{\sin^2\theta}{n^2}}} \tag{2}$$

where m = 1,2,3... and θ is the incidence angle measured from the normal.

The first thickness (or interference maxima) is given by

$$\tau = \lambda\ 2n \left(1 - \frac{\sin^2\theta}{n^2}\right)^{-\frac{1}{2}} \tag{3}$$

for m = 1 and other thicknesses are given by

$$\tau = (2)\lambda\ 2n \left(1 - \frac{\sin^2\theta}{n^2}\right)^{-\frac{1}{2}} \tag{4}$$

for m = 2 and

$$t = (3)\lambda \, 2n \left(1 - \frac{\sin^2\theta}{n^2}\right)^{-\frac{1}{2}} \tag{5}$$

for m = 3, etc., with the thickness differential between successive maxima being equivalent to that given by Eq. (3).

In each case the refractive index, n, had to be measured before a thickness could be calculated. This measurement of n has been described previously (Refs. 4 and 5) and involves using Eq. (1) for two different incidence angles, which were approximately 18 and 68 deg in this study. (Thickness was based on interference maxima for 18-deg incidence.)

Optical constants were derived for all of the gases except N_2O and air. The experimental data obtained for the N_2O showed that the absorption band locations shifted with film thickness and hence gave relatively large errors in the n's and k's determined in those wavenumber regions. This was the only gas exhibiting such behavior. Two attempts were made for this gas with the same results. The n's and k's for air also are not presented as they would be very similar to those values determined for nitrogen and oxygen.

4.1 CO ON 20 K GERMANIUM

The CO transmission spectra were taken on deposits whose thicknesses ranged from 0.258 to 4.13 μm (Fig. 4). The calculated value for the index of refraction at $\lambda = 0.6328\ \mu$m is 1.27, and the density of the condensed gas is 0.80 gm/cm^3. The corresponding Lorentz-Lorenz value is 0.21 cm^3/gm. Absorptions are noted at 2095, 2140, and 2210 cm^{-1}, and a very small absorption at 2350 cm^{-1}. The fundamental stretching vibration of CO occurs at 2143 cm^{-1} (Ref. 6) in the gaseous state, which is in very close agreement with the observed vibration at 2140 cm^{-1}. The broad absorption at 2210 cm^{-1} is felt to result from a combination of the fundamental and a lattice vibrations, similar to the vibration noted in CO_2 deposits. The absorption at 2095 cm^{-1} corresponds to the fundamental vibration of the isotope $C^{13}O^{16}$, which occurs at 2093 cm^{-1}. The weak absorption at 2350 cm^{-1} is caused by traces of CO_2.

4.2 NO ON 20 K GERMANIUM

Transmission spectra of NO deposited on 20 K germanium were obtained for thicknesses of from 0.239 to 4.78 μm (20 interference maxima), an example of which is shown in Fig. 5.

The refractive index at $\lambda = 0.6328$ μm was measured to be 1.37, and the density was determined to be 1.17 gm/cm^3. The resulting Lorentz-Lorenz value is 0.191 cm^3/gm at $\lambda = 0.6328$ μm. The fundamental vibration band of NO in the gaseous state (Ref. 5) occurs at 1876 cm^{-1}. From the transmission data, a narrow, fairly strong absorption is observed at 1860 cm^{-1}, corresponding to this fundamental vibration. At about twice this frequency (3580 cm^{-1}) a weaker absorption is noted, corresponding to 2 ν_1.

In the spectra, many other lines are observed, the most obvious being the very strong absorption at 1760 cm^{-1}. Other absorptions are 1300, 1600, 2030, 2240, and 2340 cm^{-1}. Warming the sample to 83 K results in the bands at 1760, 1860, 2030, and 3580 cm^{-1} being greatly decreased in magnitude. Most of the NO has already sublimated. The spectrum taken at this temperature is shown in Fig. 6. Another feature of the spectrum at this temperature is the absence of the channel spectra, indicating that interference is no longer occuring in the sample. The absorptions at 1300, 1600, 2240, and 2340 cm^{-1} are still seen. At the chamber pressure of 2×10^{-6} torr, NO sublimates at about 55 K. The probable contaminants causing the absorptions at 1600 and 2340 cm^{-1} are H_2O and CO_2, respectively. The probable contaminant causing the absorptions at 1300 and 2240 cm^{-1} is N_2O, which sublimates at about 84 K. The absorption at 1760 cm^{-1} is possibly N_2O_4, which has a very strong absorption at this frequency. The cause of the absorption at 2030 cm^{-1} is unknown.

4.3 CH_4 ON 20 K GERMANIUM

Transmission spectra were obtained for deposits of CH_4 on 20 K germanium. These deposits ranged in thickness from 0.242 to 11.35 μm. The index of refraction was measured to be 1.35 at $\lambda = 0.6328$ μm, and the density was 0.426 gm/cm^3. The resulting Lorentz-Lorenz value is 0.505 cm^3/gm.

In Fig. 7 ($\tau = 5.57$-μm) absorptions are observed at 1300, 1350, 1540, 2340, 2590, 2830, 3010, and 3060 cm^{-1}. These absorption lines have been identified as:

Frequency, cm^{-1}	Vibration
1300	ν_4
1350	ν_4+lattice
1540	ν_2
2590	$2\nu_4$
2820	ν_1
3010	ν_3
3060	ν_3+lattice

The absorption at 2340 cm^{-1} is probably due to the presence of trace amounts of CO_2. After a thickness of 11.98 μm was deposited, the temperature was increased to 35 K. A spectrum taken at this temperature shows little change (Fig. 8). Evidence that the bands at 1350 and 3060 cm^{-1} are combinations of fundamental and lattice vibrations is shown in Fig. 9. This spectrum shows the transmission after the substrate has been raised to 54 K and recooled to 20 K. The bands at 1350 and 3060 cm^{-1} are no longer present, indicative of a change in the structure of the deposit.

4.4 HCl ON 20 K GERMANIUM

Transmission spectra were obtained for thicknesses of between 0.505 and 2.78 μm of HCl cryodeposited on germanium at 20 K, an example of which is shown in Fig. 10 for the 2.78-μm-thick film. The index of refraction at $\lambda = 0.6328$ μm was determined to be 1.30, and the density of the deposit was 0.955 gm/cm^3. The corresponding Lorentz-Lorenz value at $\lambda = 0.6328$ μm is 0.194 cm^3/gm. In the spectra taken from this sample, absorption bands are observed at 2340, 2780, and 2920 cm^{-1}. The fundamental vibration of HCl occurs in the gaseous state at 2886 cm^{-1} (Ref. 6). Therefore, it seems likely that the absorption band at 2780 cm^{-1} is the fundamental vibration in the condensed state.

The sample was warmed to 55 K. A transmission spectrum taken at this temperature (Fig. 11) shows that the absorption band at 2780 cm^{-1} has split into three distinct bands located at 2710, 2750, and 2780 cm^{-1}. As the sample is warmed further to 75 K (Fig. 12), a new absorption is noted at 2620 cm^{-1}, and the fundamental vibration is now only two bands located at 2710 and 2750 cm^{-1}, whereas the absorption at 2910 cm^{-1} has shifted up to 2990 cm^{-1}. The absorptions at the fundamental vibration are much stronger, approaching zero transmission. Warming the sample to 92 K (Fig. 13) shows that the deposit is no longer present. (At the chamber pressure of 4×10^{-1} torr, HCl sublimates at about 75 K, whereas CO_2, the probable contaminant causing the absorption at 2340 cm^{-1}, sublimates at about 87 K.) The broad, narrow band occuring at 2920 cm^{-1} is probably a combination of the fundamental and lattice vibrations.

4.5 N_2O ON 20 K GERMANIUM

Transmission spectra of N_2O deposited on 20 K germanium were obtained for thicknesses of from 0.262 to 4.19 μm (16 interference maxima). The index of refraction at $\lambda = 0.6328$ μm and the density were determined to be 1.27 and 0.988 gm/cm^3, respectively. The corresponding Lorentz-Lorenz value at $\lambda = 0.6328$ μm is 0.169 cm^3/gm.

As shown in the spectra for the 2.36-μm-thick film (Fig. 14), N_2O has many absorptions in the infrared (Ref. 7). Absorptions are noted at 580, 1160, 1295, 2190, 2240, 2460, 2570,

2800, 3380, and 3500 cm^{-1}. All of these bands except the 2190-cm^{-1} band correspond within about twenty wavenumbers to absorption bands in the gaseous state. These assignments are given below:

Frequency, cm^{-1}	Vibration
580	ν_2
1160	$2\nu_2$
1295	ν_3
2240	ν_1
2460	$\nu_3+2\nu_2$
2570	$2\nu_3$
2800	$\nu_1+\nu_2$
3380	$\nu_1+2\nu_2$
3500	$\nu_1+\nu_3$

The cause of the 2190-cm^{-1} absorption band is unknown, but possibly arises from an isotope of N_2O.

After a deposition of 4.19 μm, the temperature of the deposit was slowly increased. At a temperature of about 29 K, a structure change occurred in the sample as evidenced by the scattering that began. Further evidence of this phase change is seen in the spectrum taken at 46 K (Fig. 15). In this figure, the absorptions are stronger than previously.

4.6 O_2 ON 20 K GERMANIUM

Transmission spectra were obtained for thicknesses of O_2 deposited on 20 K germanium (Fig. 16). These thicknesses ranged from 0.263 to 14.45 μm. The index of refraction was 1.25 at λ = 0.6328 μm, the density 1.22 gm/cm^3, and the Lorentz-Lorenz value 0.121 cm^3/gm.

It is known that condensed O_2 is slightly infrared active (Ref. 8). This absorption occurs at the fundamental frequency of 1550 cm^{-1}, is very weak, and was undetectable for the thicknesses examined in this experiment. In the spectra, two weak absorptions are seen at 2140 and 2340 cm^{-1}. These absorptions are probably attributable to trace quantities of CO and CO_2, respectively. Warmup of the O_2 film to 30 K and subsequent recooling to 20 K showed no change in the spectral transmittance, indicating no change was observed for these thicknesses between the α and β phases.

4.7 N_2 ON 20 K GERMANIUM

Nitrogen is not active in the infrared (Fig. 17). Spectra were taken for thicknesses ranging from 0.261 to 5.22 μm. The index of refraction at λ = 0.6328 μm was 1.26, the density of the deposit 0.83 gm/cm^3, and the Lorentz-Lorenz value 0.194 cm^3/gm. The only noticeable N_2 effect on transmission is the channel spectra.

4.8 Ar ON 20 K GERMANIUM

Argon, not being infrared active, should show no absorptions in the region of interest. Transmission spectra were obtained for deposit thicknesses ranging from 0.266 to 6.93 μm (Fig. 18). The measured index of refraction at λ = 0.6328 μm was 1.23. Unfortunately, the QCM data obtained were not good, and this prevented a determination of the density. As was expected, the deposits of Ar showed no absorptions, and the only noticeable effect was the presence of the channel spectra.

4.9 Air ON 20 K GERMANIUM

Thin films of air were cryodeposited on 20 K germanium substrates (Fig. 19). Because these deposits were very transparent and caused little scattering, it was possible to form relatively thick deposits, ranging from 0.266 to 14.65 μm (55 interference maxima). The index of refraction at the He-Ne laser wavelength of 0.6328 μm was determined to be 1.23, and the density of the deposit was 1.05 gm/cm^3. The resulting Lorentz-Lorenz value was 0.142 cm^3/gm. Two absorptions were observed in the spectra, one at 1600 cm^{-1} and one at 2350 cm^{-1}, corresponding to H_2O and CO_2, respectively.

5.0 OPTICAL PROPERTIES DETERMINATION

To account for the influence of these constituents as contaminants it is necessary to know the solid, condensed phase optical properties. These properties are necessary to compute the reflectance change of a surface or to compute the transmittance change of an optical component. Knowing these properties can help correct for or predict the anticipated effects of condensed constituents on an actual surface. The optical properties desired are the refractive index, n, and the absorption index, k.

In order to determine the complex refractive index ($\bar{n}$ = n - ik) of the thin solid film from the transmittance versus thickness data for wavenumbers between 700 and 3700 cm^{-1}, an analytical model of film plus substrate transmission was developed (Refs. 9 and 10). It was

assumed that the germanium window acted as a thick film, and thus there was no phase coherence between multiple, internal-reflected rays. Moreover, the real part of the germanium complex index, n_g, is known and given by Ref. 11:

$$n_g = A + BL + CL^2 + D\lambda^2 + E\lambda^4 \tag{6}$$

where

$$L = \left(\lambda^2 - 0.028\right)^{-1},$$

$$A = 3.99931,$$

$$B = 0.391707,$$

$$C = 0.163492,$$

$$D = 0.000006, \text{ and}$$

$$E = 0.000000053.$$

The geometry describing the transmittance is shown in Fig. 20. For convenience the different layers have been subscripted 0, 1, 2, and 3, where subscripts 0 and 3 are vacuum and 1 and 2 are the thin condensed film and the thick germanium substrate, respectively. The model employed to fit the experimental results is for normal incidence only. As shown in Fig. 20, E_o^+ is the amplitude of the incident radiation that undergoes an infinite number of multiple reflections after passing into the thin film. Following multiple reflections the total amplitude of reflected and transmitted radiation is given by B_1 and E_2^+, respectively. E_2^+ internally reflects from the back of the germanium window, becomes A_1, and C_1, and again undergoes thin-film multiple reflection in medium 1. This results in the rays B_2 and A_2, and so on. Analytically the relationships between the amplitudes of the various waves are the following:

$$\begin{aligned} E_2^+ &= t_{012} E_o^+ \\ A_2 &= A_1 r_{210} \\ A_4 &= A_3 r_{210} \\ A_6 &= A_5 r_{210} \end{aligned} \tag{7}$$

with

$$\begin{aligned} A_1 &= E_2^+ r_2 \\ A_3 &= A_2 r_2 \\ A_5 &= A_4 r_2 \end{aligned} \tag{8}$$

with

$$C_1 = t_2 E_2^+$$
$$C_2 = t_2 A_2 \tag{9}$$
$$C_3 = t_2 A_4$$

and with

$$B_1 = r_{012} E_o^+$$
$$B_2 = A_1 t_{210} \tag{10}$$
$$B_3 = A_3 t_{210}$$
$$B_4 = A_5 t_{210}$$

where t_2 designates the amplitude transmittance of light traveling from medium 2 to medium 3, r_2 designates the amplitude reflection of light incident upon medium 3 from medium 2, r_{012} designates the amplitude reflection of light that is incident from medium 0 and is reflected back into medium 0 after undergoing thin-film interference in medium 1, r_{210} designates the amplitude reflection of light that is incident from medium 2 and is reflected back into medium 2 after undergoing thin-film interference in medium 1, t_{012} designates the amplitude transmittance of light incident from medium 0 and transmitted into medium 2 after undergoing thin-film interference in medium 1, and t_{210} designates the amplitude transmittance of light incident from medium 2 and transmitted into medium 0 after undergoing thin-film interference in medium 1.

The power transmitted through the thin-film/thick-film combination is given by

$$\xi = n_3 \left[C_1\right]^2 + n_3 \left[C_2\right]^2 + n_3 \left[C_3\right]^2 + \ldots \tag{11}$$

where $n_3 = n_0$ since medium 3 and medium 0 are both considered as vacuum and with the constant $c/4\pi$ (c being the speed of light in vacuum) being omitted for convenience since this constant will be lost when dividing to determine the overall transmittance.

Substituting Eq. (9) into Eq. (11) yields the transmitted power as

$$\xi = n_o |t_2|^2 \left[|E_2^+|^2 + |A_2|^2 + |A_4|^2 + |A_6|^2 + \ldots\right] \tag{12}$$

Next, combining Eqs. (7) and (8) yields

$$A_2^2 = R_2 R_{210} E_2^{+2}$$
$$A_4^2 = R_2^2 R_{210}^2 E_2^{+2} \tag{13}$$
$$A_6^2 = R_2^3 R_{210}^3 E_2^{+2}$$

where

$$R_2 = r_2^2 \tag{14}$$

$$R_{210} = r_{210}^2 \tag{15}$$

$$T_2 = t_2^2 \tag{16}$$

Inserting Eq. (13) into Eq. (12) results in the transmitted power being given by

$$\xi = n_0 T_2 E_2^{+2} \left(1 + R_2 R_{210} + R_2^2 R_{210}^2 + R_2^3 R_{210}^3 + \ldots\right) \tag{17}$$

where the infinite sum converges to the closed-form expression,

$$\xi = \frac{n_0 T_2 E_2^{+2}}{1 - R_2 R_{210}} \tag{18}$$

The transmittance is defined as the transmitted power divided by the incident power. The incident power is given by

$$\xi_0 = n_0 E_0^{+2} \tag{19}$$

and the expression for the overall transmittance is obtained by ratioing Eq. (18) to Eq. (19), i.e.,

$$T = \frac{\xi}{\xi_o} = \frac{T_2 |E_2^+|^2}{\left(1 - R_2 R_{210}\right) \left[E_o^+\right]^2} \tag{20}$$

But from Eq. (7)

$$\frac{|E_2^+|^2}{|E_o^+|^2} = |t_{012}|^2 = T_{012} \tag{21}$$

and the final result for the overall normal transmittance is given by

$$T = \frac{T_2 T_{012}}{\left(1 - R_2 R_{210}\right)} \tag{22}$$

The result in Eq. (22) is valid only when the substrate is a nonabsorbing medium. If the substrate is also absorbing, i.e., the imaginary part of the complex refractive index of the substrate is nonzero, then Eq. (22) becomes

$$T = \frac{T_2 T_{012} e^{-\alpha_g D}}{1 - R_2 R_{210} e^{-2\alpha_g D}} \tag{23}$$

where

D = the thickness of the substrate (germanium),

$\alpha_g = \frac{4\pi k_g}{\lambda}$ is the absorption coefficient of the substrate (germanium),

k_g = imaginary component of complex refractive index of the substrate (germanium), and

λ = wavelength in vacuum.

Having developed Eq. (23), which is the normal transmittance of a thin film deposited upon a thick partially transmitting film, it is now necessary to define the expressions T_2, T_{012}, R_2, and R_{210} in terms of the optical constants of the thin film, the substrate, and wavelength. The derivation of these quantities is straightforward, although tedious, and is outlined in detail in Ref. 9. For completeness, the expressions required to evaluate Eq. (23) are listed below:

$$R_2 = |r_2|^2 = \left| \frac{\bar{n}_2 - n_o}{\bar{n}_2 + n_o} \right|^2 \tag{24}$$

$$T_2 = |t_2|^2 = \left| \frac{2\bar{n}_2}{(n_o + \bar{n}_2)} \right|^2 \tag{25}$$

The expressions for T_{012} and R_{210} are somewhat more complicated to evaluate and will be considered separately from R_2 and T_2. The expressions for T_{012} and R_{210} based on the work of Ref. 10 are given by

$$T_{012} = \frac{|t_a|^2 |t_b|^2 e^{-2b}}{\left\{ 1 + |r_a|^2 |r_b|^2 e^{-4b} + 2e^{-2b} \left[\mathrm{Re}\left(r_a r_b\right) \cos 2a + \mathrm{Im}\left(r_a r_b\right) \sin 2a \right] \right\}} \tag{26}$$

and

$$R_{210} = \frac{\left\{ |r_a|^2 + |r_b|^2 e^{-4b} + 2e^{-2b} \left[\mathrm{Re}\left(r_b r_a^*\right) \cos 2a + \mathrm{Im}\left(r_b r_a^*\right) \sin 2a \right] \right\}}{\left\{ 1 + |r_a|^2 |r_b|^2 e^{-4b} + 2e^{-2b} \left[\mathrm{Re}\left(r_a r_b\right) \cos 2a + \mathrm{Im}\left(r_b r_a^*\right) \sin 2a \right] \right\}} \tag{27}$$

where

$$r_a = \frac{\bar{n}_2 - \bar{n}_1}{\bar{n}_2 + \bar{n}_1} \tag{28}$$

$$r_b = \frac{\bar{n}_1 - n_o}{\bar{n}_1 + n_o} \tag{29}$$

$$t_a = \frac{2\bar{n}_1}{\bar{n}_1 + \bar{n}_2} \tag{30}$$

$$t_b = \frac{2n_o}{n_o + \bar{n}_1} \tag{31}$$

$$\bar{n}_1 = n_1 - ik_1 = n - ik = \bar{n} \tag{32}$$

$$\bar{n}_2 = n_g - ik_g \tag{33}$$

$$a = \frac{2\pi d_1 n_1}{\lambda} \tag{34}$$

$$b = \frac{2\pi d_1 k_1}{\lambda} \tag{35}$$

where d_1 = cryodeposit thickness and * denotes the complex conjugate. The optical constants of the cryopumped constituents were determined by using this analytical transmission model in conjunction with a nonlinear least-squares convergence routine. Also, the subtractive Kramers-Kronig relation between n and k was used in comparison with the nonlinear least-squares determination of n. The subtractive Kramers-Kronig relation is given by

$$n(\nu) = n(\nu_m) + \frac{2}{\pi} P \int_0^\infty \left[\frac{k(\nu')\nu' - k(\nu)\nu}{(\nu')^2 - \nu^2} - \frac{k(\nu')\nu' - k(\nu_m)\nu_m}{(\nu')^2 - \nu_m^2} \right] d\nu' \tag{36}$$

where ν_m is a reference frequency (for CO ν_m = 2500 cm^{-1}, n = 1.232; for NO ν_m = 2500 cm^{-1}, n = 1.326; for CH_4 ν_m = 2200 cm^{-1}, n = 1.330; for HCl ν_m = 1700 cm^{-1}, n = 1.278; for O_2 ν_m = 2200 cm^{-1}, n = 1.264; for N_2 ν_m = 2200 cm^{-1}, n = 1.229; and for Ar ν_m = 2200 cm^{-1}, n = 1.225) and P indicates the Cauchy principal value of the integral. Integration was performed using the simple trapezoidal rule; the $k(\nu')$ values used in Eq. (36) were those determined by the nonlinear least-squares technique.

Transmittance data recorded for all deposits discussed here were digitized every 2 cm^{-1}. The optical properties were computed every 10 cm^{-1} except in regions of strong absorption where computations were performed every 2 cm^{-1}. The optical properties were initially computed by the nonlinear least-squares determination using Eq. (23). However in some instances the program did not appear to converge upon a unique value of n. This usually occurred in regions of strong absorption or low wavenumber or for cases where it was only possible to form a few small thicknesses of the deposit. The n value appears to be primarily defined by the period of the transmission versus thickness curve at each wavenumber. At small thicknesses, or high absorption, or low wavenumbers, the transmission versus thickness (for each wavenumber) curve is not well defined, i.e., the period of the interference as a function of thickness is not well defined. The k value, which is primarily

defined by the magnitude of the transmittance, did not have this difficulty and was well defined over the whole spectral region (700 to 3700 cm^{-1}). Thus, to determine n, the k values were used with the subtractive Kramers-Kronig relationship to compute n; these new n values were then used in the analytical model (along with the k values) to see if good agreement occurred with the transmittance data. For all wavenumbers, the Kramers-Kronig n values along with the least-squares k values yielded good agreement when the analytical model and transmittance data were compared.

Generally, the nonlinear least-squares (thin-film model) values did converge, and a comparison of the Kramers-Kronig and thin-film results are shown for each species investigated. The values listed in the tables are the Kramers-Kronig n values along with the thin-film k values. The slanted dashed line on the k versus ν plots represents the minimum absorption index values that can be determined due to the error limits on the film-substrate transmission measurements. Values below the dashed line are shown but should not be considered as accurate.

5.1 CO OPTICAL CONSTANTS

The optical properties n,k, which are the refractive and absorption indices of carbon monoxide films, were determined from 15 thicknesses. These curves are shown in Fig. 21 and tabulated in Table 1. The refractive index, n, is essentially constant between 1.23 and 1.24, except for the region of the fundamental stretching vibration band centered at 2140 cm^{-1}. The values obtained using the nonlinear least-squares technique in this region go both higher and lower than obtained using the Kramers-Kronig technique. The k curve shows an absorption index maximum of 0.34 at 2140 cm^{-1}. The transmission of the CO film on the germanium at 1100, 2146, and 3300 cm^{-1} is shown in Fig. 22 as a function of film thickness. The experimental curve and the calculated curve using the n's and k's determined are in close agreement.

5.2 NO OPTICAL CONSTANTS

The n's and k's of 20 K nitric-oxide films were determined from 18 thicknesses (see Fig. 23 and Table 2). The refractive indices over much of the wavenumber range varied between 1.30 and 1.35. Between 1500 and 2000 cm^{-1} there was considerable variation, as shown in Fig. 23. Most of the major variation in k occurs between 1700 and 1900 cm^{-1} with the strongest peak occurring at a k value of 0.9, at 1760 cm^{-1}, and another peak at 1860 cm^{-1}. These bands occur in the region of the fundamental absorption band for NO. The agreement between the nonlinear least-squares and Kramers-Kronig techniques for determining n is quite good. The comparison of theory and data for determining the transmittance of 20 K

germanium with the condensed NO films as a function of thickness is shown in Fig. 24. The 1400- and 2700-cm^{-1} curves correspond to regions of low absorption, whereas the 1760-cm^{-1} curve is for the highly absorbing region. As observed the thin-film interference is damped out for the highly absorbing wavenumbers.

5.3 HCl OPTICAL CONSTANTS

The refractive and absorption indices, shown in Fig. 25 and Table 3, were obtained for 10 thicknesses of HCl. The vibration band located at 2780 cm^{-1} is the only region of appreciable absorption, and this band only shows an absorption index of 0.28, which is considerably less than observed for the NO band. The refractive index varied between 1.25 and 1.29 over most of the wavenumber range with the exception being in the vicinity of the 2780-cm^{-1} absorption bands. The agreement between the two techniques of refractive index measurement is again quite good. Figure 26 shows the comparison of theory and data for 20 K HCl films for 1000-, 3000-, and 2768-cm^{-1} wavenumber regions. The 1000-and 3000-cm^{-1} curves are for low absorption regions, whereas the 2768-cm^{-1} curve is for the high absorption index region.

5.4 CH_4 OPTICAL CONSTANTS

The 20 K methane optical constants were determined using 24 film thicknesses, and the results are shown in Fig. 27 and Table 4. The refraction index values ranged from 1.32 to 1.35 over most of the 700- to 3700-cm^{-1} range. The two regions of highest absorption were at 1310 cm^{-1} ($k = 0.27$) and at 3020 cm^{-1} ($k = 0.65$), which correspond to the ν_4 and ν_3 vibration bands, respectively. The comparison of theory and data for CH_4 films on 20 K germanium are shown in Fig. 28 for the 1300-, 2100-, and 3020-cm^{-1} regions. Good agreement between theory and data is again observed.

5.5 O_2, N_2, AND Ar OPTICAL CONSTANTS

Since the homonuclear gases O_2 and N_2 and the monoatomic gas argon showed no absorption in the 700- to 3700-cm^{-1} wavenumber range, only the refractive index curves are presented. Figure 29 and Table 5 show the refractive indices obtained for 20 thicknesses of O_2 condensed on 20 K germanium. The refractive index is essentially constant (between 1.26 and 1.27) over the entire wavenumber range. The comparison between theory and data is presented in Fig. 30 and shows excellent agreement.

Similar measurements were made for 15 N_2 film thicknesses condensed on 20 K germanium (Fig. 31 and Table 6). Refractive index values of 1.22 and 1.23 were observed for all

wavenumbers. The comparison for theory and expermental values for N_2 films is shown in Fig. 32 from 3610-, 2200-, and 710-cm $^{-1}$ curves. Good agreement is again shown.

Refractive indices for argon are presented in Fig. 33 and Table 7. These values were derived using 16 thicknesses of argon films condensed on 20 K germanium. As expected, the refractive indices are essentially constant with a value of 1.22 observed for most of the wavenumber range. Comparison of experimental and theoretical values in Fig. 34 show good agreement.

6.0 SUMMARY

Experimentally determined transmission measurements of condensed gases on a cryogenically cooled germanium window have been made. Thin films of CO, NO, CH_4, HCl, N_2O, O_2, N_2, Ar, and air were deposited at 20 K. The infrared spectral transmission was studied over the 500- to 3700-cm^{-1} wavenumber range. The film thickness was accurately determined using a two-angle laser-interference technique. The density of the films was determined using quartz-crystal microbalances and by determining the refractive index at 0.6328 μm to allow accurate thickness determination.

From the transmission data, the optical properties n and k, which are the real and imaginary parts of the refractive index, were determined for the 700- to 3700-cm^{-1} wavenumber range. These results are presented in graphical and tabular form for a wavenumber interval of 2 cm^{-1}. The optical properties presented are important for calculating the effects of possible deposits upon cryogenically cooled surfaces. Such surfaces as cryogenically cooled sensor optics and telescopes will be functioning in the wavenumber region investigated. The interpretation of information from these types of instruments, when contaminated with thin films, will require spectral knowledge of n and k.

REFERENCES

1. Roux, J. A., Wood, B. E., and Smith, A. M. "Infrared Optical Properties of Bipropellant Cryocontaminants." AEDC-TR-79-50, August 1979.

2. Roux, J. A., Wood, B. E., and Smith, A. M. "IR Optical Properties of Thin H_2O, NH_3, and CO_2 Cryofilms." AEDC-TR-79-57, September 1979.

3. Pipes, J. G., Roux, J. A., Smith, A. M., and Scott, H. E. "Infrared Transmission of Contaminated Cryocooled Optical Windows." *AIAA Journal*, Vol. 16, No. 9, Sept. 1978, pp. 984-990.

4. Tempelmeyer, K. E. and Mills, D. W., Jr. "Refractive Index of Carbon Dioxide Cryodeposit." *Journal of Applied Physics*, Vol. 39, 1968, pp. 2968-2969.

5. Smith, A. M., Tempelmeyer, K. E., Müller, P. R., and Wood, B. E. "Angular Distribution of Visible and Near IR Radiation Reflected from CO_2 Cryodeposits." *AIAA Journal*, Vol. 7, No. 12, Dec. 1969, pp. 2274-2280.

6. Herzberg, G. "*Molecular Spectra and Molecular Structure*, I. *Spectra of Diatomic Molecules*. D. Van Nostrand Company, Inc., Princeton, N. J., 1950.

7. Herzberg, G. *Infrared and Raman Spectra of Polyatomic Molecules*. D. Van Nostrand Company, Inc., Princeton, N. J., 1945.

8. Cairns, B. R. and Pimentel, G. C. "Infrared Spectra of Solid α- and β-Oxygen." *Journal of Chemical Physics*, Vol. 43, No. 10, 1965, pp. 3432-3438.

9. Vašicek, A. *Optics of Thin Films*. North-Holland Publishing Company, Interscience Publishers, Inc., New York, 1960.

10. Heavens, O. S. *Optical Properties of Thin Films*. Dover Publications, Inc., New York, 1965.

11. Herzberger, M. and Salzberg, C. D. "Refractive Indices of Infrared Optical Materials and Color Correction of Infrared Lenses." *Journal of the Optical Society of America*, Vol. 52, Number 4, April 1962, pp. 420-426.

1. Pyroelectric detector and collection optics.
2. Stainless steel high vacuum chamber, 85 cm tall by 70 cm in diameter (33.5 in. by 27.5 in. in diameter).
3. Cryogenically cooled infrared window; germanium, 4 mm thick by 70 mm square (0.158 in. by 2.76 in.) and QCM.
4. Helium-neon laser (0.6328 μm) beam (one of two shown) employed to measure cryofilm thickness.
5. Infrared beam, 38 mm in diameter (1.5 in.).
6. 2-mw He-Ne laser.
7. Michelson interferometer.
8. Infrared source and collimator mirror.

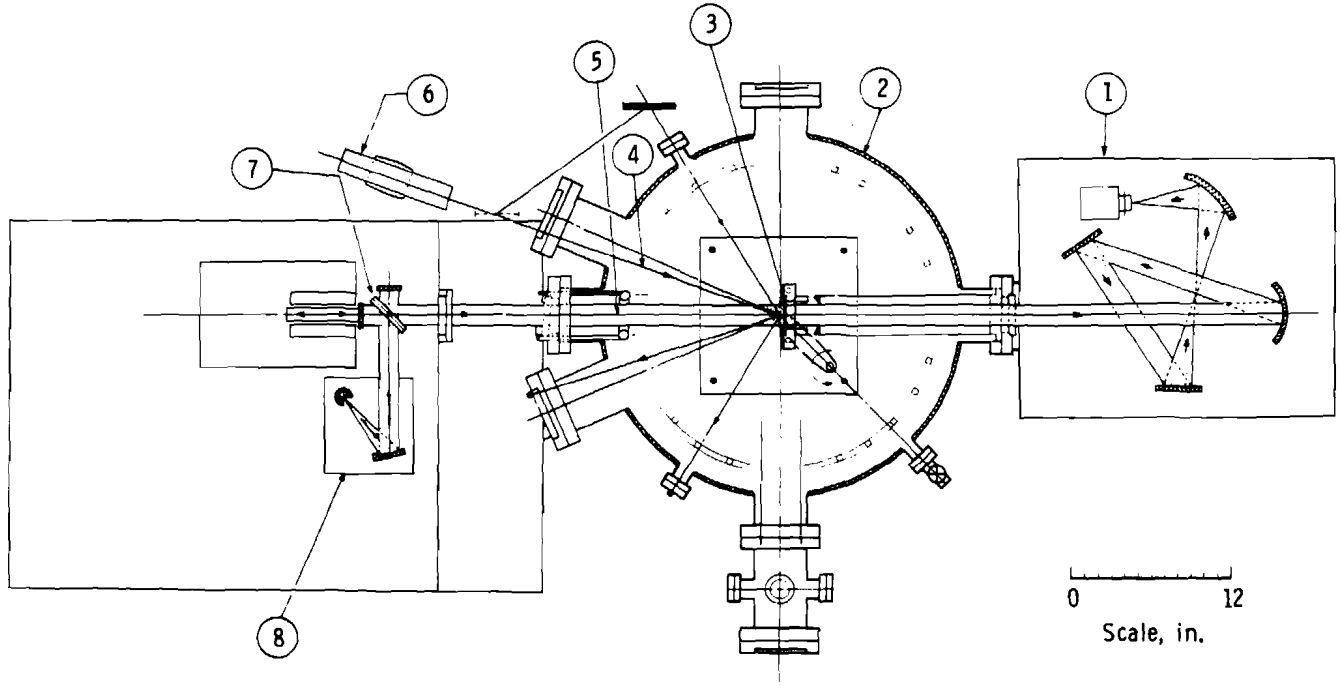

Figure 1. Schematic of the Infrared Optical Transmission Chamber (IROTC) with FTS-14 interferometer-spectrometer.

1. Infrared beam, 38-mm-diameter (1.5.).
2. Optical stop required to underfill cryocooled window with infrared beam. Also, this stop is supported by a 3-in. -ID pipe that prevents gas added to chamber from cryopumping on rear of window.
3. Aluminum holder with cryogenic passageways.
4. Germanium window heat sunk with an indium gasket to the aluminum holder.
5. Cover plate.
6. Gaseous helium or liquid nitrogen inlet.
7. Gaseous helium or liquid nitrogen outlet.
8. Crosshatched area illustrates area of window heat sunk to holder. Clear diameter is 50.7 mm (2 in.) while infrared beam diameter is 38 mm (1.5 in.).
9. QCM heat sunk with indium gasket to aluminum holder.

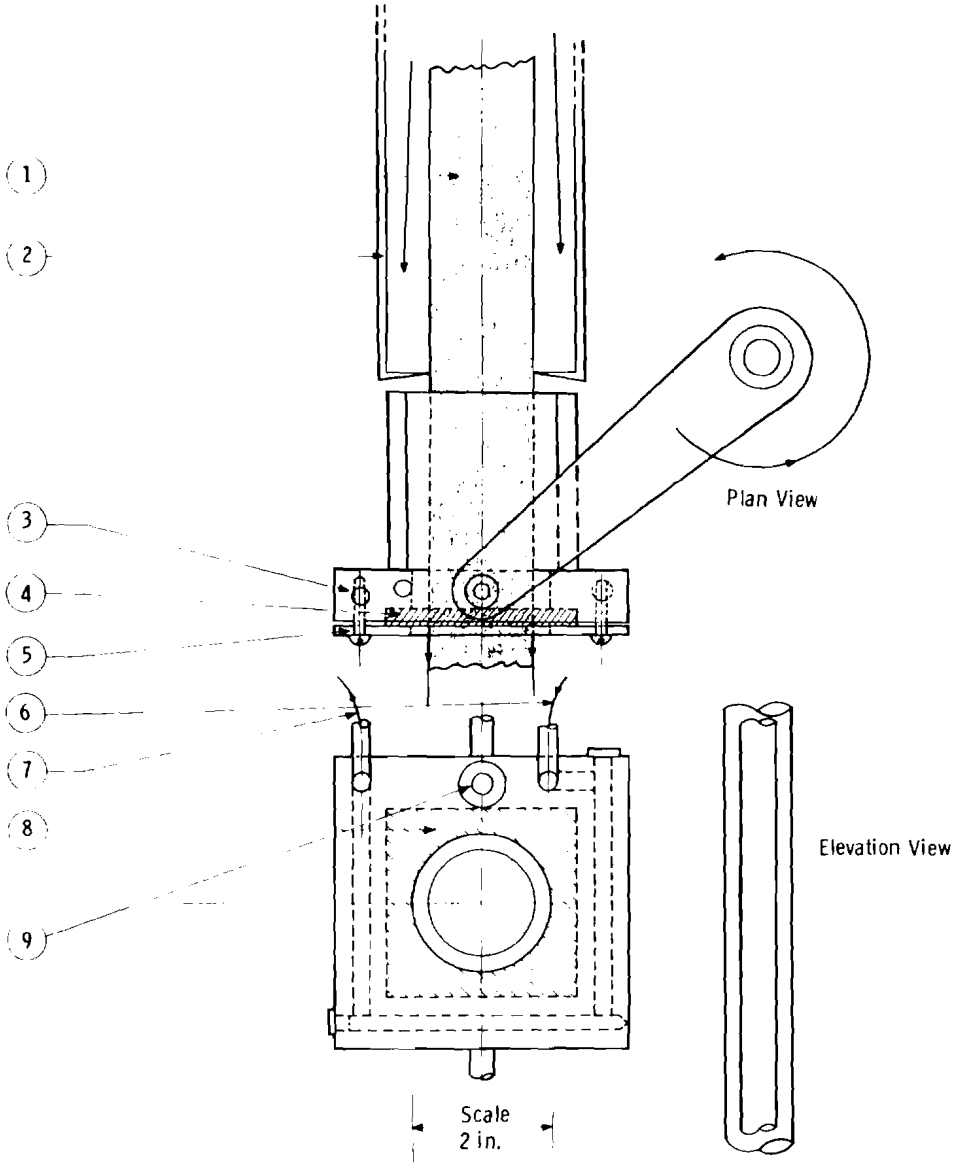

Figure 2. Plan and elevation views of cryogenically cooled window holder.

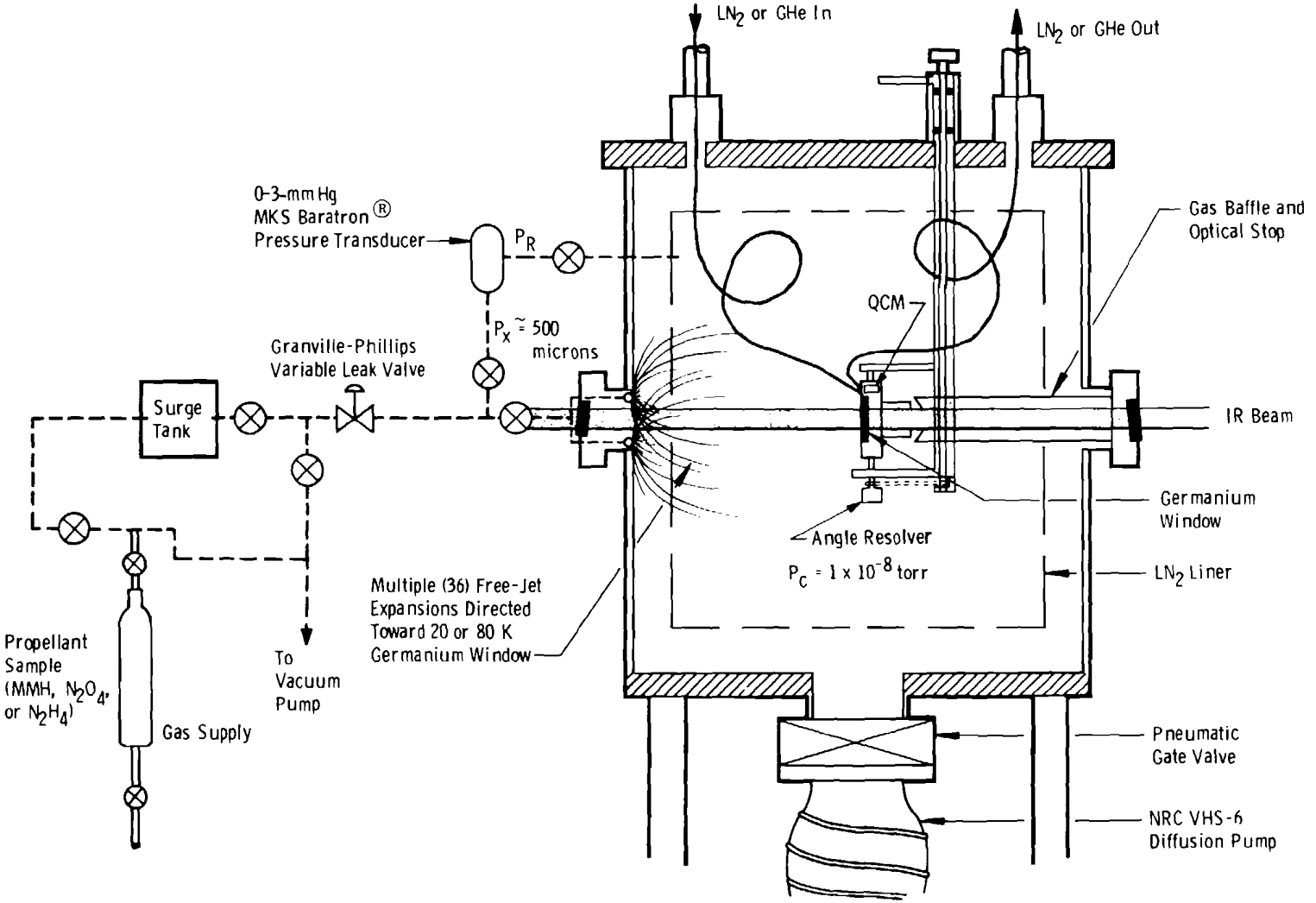

Figure 3. Gas deposition system.

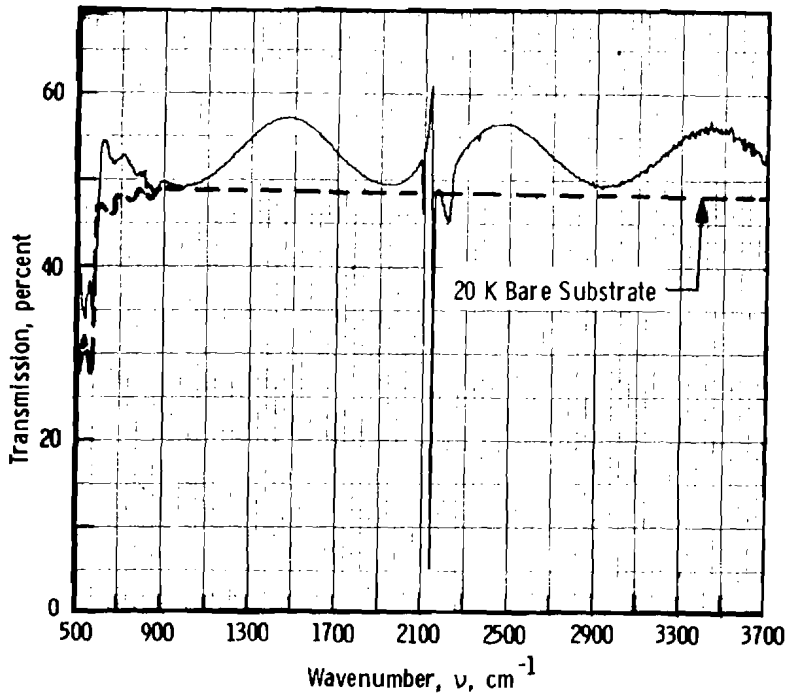

Figure 4. Transmittance of a 4.13-μm-thick CO film on 20 K germanium.

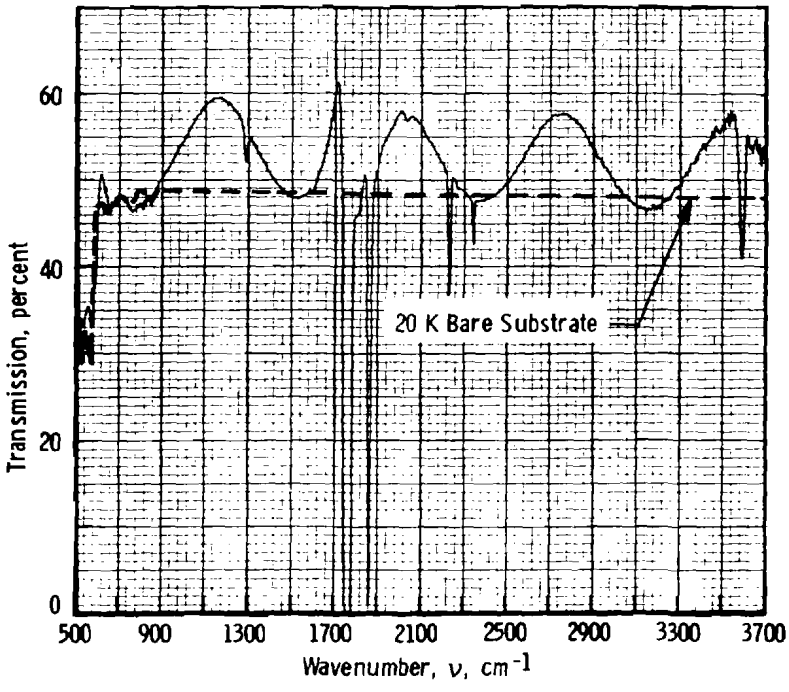

Figure 5. Transmittance of a 4.78-μm-thick NO film on 20 K germanium.

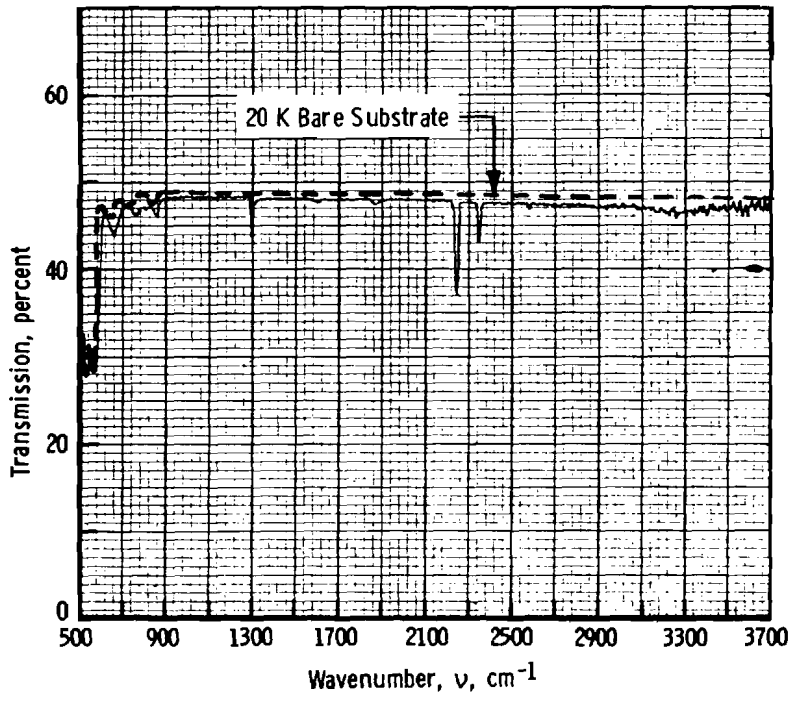

Figure 6. Transmittance of an NO film after warmup to 83 K.

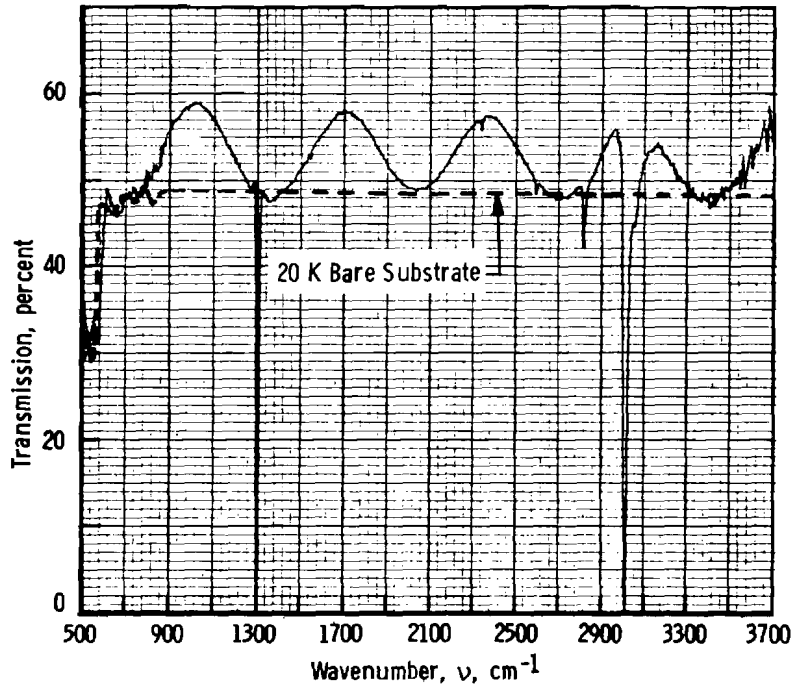

Figure 7. Transmittance of a 5.57-μm-thick CH_4 film on 20 K germanium.

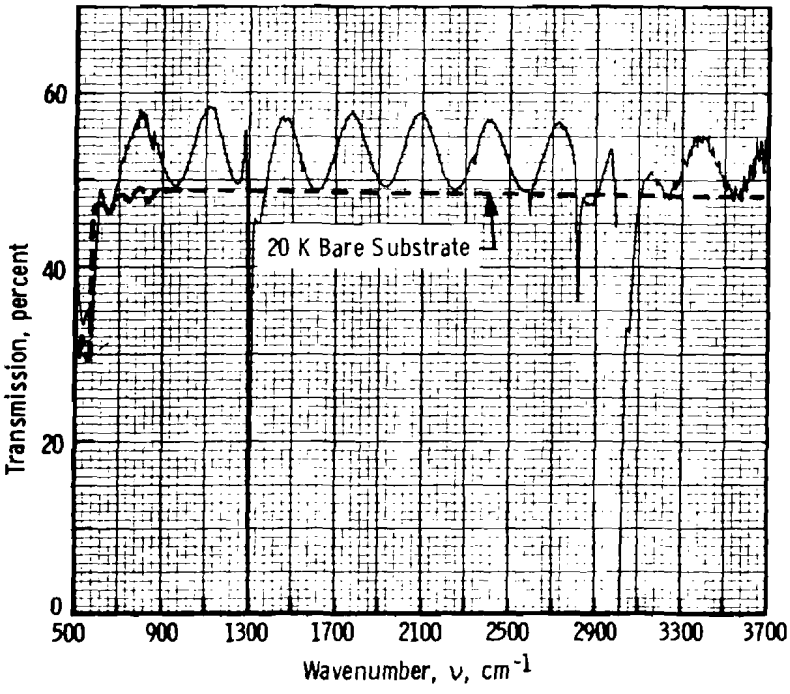

Figure 8. Transmittance of a 11.98-μm-thick CH_4 film after warmup to 35 K.

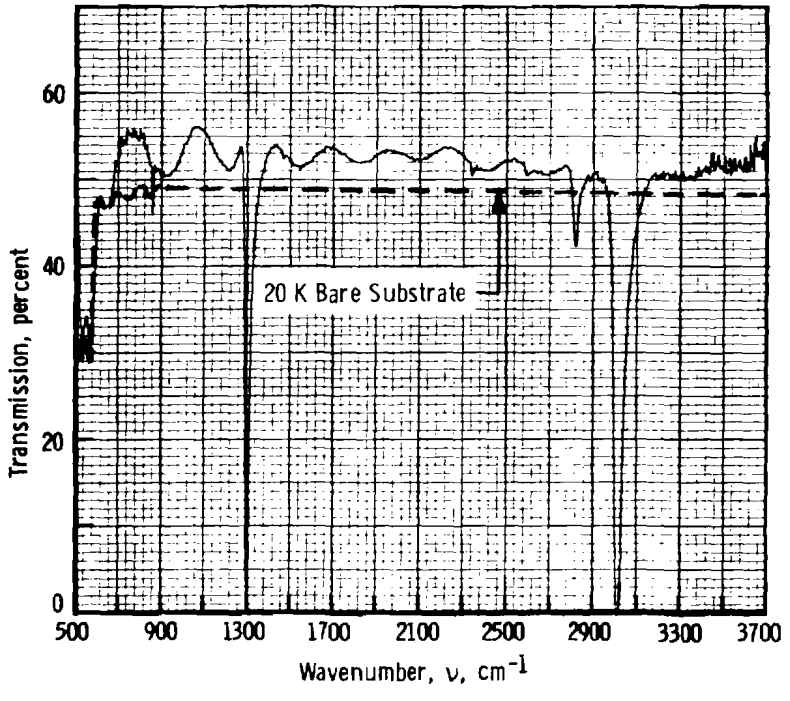

Figure 9. Transmittance of 12.0-μm-thick CH_4 film after warmup to 54 K and recooling to 20 K.

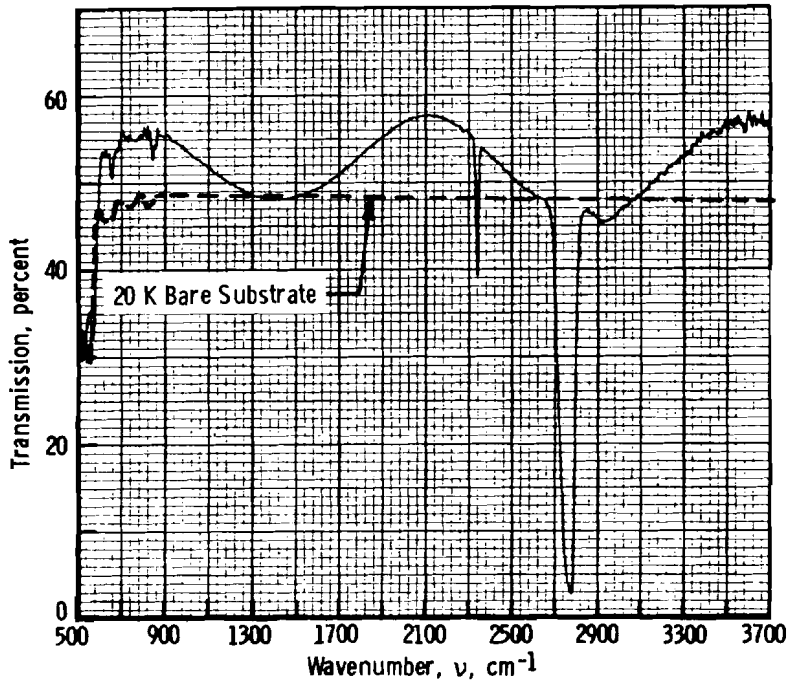

Figure 10. Transmittance of a 2.78-μm-thick HCl film on 20 K germanium.

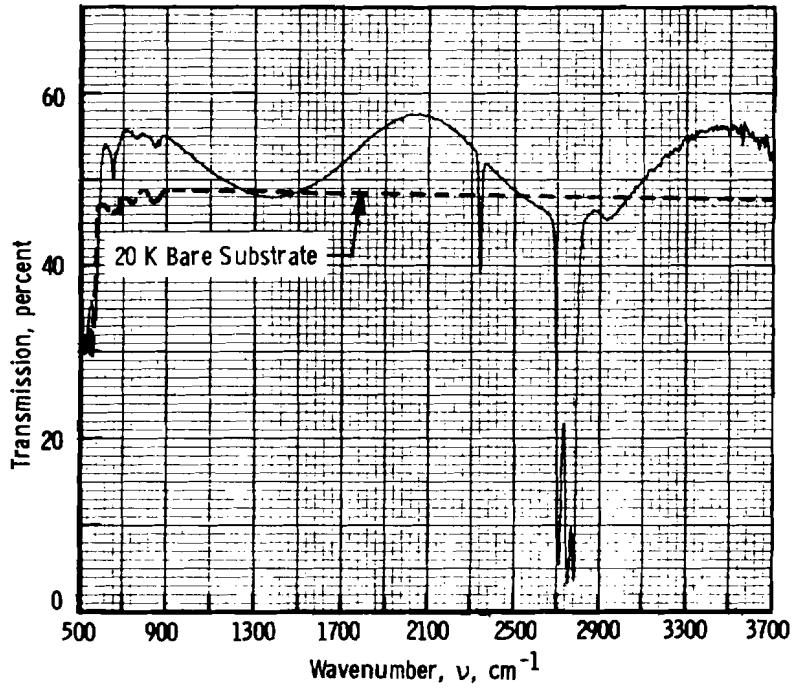

Figure 11. Transmittance of a 2.78-μm-thick HCl film after warmup to 55 K.

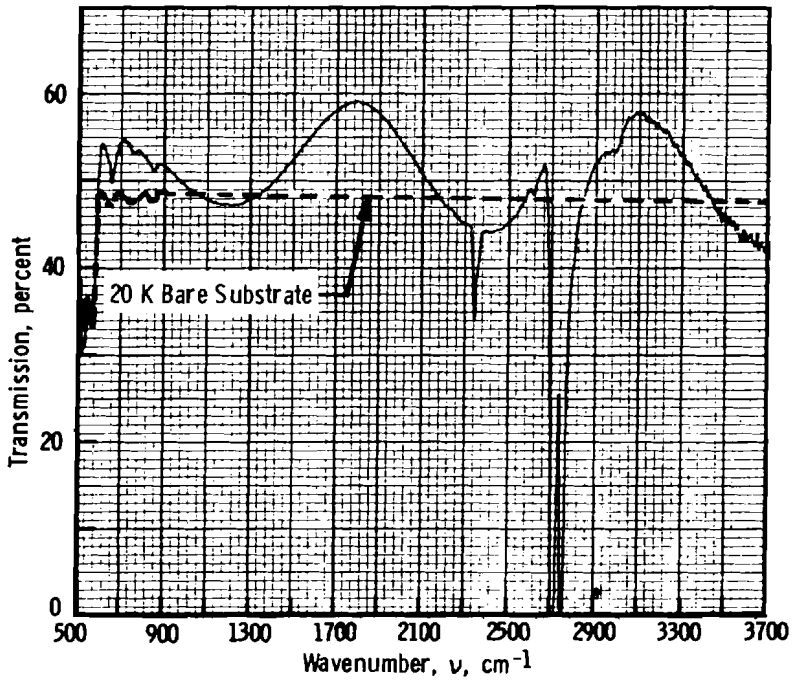

Figure 12. Transmittance of a 2.78-μm-thick film after warmup to 75 K.

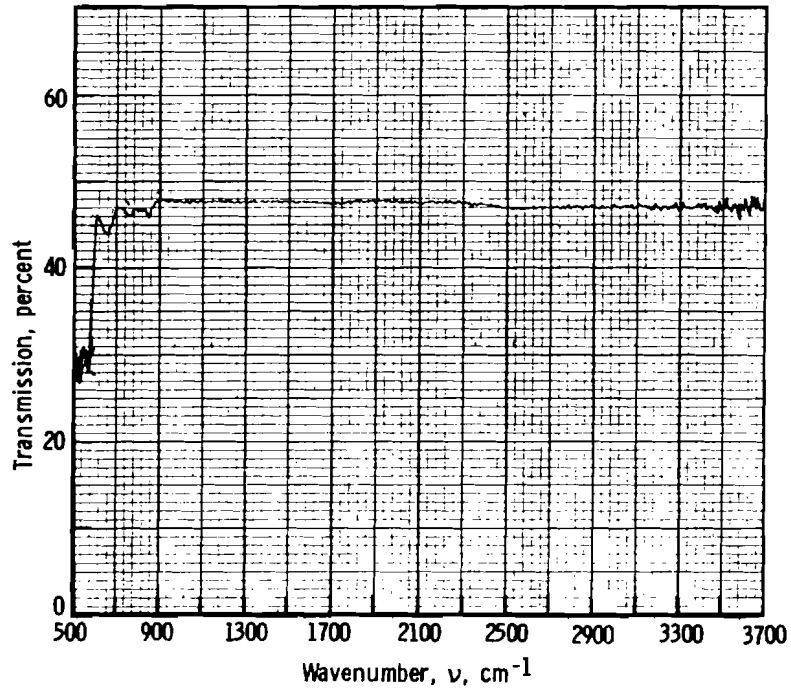

Figure 13. Transmittance of a germanium window after warmup to 92 K (HCl has already sublimated).

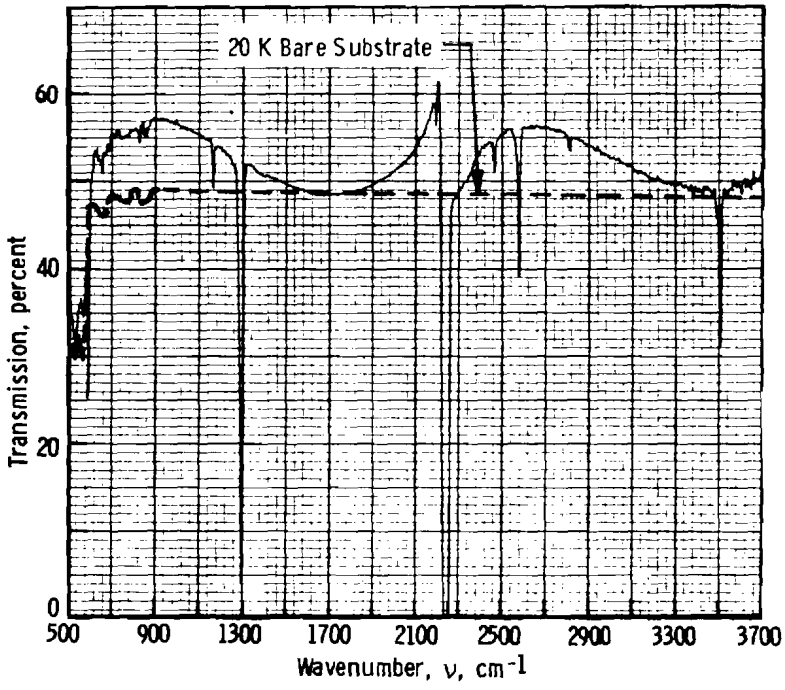

Figure 14. Transmittance of a 2.36-μm-thick N_2O film on 20 K germanium.

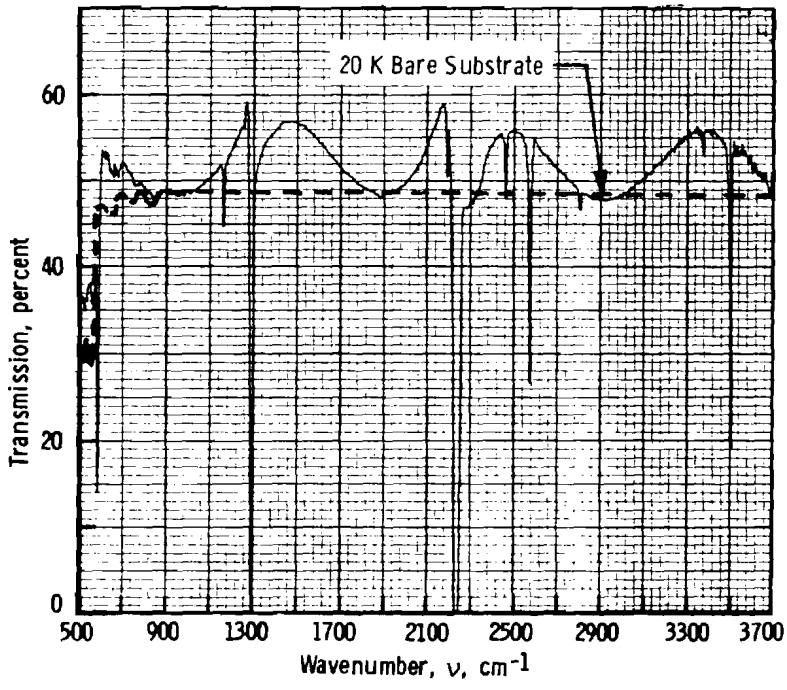

Figure 15. Transmittance of a 4.19-μm-thick N_2O film after warmup to 46 K.

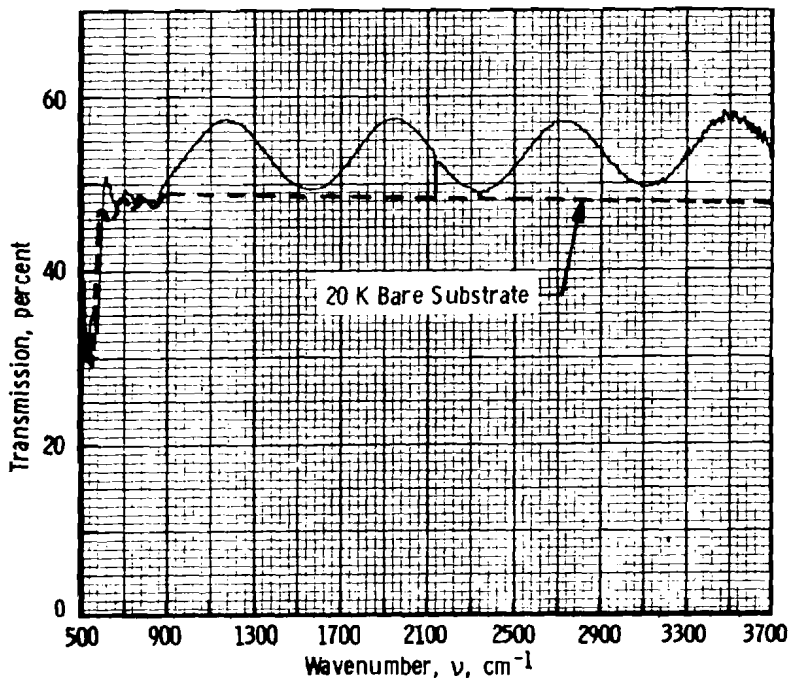

Figure 16. Transmittance of a 5.26-μm-thick oxygen film on 20 K germanium.

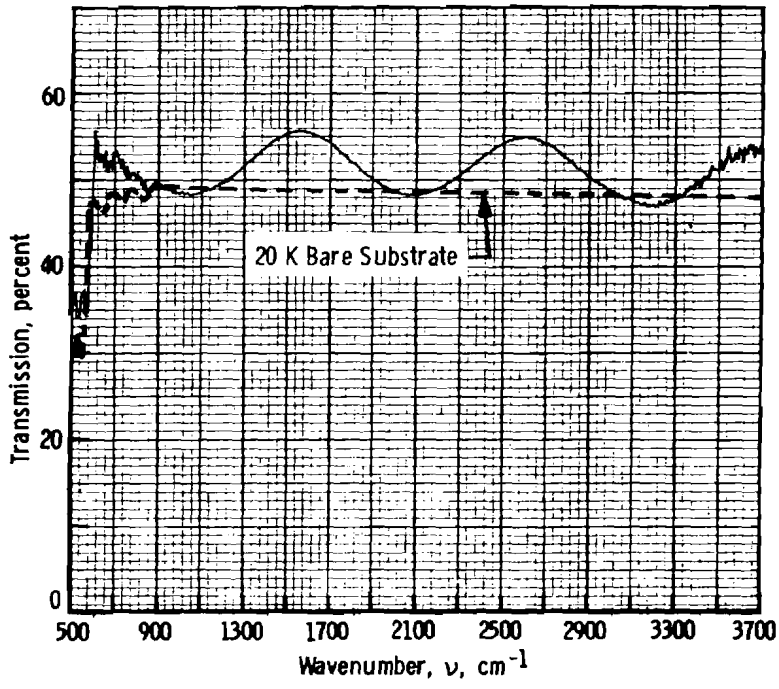

Figure 17. Transmittance of a 40-μm-thick N_2 film on 20 K germanium.

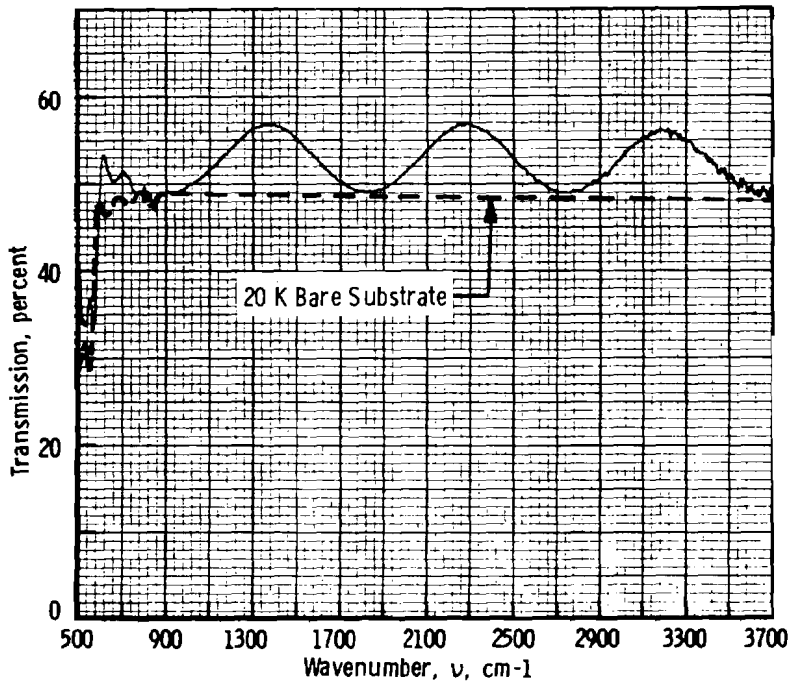

Figure 18. Transmittance of a 4.52-μm-thick argon film on 20 K germanium.

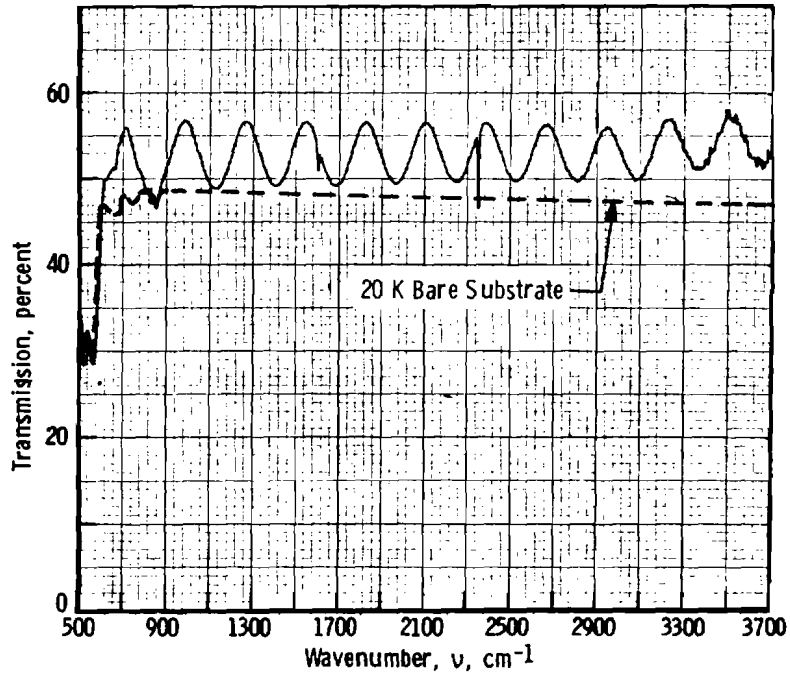

Figure 19. Transmittance of a 14.65-μm-thick condensed air film on 20 K germanium.

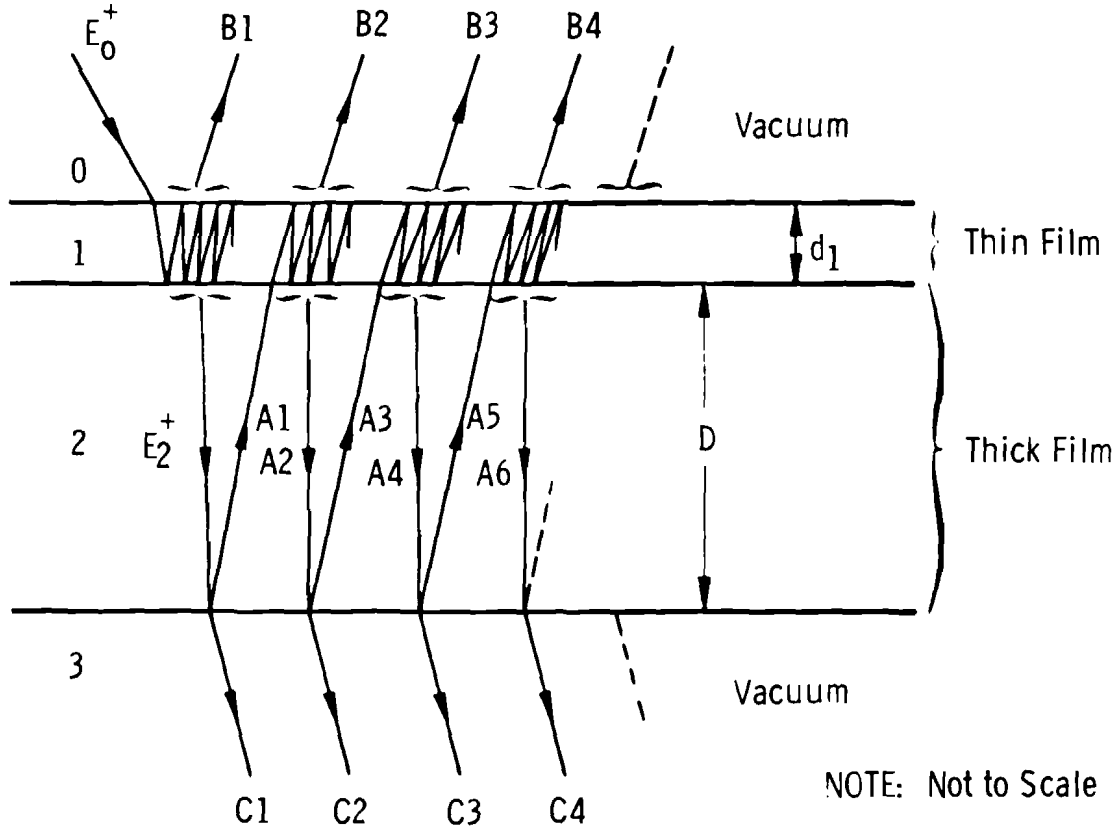

Figure 20. Geometry depicting analytical model for a thin film formed on a thick film.

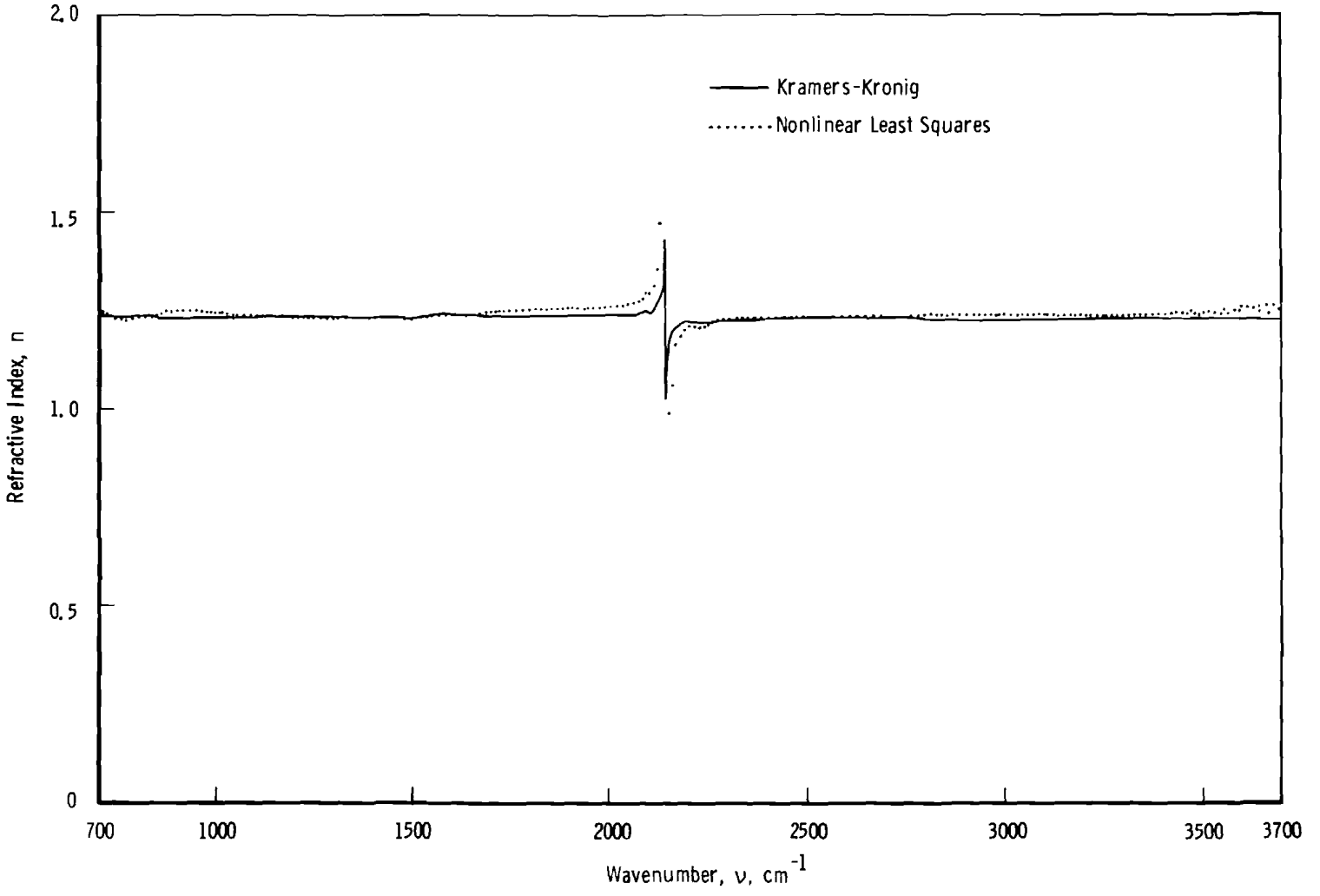

Figure 21. Optical properties of CO condensed on 20 K germanium.

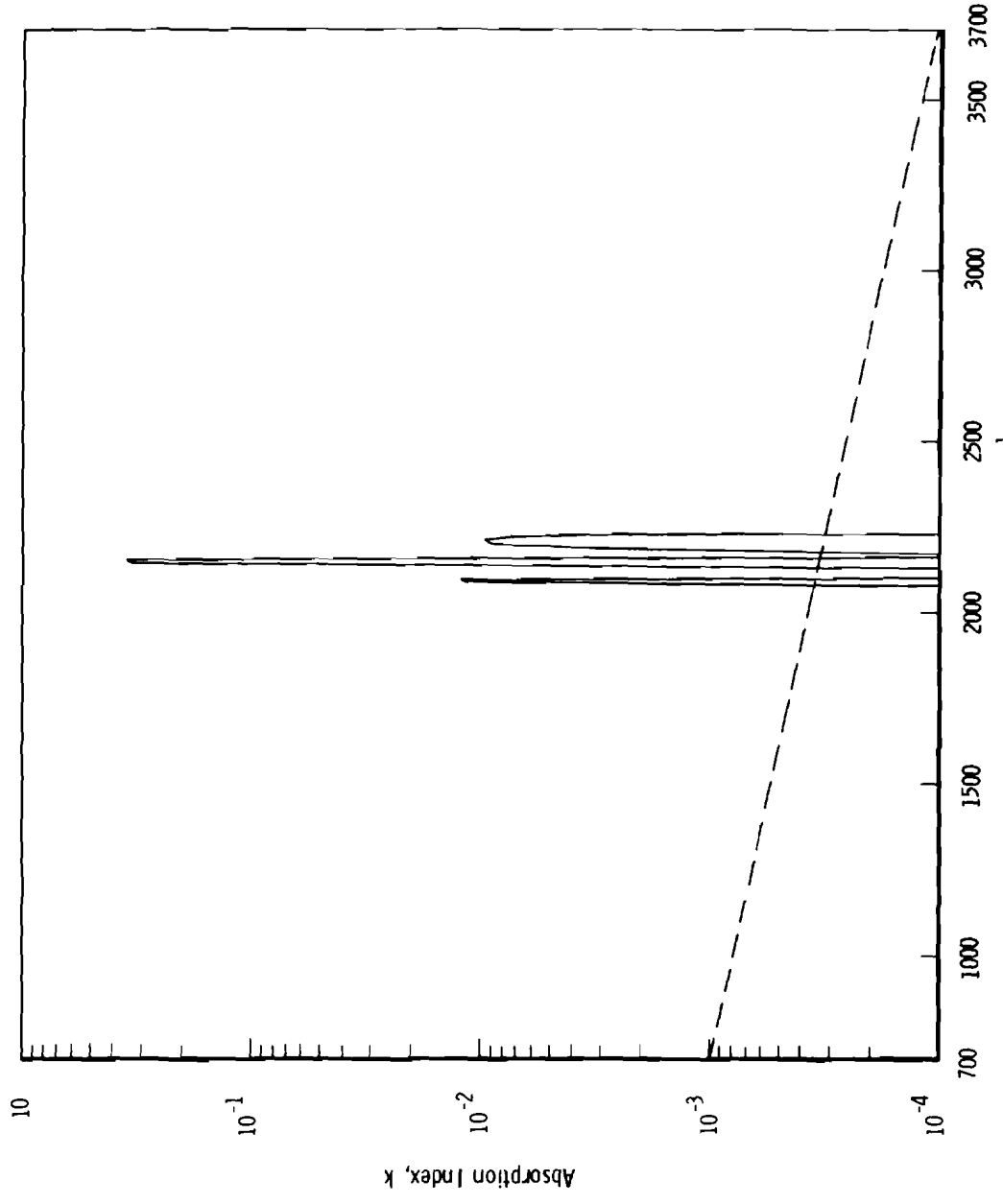

Figure 21. Concluded.

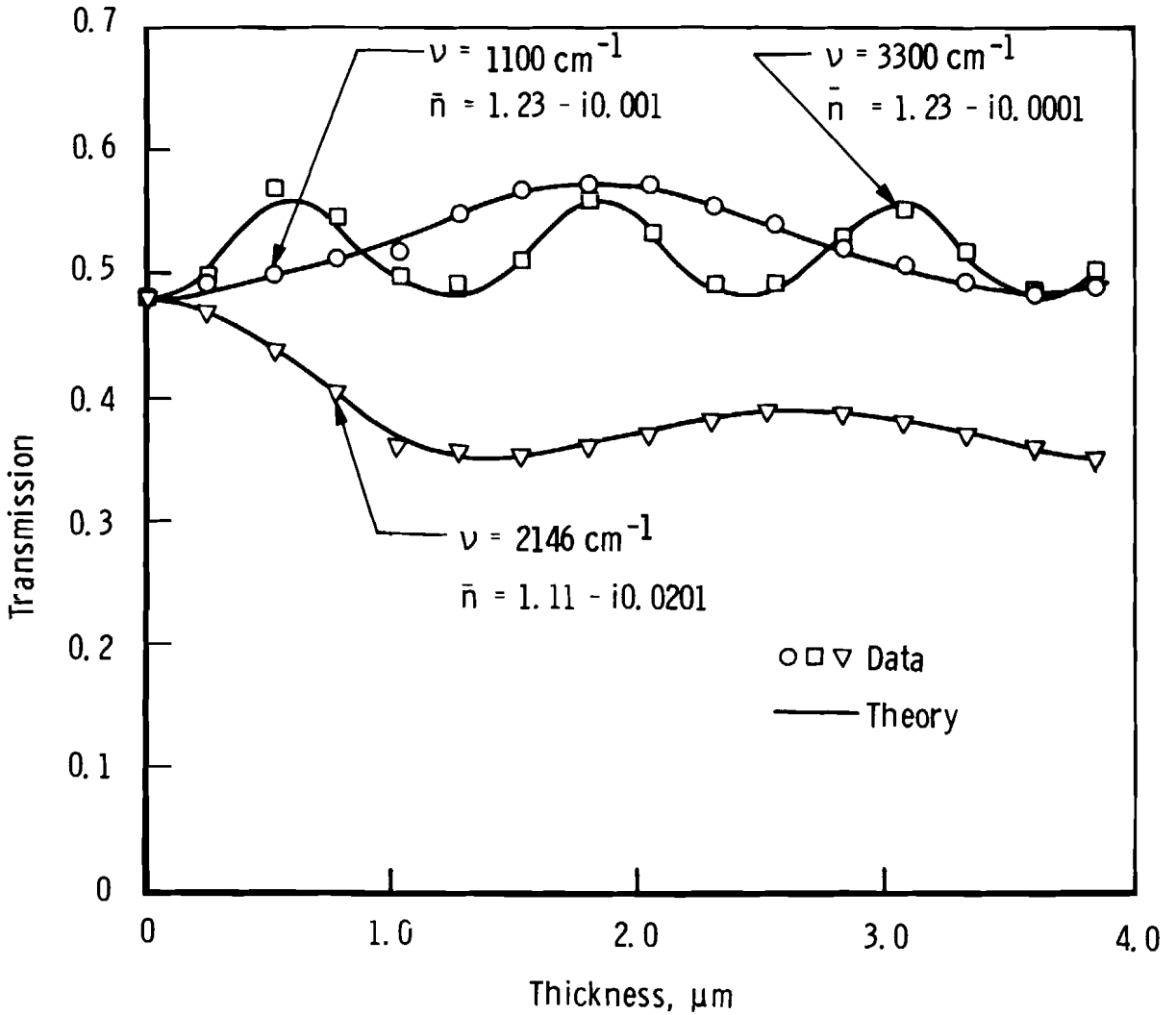

Figure 22. Comparison of theory and data for 20 K solid CO for three different wavenumbers.

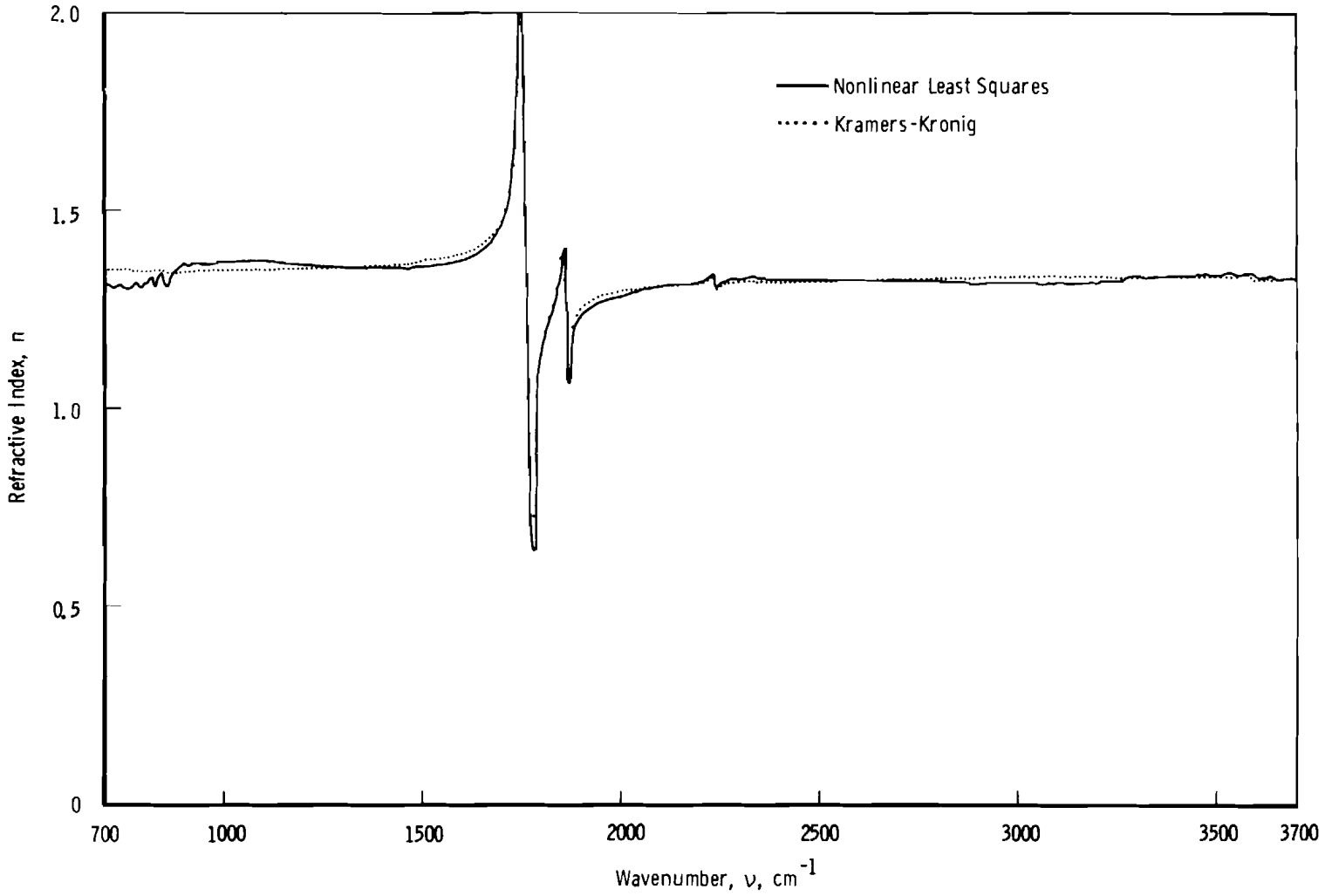

Figure 23. Optical properties of NO condensed on 20 K germanium.

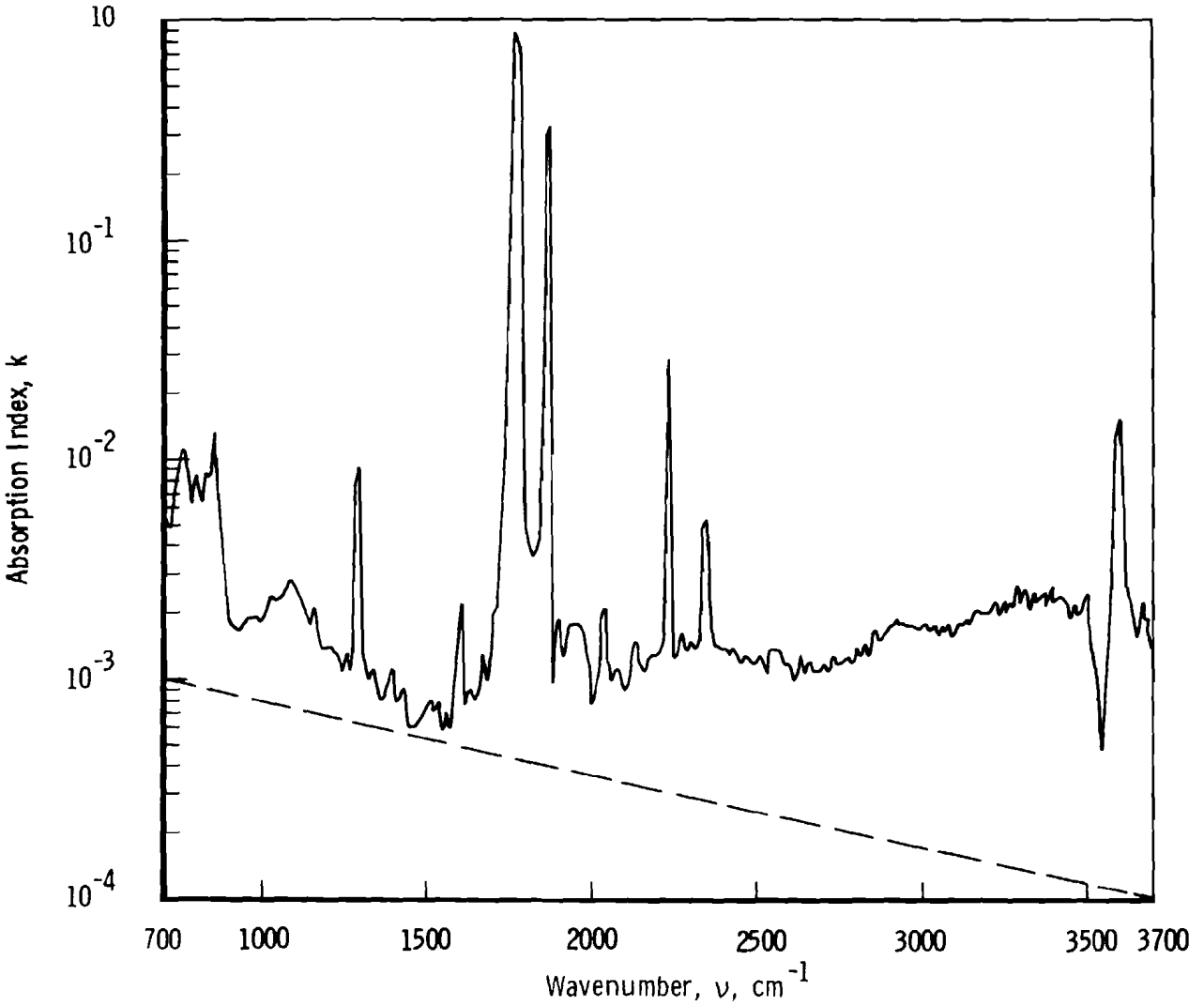

Figure 23. Concluded.

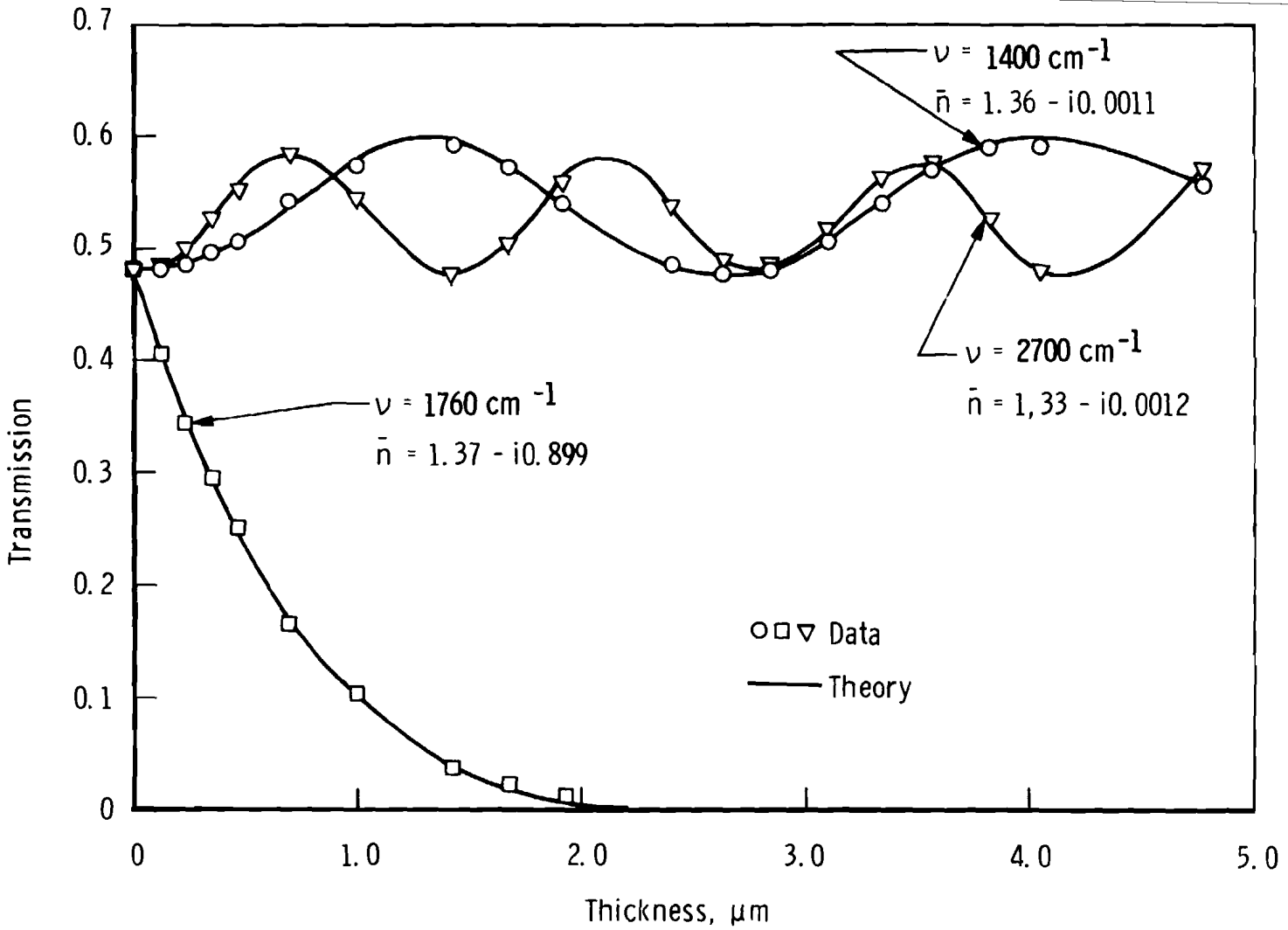

Figure 24. Comparison of theory and data for 20 K solid NO for three different wavenumbers.

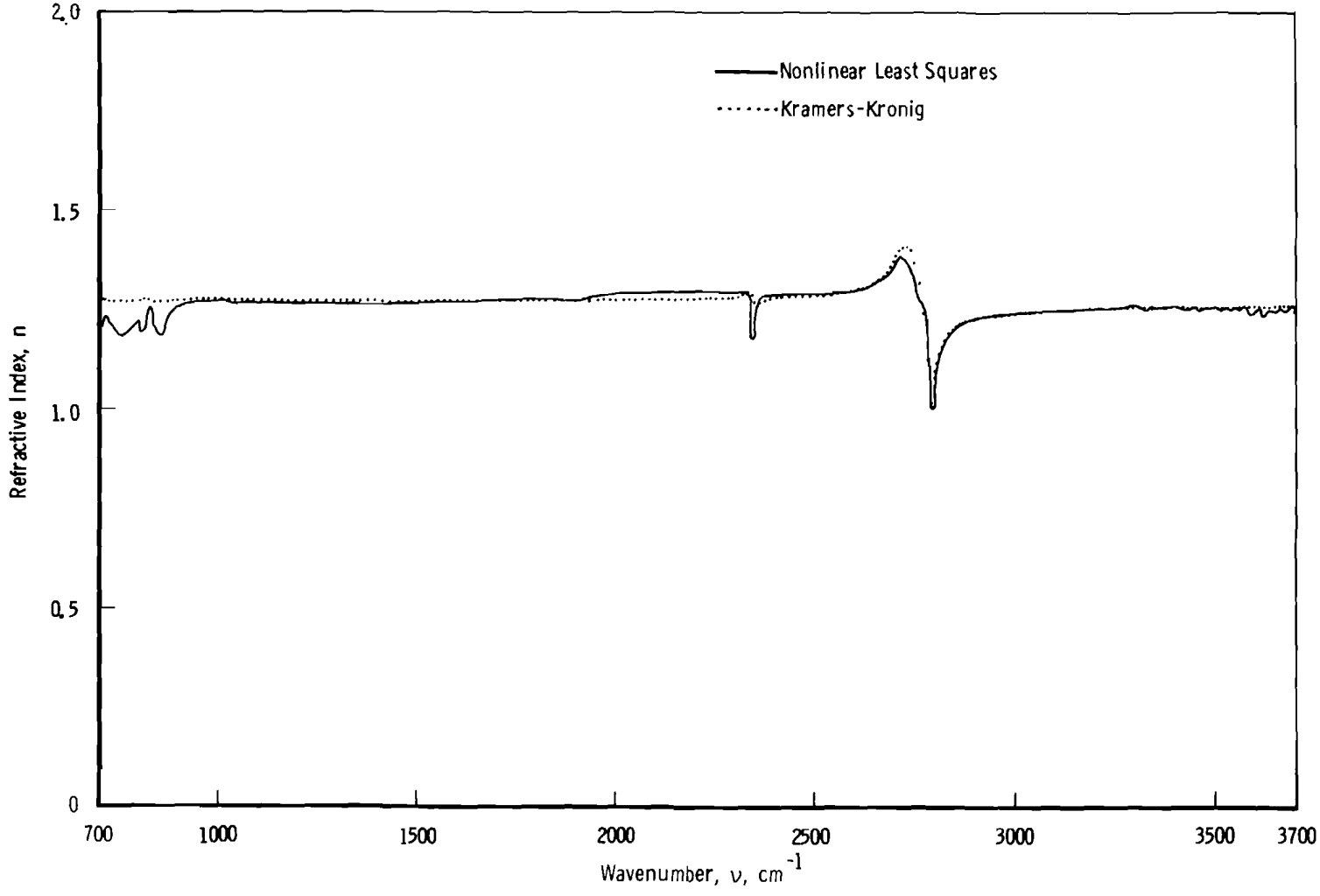

Figure 25. Optical properties of HCl condensed on 20 K germanium.

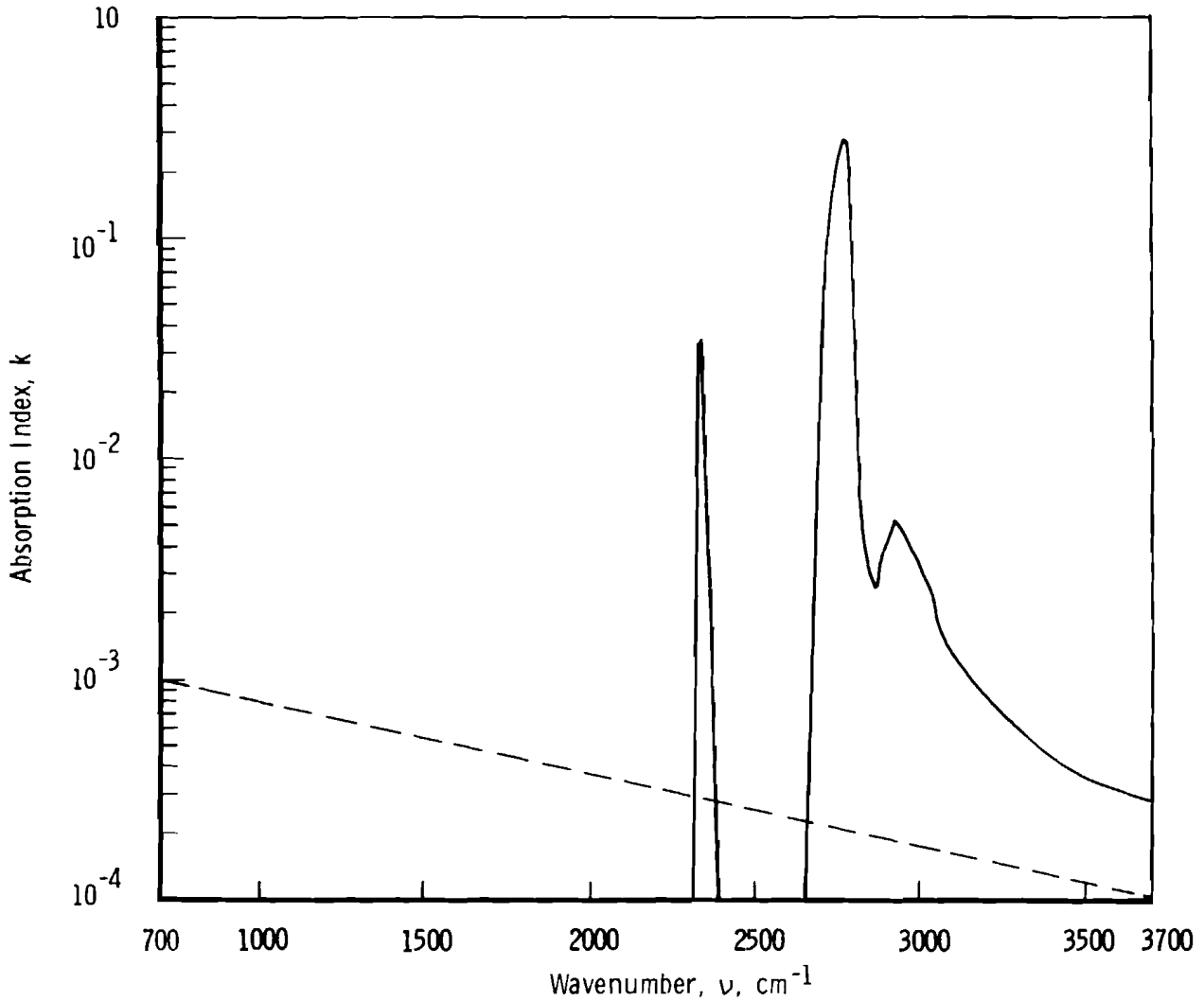

Figure 25. Concluded.

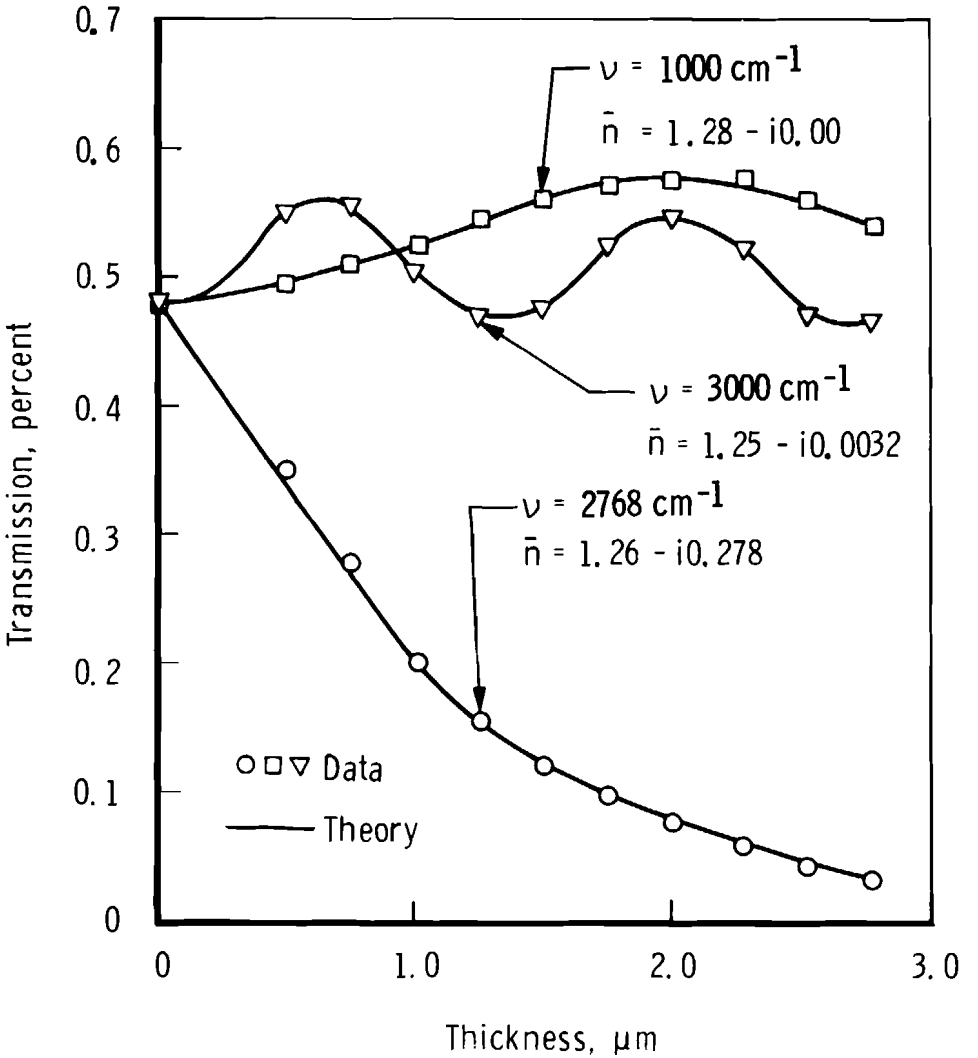

Figure 26. Comparison of theory and data for 20 K solid HCl for three different wavenumbers.

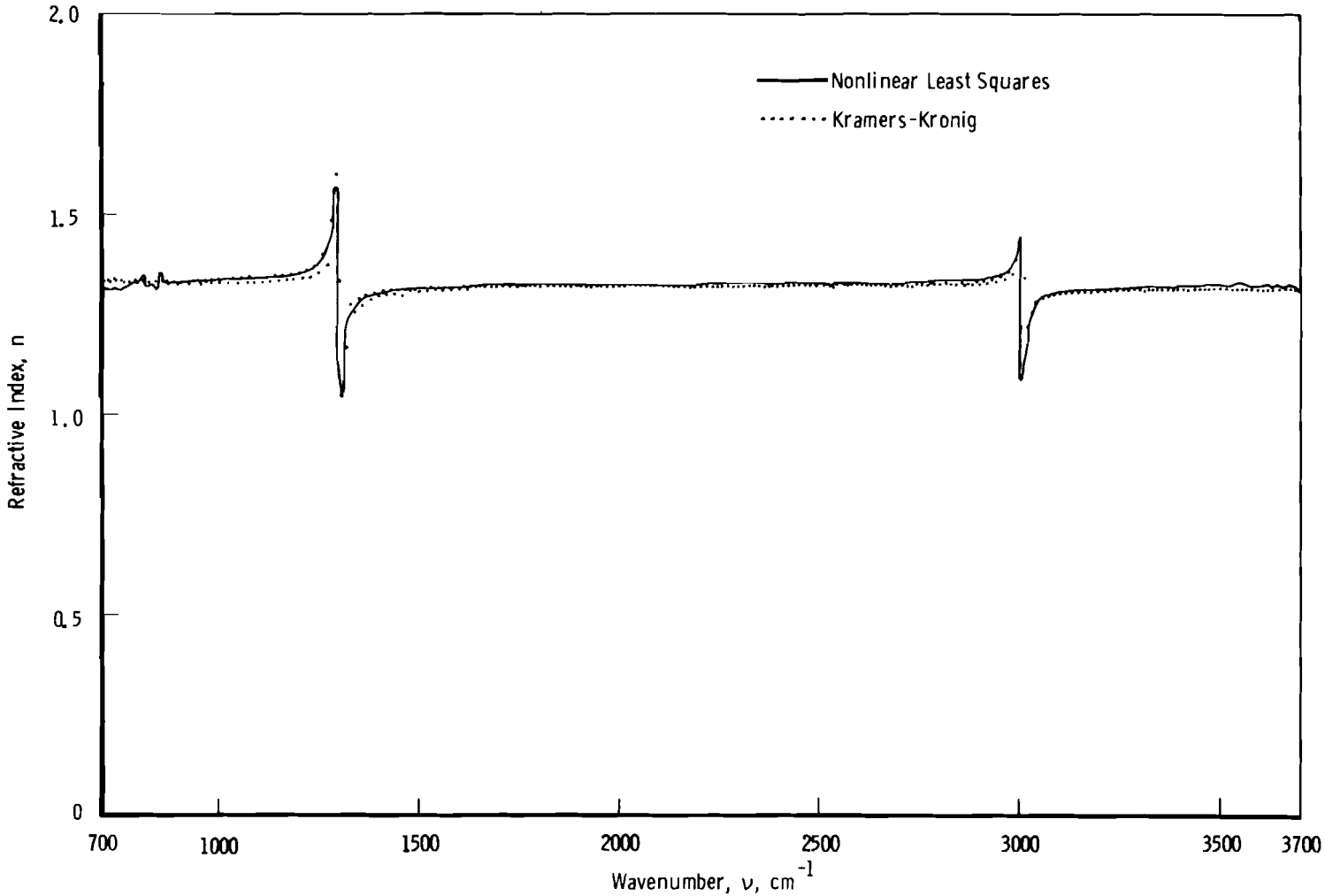

Figure 27. Optical properties of CH_4 condensed on 20 K germanium.

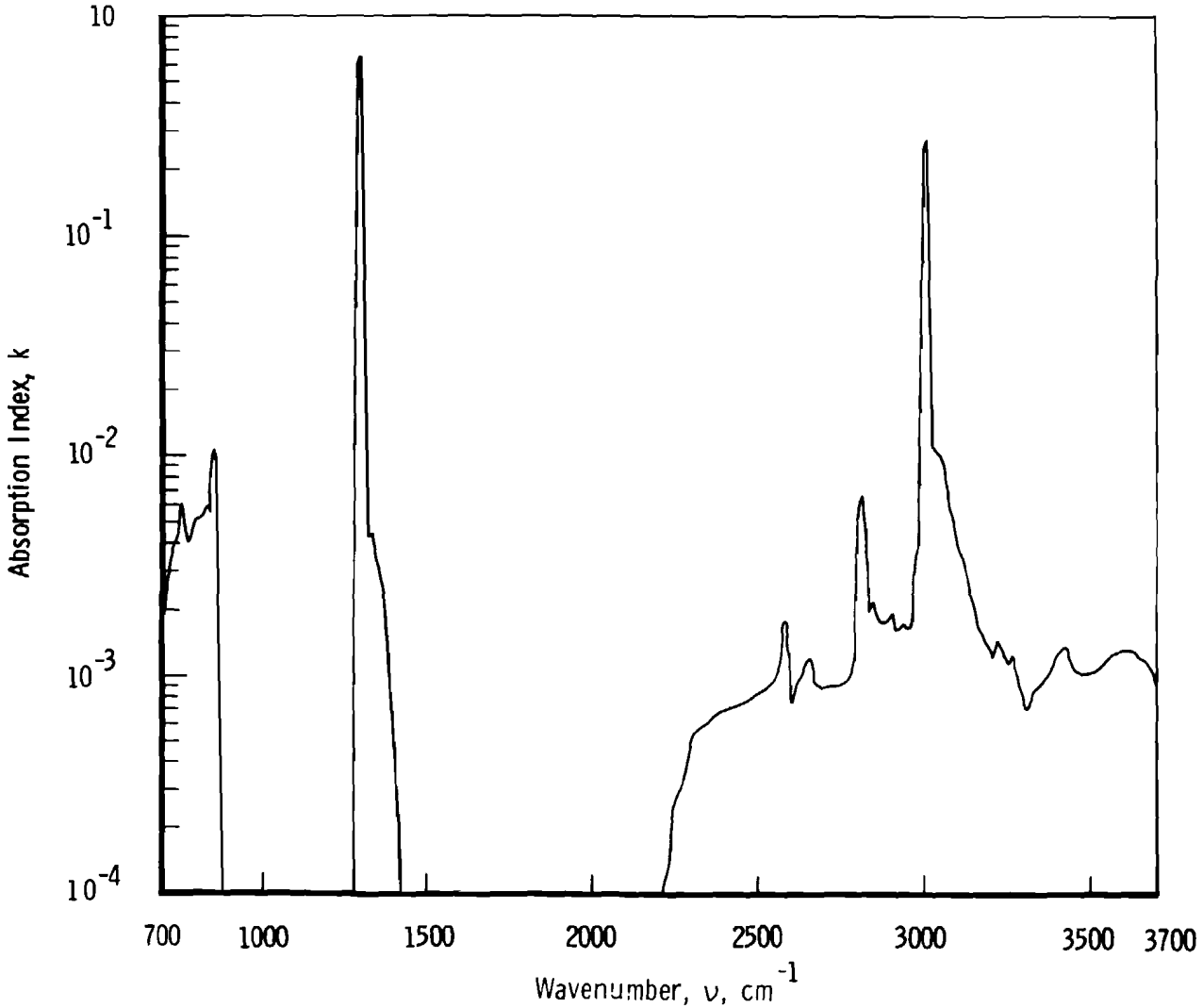

Figure 27. Concluded.

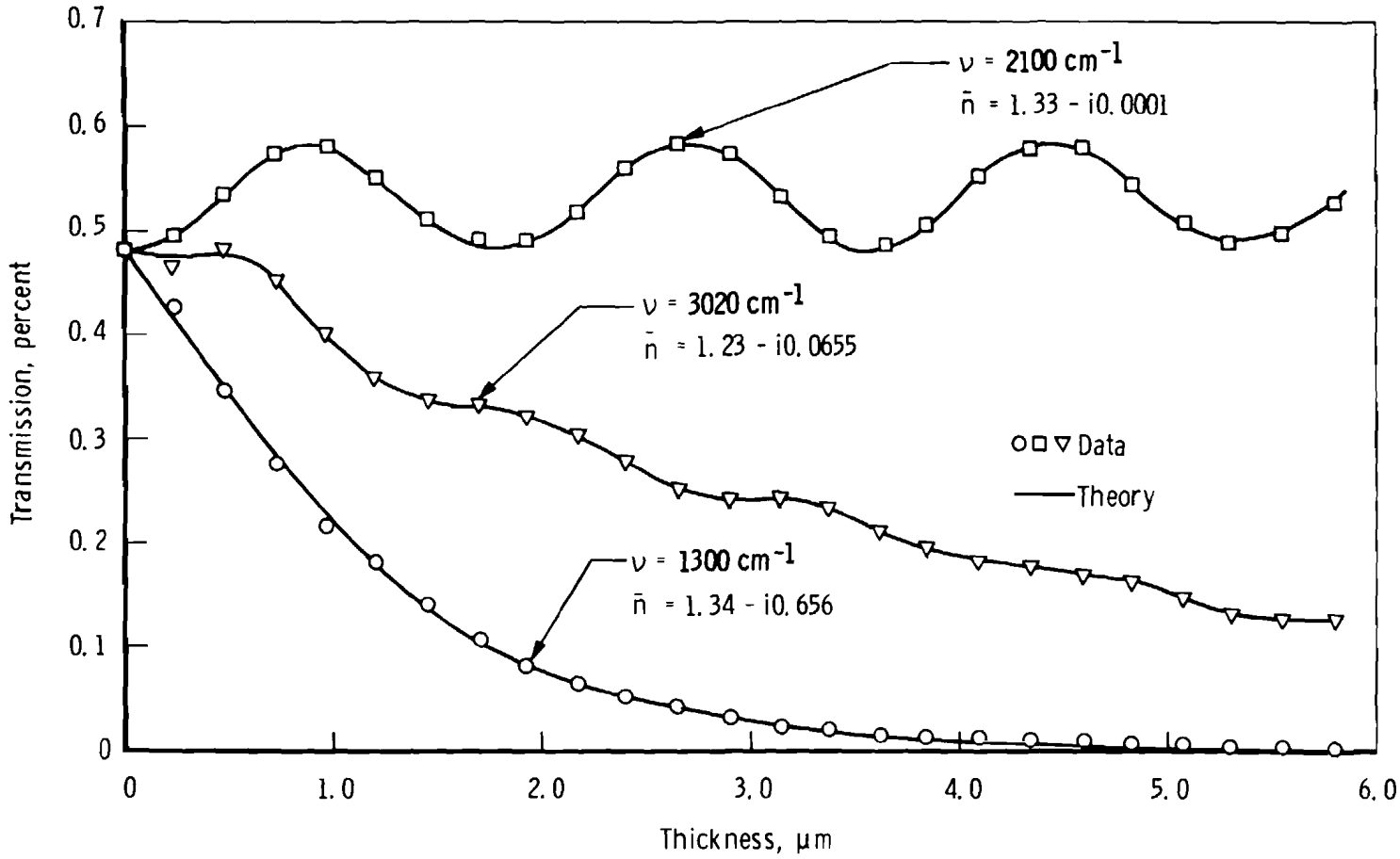

Figure 28. Comparison of theory and data for 20 K solid CH_4 for three different wavenumbers.

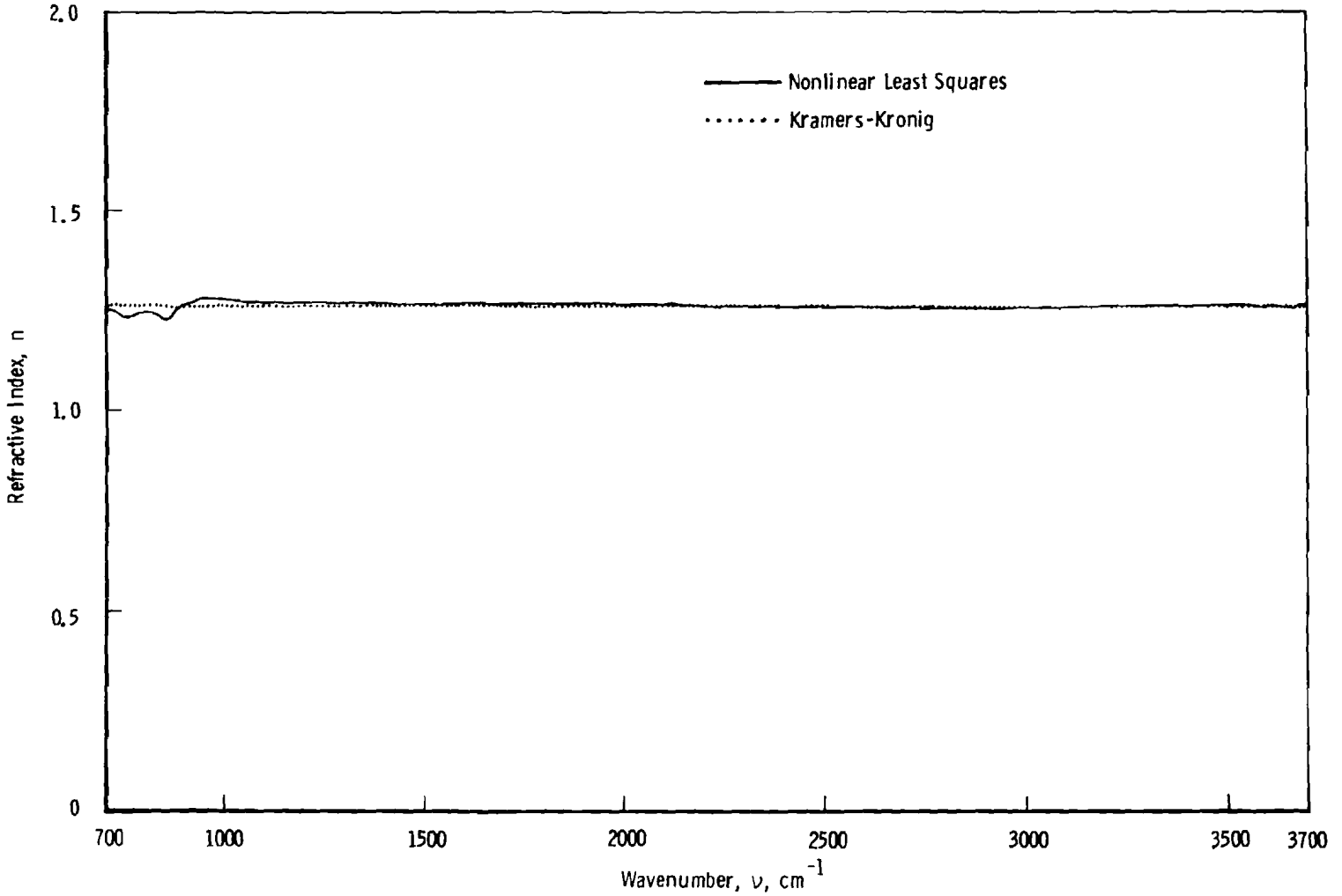

Figure 29. Optical properties of O_2 condensed on 20 K germanium.

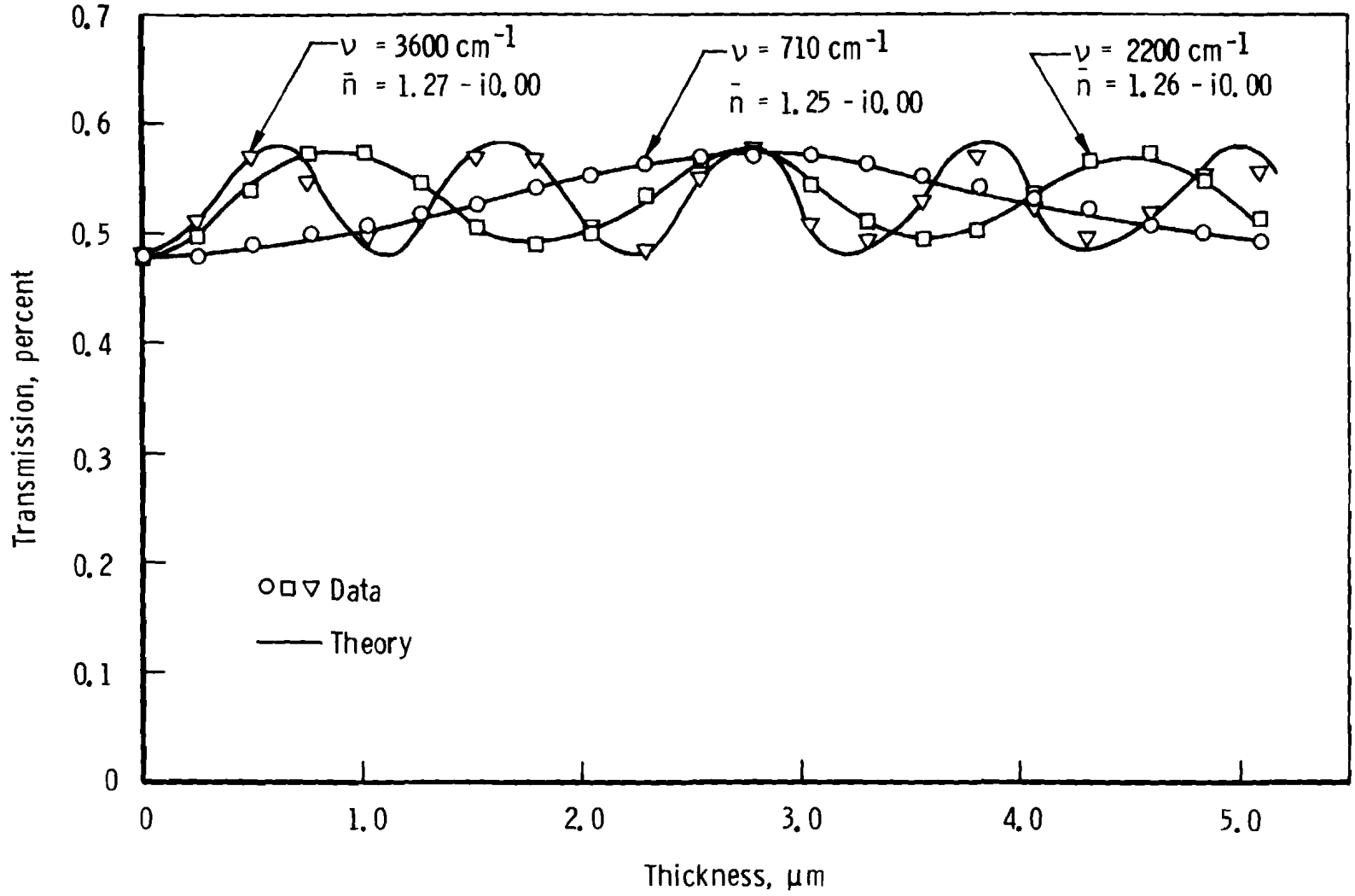

Figure 30. Comparison of theory and data for 20 K solid O_2 for three different wavenumbers.

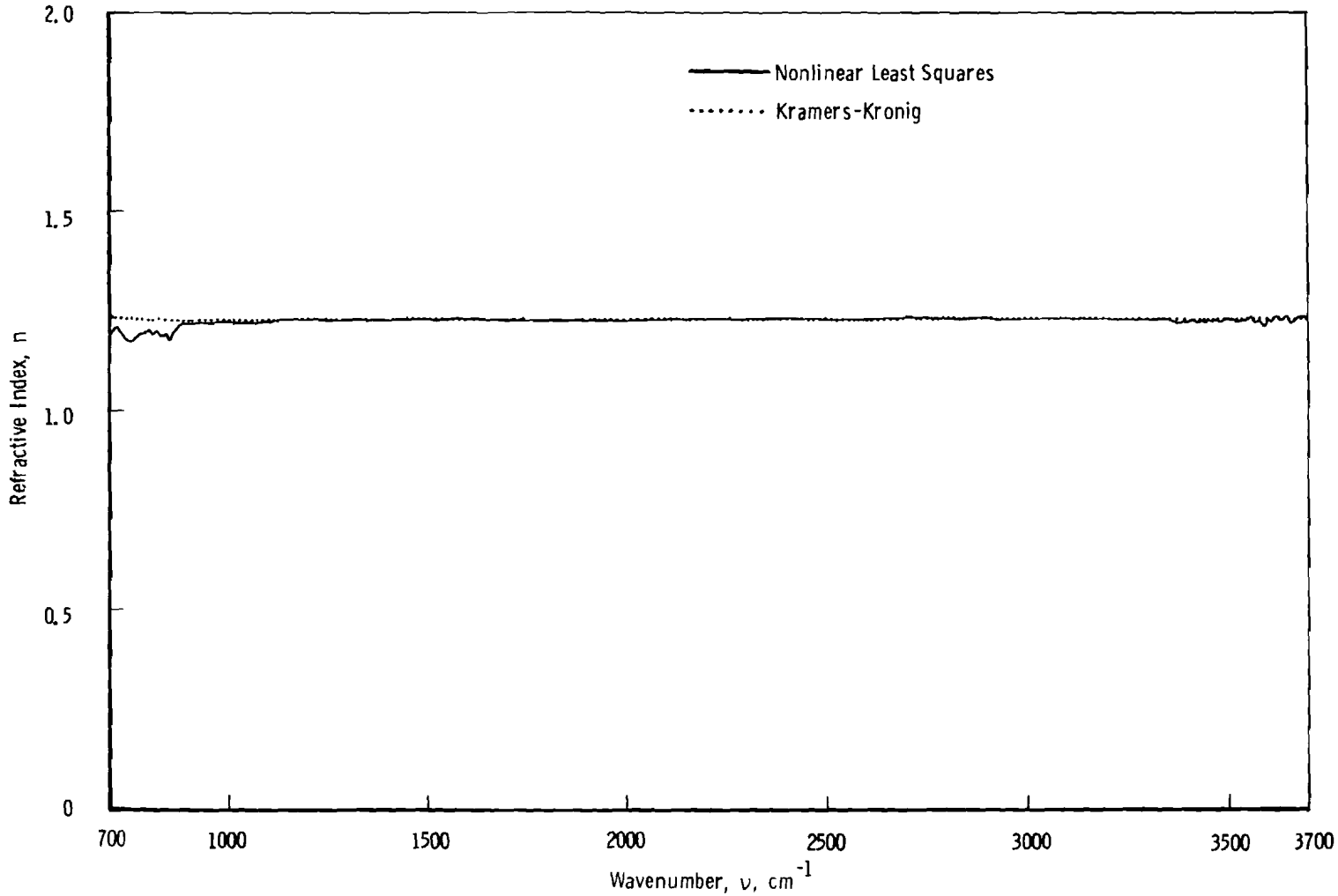

Figure 31. Optical properties of N_2 condensed on 20 K germanium.

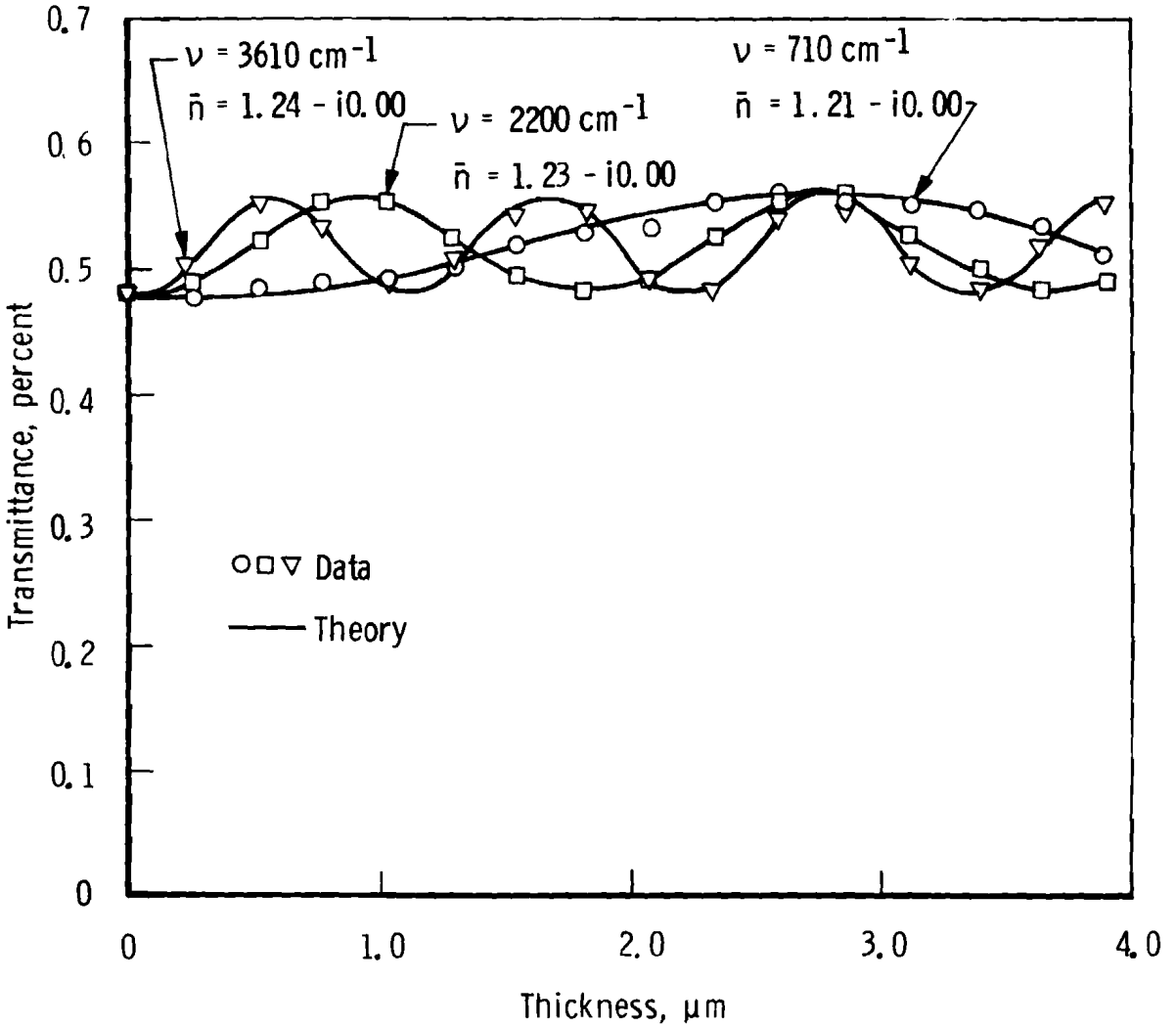

Figure 32. Comparison of theory and data for 20 K solid N_2 for three different wavenumbers.

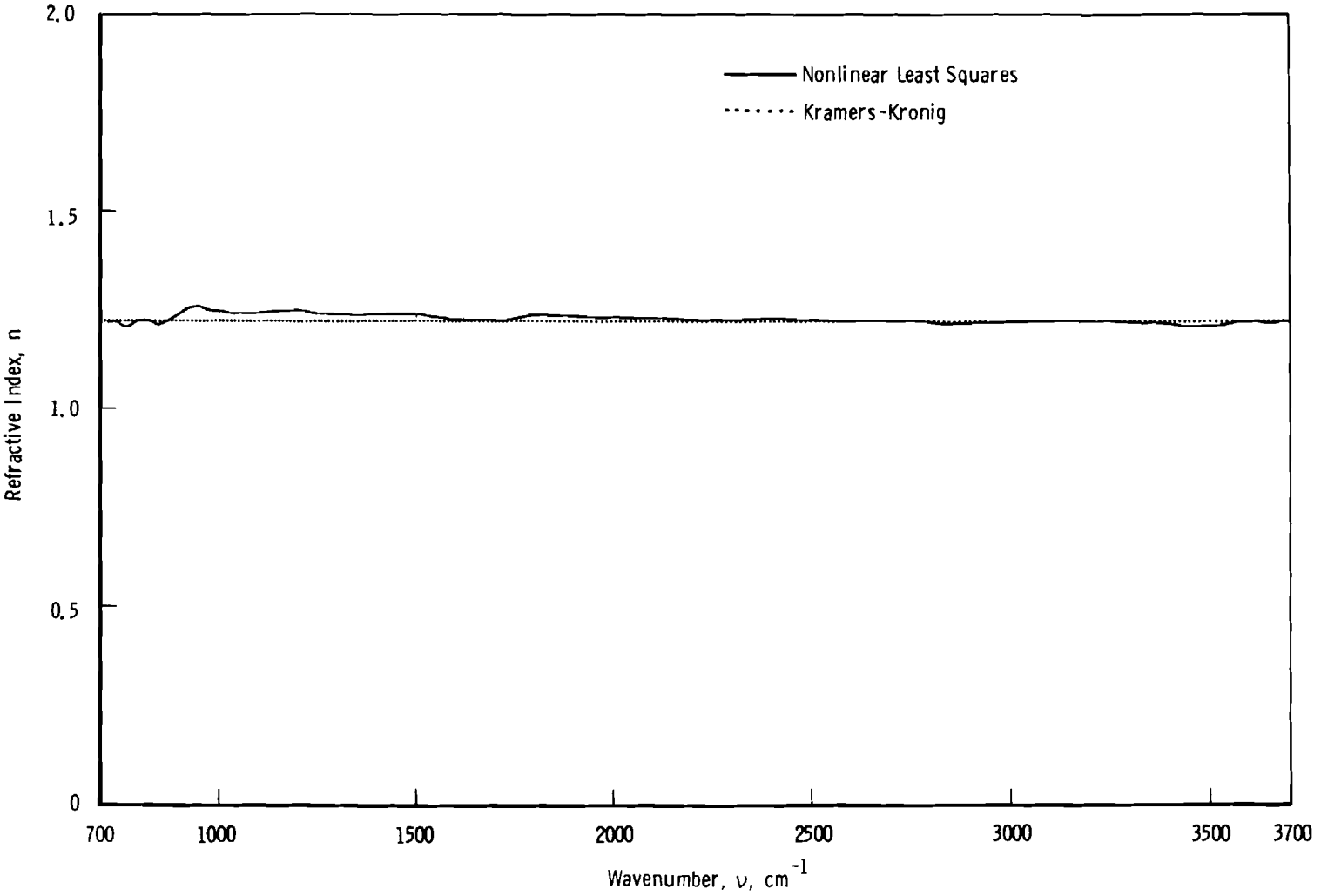

Figure 33. Optical properties of argon condensed on 20 K germanium.

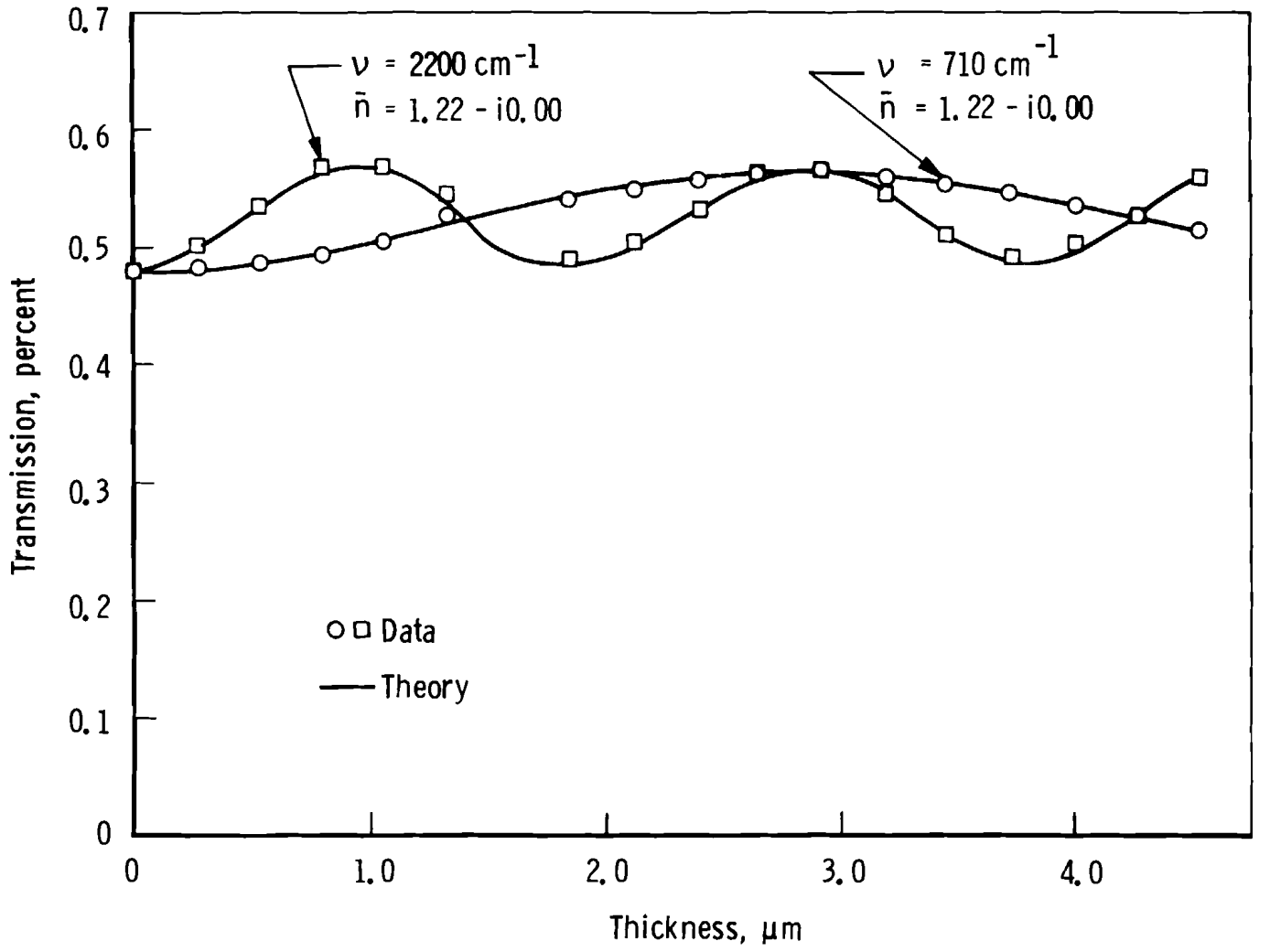

Figure 34. Comparison of theory and data for 20 K solid argon for three different wavenumbers.

Table 1. Solid CO Optical Properties at 20 K

ν, cm^{-1}	n	k	ν, cm^{-1}	n	k
3700		0.000500	3250	1.233432	0.000100
3690	1.233829	0.000100	3240	1.233433	0.000100
3680	1.233496	0.000200	3230	1.233415	0.000100
3670	1.233660	0.000500	3220	1.233415	0.000100
3660	1.233541	0.000100	3210	1.233398	0.000100
3650	1.233542	0.000300	3200	1.233397	0.000100
3640	1.232940	0.000100	3190	1.233380	0.000100
3630	1.232464	0.000600	3180	1.233379	0.000100
3620	1.233861	0.003300	3170	1.233363	0.000100
3610	1.235169	0.000300	3160	1.233361	0.000100
3600	1.234471	0.000100	3150	1.233345	0.000100
3590	1.233952	0.000200	3140	1.233342	0.000100
3580	1.234108	0.000300	3130	1.233327	0.000100
3570	1.233986	0.000100	3120	1.233323	0.000100
3560	1.233963	0.000100	3110	1.233308	0.000100
3550	1.233824	0.000100	3100	1.233304	0.000100
3540	1.233848	0.000100	3090	1.233290	0.000100
3530	1.233760	0.000100	3080	1.233285	0.000100
3520	1.233778	0.000100	3070	1.233270	0.000100
3510	1.233713	0.000100	3060	1.233265	0.000100
3500	1.233725	0.000100	3050	1.233250	0.000100
3490	1.233675	0.000100	3040	1.233244	0.000100
3480	1.233674	0.000100	3030	1.233230	0.000100
3470	1.233610	0.000100	3020	1.233223	0.000100
3460	1.233663	0.000200	3010	1.233209	0.000100
3450	1.233666	0.000100	3000	1.233202	0.000100
3440	1.233657	0.000100	2990	1.233187	0.000100
3430	1.233607	0.000100	2980	1.233179	0.000100
3420	1.233620	0.000100	2970	1.233164	0.000100
3410	1.233583	0.000100	2960	1.233156	0.000100
3400	1.233593	0.000100	2950	1.233141	0.000100
3390	1.233561	0.000100	2940	1.233132	0.000100
3380	1.233569	0.000100	2930	1.233116	0.000100
3370	1.233541	0.000100	2920	1.233106	0.000100
3360	1.233547	0.000100	2910	1.233091	0.000100
3350	1.233521	0.000100	2900	1.233080	0.000100
3340	1.233526	0.000100	2890	1.233064	0.000100
3330	1.233503	0.000100	2880	1.233053	0.000100
3320	1.233507	0.000100	2870	1.233036	0.000100
3310	1.233485	0.000100	2860	1.233024	0.000100
3300	1.233488	0.000100	2850	1.233007	0.000100
3290	1.233467	0.000100	2840	1.232994	0.000100
3280	1.233469	0.000100	2830	1.232976	0.000100
3270	1.233450	0.000100	2820	1.232962	0.000100
3260	1.233451	0.000100	2810	1.232944	0.000100

Table 1. Continued.

ν, cm^{-1}	n	k	ν, cm^{-1}	n	k
2800	1.232928	0.000100	2330	1.230039	0.000100
2790	1.232909	0.000100	2320	1.229829	0.000100
2780	1.232893	0.000100	2310	1.229505	0.000100
2770	1.232873	0.000100	2300	1.229223	0.000100
2760	1.232855	0.000100	2290	1.228787	0.000100
2750	1.232834	0.000100	2280	1.228380	0.000100
2740	1.232815	0.000100	2270	1.227743	0.000100
2730	1.232793	0.000100	2260	1.227074	0.000100
2720	1.232773	0.000100	2250	1.225964	0.000100
2710	1.232750	0.000100	2240	1.224359	0.000100
2700	1.232728	0.000100	2238	1.223657	0.000100
2690	1.232703	0.000100	2234	1.222032	0.000503
2680	1.232679	0.000100	2232	1.220977	0.001261
2670	1.232652	0.000100	2230	1.220327	0.002508
2660	1.232627	0.000100	2228	1.220033	0.003973
2650	1.232598	0.000100	2226	1.220474	0.005291
2640	1.232570	0.000100	2224	1.220953	0.006138
2630	1.232540	0.000100	2222	1.221629	0.006722
2620	1.232509	0.000100	2220	1.221935	0.007097
2610	1.232476	0.000100	2218	1.222278	0.007456
2600	1.232443	0.000100	2216	1.222383	0.008121
2590	1.232407	0.000100	2214	1.223047	0.008877
2580	1.232371	0.000100	2212	1.223809	0.009442
2570	1.232332	0.000100	2210	1.224907	0.009493
2560	1.232291	0.000100	2208	1.225565	0.009289
2550	1.232249	0.000100	2206	1.226231	0.008900
2540	1.232204	0.000100	2204	1.226352	0.008538
2530	1.232157	0.000100	2202	1.226664	0.008394
2520	1.232108	0.000100	2200	1.226828	0.008384
2500	1.232000	0.000100	2198	1.227543	0.008242
2480	1.231879	0.000100	2196	1.227972	0.007667
2470	1.231810	0.000100	2194	1.228325	0.006659
2460	1.231743	0.000100	2192	1.227863	0.005841
2450	1.231661	0.000100	2190	1.227594	0.005351
2440	1.231587	0.000100	2188	1.227041	0.004989
2430	1.231491	0.000100	2186	1.226893	0.004599
2420	1.231408	0.000100	2184	1.226352	0.004170
2410	1.231295	0.000100	2182	1.226166	0.003679
2400	1.231199	0.000100	2180	1.225393	0.002974
2390	1.231064	0.000100	2178	1.224795	0.002355
2380	1.230952	0.000100	2176	1.223592	0.001772
2370	1.230789	0.000100	2174	1.222660	0.001199
2360	1.230655	0.000100	2172	1.221038	0.000685
2350	1.230455	0.000100	2170	1.219549	0.000199
2340	1.230290	0.000100	2168	1.217419	0.000100

Table 1. Continued.

ν, cm^{-1}	n	k	ν, cm^{-1}	n	k
2160	1.208019	0.000100	1890	1.236519	0.000100
2156	1.199784	0.000100	1880	1.236314	0.000100
2154	1.193860	0.000100	1870	1.236322	0.000100
2152	1.185704	0.000100	1860	1.236135	0.000100
2150	1.172238	0.000748	1850	1.236151	0.000100
2148	1.151502	0.003339	1840	1.235979	0.000100
2146	1.111849	0.020103	1830	1.236001	0.000100
2144	1.035327	0.060232	1820	1.235841	0.000100
2142	1.102075	0.297940	1810	1.235868	0.000100
2140	1.329037	0.340710	1800	1.235719	0.000100
2138	1.431818	0.085606	1790	1.235749	0.000100
2136	1.370664	0.037510	1780	1.235609	0.000100
2134	1.327975	0.007499	1770	1.235642	0.000100
2132	1.306179	0.001176	1760	1.235509	0.000100
2130	1.287710	0.000100	1750	1.235545	0.000100
2120	1.261650	0.000100	1740	1.235419	0.000100
2110	1.251298	0.000100	1730	1.235457	0.000100
2100	1.245991	0.000100	1720	1.235336	0.000100
2098	1.243159	0.000100	1710	1.235376	0.000100
2096	1.240309	0.001783	1700	1.235260	0.000100
2094	1.240693	0.009371	1690	1.235301	0.000100
2092	1.247696	0.011930	1680	1.235189	0.000100
2090	1.251809	0.006004	1670	1.235231	0.000100
2088	1.251249	0.001622	1660	1.235123	0.000100
2086	1.248363	0.000100	1650	1.235166	0.000100
2084	1.247099	0.000100	1640	1.235061	0.000100
2080	1.245164	0.000100	1630	1.235104	0.000100
2070	1.243425	0.000100	1620	1.235003	0.000100
2060	1.241853	0.000100	1610	1.235054	0.000100
2050	1.241169	0.000100	1600	1.234949	0.000100
2040	1.240214	0.000100	1590	1.234988	0.000100
2030	1.239833	0.000100	1580	1.234897	0.000100
2020	1.239156	0.000100	1570	1.235032	0.000100
2010	1.238924	0.000100	1560	1.234847	0.000100
2000	1.238407	0.000100	1550	1.235075	0.000100
1990	1.238259	0.000100	1540	1.234799	0.000100
1980	1.237845	0.000100	1530	1.234884	0.000100
1970	1.237751	0.000100	1520	1.234753	0.000100
1960	1.237406	0.000100	1510	1.234741	0.000100
1950	1.237348	0.000100	1500	1.234709	0.000100
1940	1.237054	0.000100	1490	1.234705	0.000100
1930	1.237021	0.000100	1480	1.234665	0.000100
1920	1.236764	0.000100	1470	1.234651	0.000100
1910	1.236749	0.000100	1460	1.234623	0.000100
1900	1.236521	0.000100	1450	1.234612	0.000100

Table 1. Concluded.

ν, cm^{-1}	n	k	ν, cm^{-1}	n	k
1440	1.234581	0.000100	990	1.233044	0.000100
1430	1.234560	0.000100	980	1.232939	0.000100
1420	1.234540	0.000100	970	1.232830	0.000100
1410	1.234519	0.000100	960	1.232695	0.000100
1400	1.234499	0.000100	950	1.232553	0.000100
1390	1.234478	0.000100	940	1.232370	0.000100
1380	1.234459	0.000100	930	1.232174	0.000100
1370	1.234438	0.000100	920	1.231902	0.000100
1360	1.234418	0.000100	910	1.231600	0.000100
1350	1.234396	0.000100	900	1.231134	0.000100
1340	1.234376	0.000100	890	1.230533	0.000100
1330	1.234357	0.000100	880	1.228926	0.000100
1320	1.234335	0.000100	870	1.226839	0.001800
1310	1.234316	0.000100	860	1.228108	0.007400
1300	1.234292	0.000100	850	1.231862	0.007500
1290	1.234269	0.000100	840	1.233956	0.005500
1280	1.234248	0.000100	830	1.233604	0.004200
1270	1.234224	0.000100	820	1.233226	0.004000
1260	1.234202	0.000100	810	1.233517	0.004900
1250	1.234179	0.000100	800	1.233619	0.003300
1240	1.234155	0.000100	790	1.232786	0.004000
1230	1.234130	0.000100	780	1.232254	0.004500
1220	1.234105	0.000100	770	1.232609	0.006300
1210	1.234079	0.000100	760	1.234465	0.007600
1200	1.234052	0.000100	750	1.236706	0.006700
1190	1.234024	0.000100	740	1.237398	0.004600
1180	1.233996	0.000100	730	1.236813	0.003500
1170	1.233966	0.000100	720	1.235972	0.003200
1160	1.233936	0.000100	710	1.235654	0.003700
1150	1.233904	0.000100	700		0.004000
1140	1.233871	0.000100			
1130	1.233836	0.000100			
1120	1.233800	0.000100			
1110	1.233762	0.000100			
1100	1.233722	0.000100			
1090	1.233679	0.000100			
1080	1.233634	0.000100			
1070	1.233587	0.000100			
1060	1.233535	0.000100			
1050	1.233482	0.000100			
1040	1.233422	0.000100			
1030	1.233360	0.000100			
1020	1.233290	0.000100			
1010	1.233217	0.000100			
1000	1.233132	0.000100			

Table 2. Solid NO Optical Properties at 20 K

ν, cm^{-1}	n	k	ν, cm^{-1}	n	k
3700		0.002500	3564	1.339223	0.001353
3690	1.332909	0.001100	3562	1.338439	0.001300
3680	1.332082	0.001900	3560	1.337999	0.001355
3670	1.331935	0.001900	3558	1.337705	0.001250
3660	1.332110	0.002300	3550	1.336493	0.000600
3650	1.331664	0.001600	3540	1.335139	0.000500
3640	1.329921	0.001722	3530	1.334254	0.000900
3638	1.330238	0.002547	3520	1.333714	0.000900
3636	1.330494	0.002729	3510	1.333200	0.001400
3634	1.330712	0.002403	3500	1.332879	0.001600
3632	1.330569	0.002573	3490	1.333054	0.002500
3630	1.330596	0.002410	3480	1.333342	0.002100
3628	1.330323	0.002322	3470	1.333205	0.002000
3626	1.330161	0.002522	3460	1.333078	0.002200
3624	1.330084	0.002590	3450	1.333175	0.002200
3622	1.329958	0.002475	3440	1.332949	0.001900
3620	1.329590	0.002455	3430	1.332773	0.002300
3618	1.329356	0.002702	3420	1.332834	0.002400
3616	1.329140	0.002694	3410	1.332930	0.002400
3614	1.328631	0.002515	3400	1.332773	0.002300
3612	1.327803	0.002789	3390	1.332898	0.002700
3610	1.327176	0.003495	3380	1.333073	0.002500
3608	1.326572	0.004049	3370	1.332981	0.002200
3606	1.325894	0.004956	3360	1.332851	0.002500
3604	1.325460	0.006411	3350	1.332948	0.002400
3602	1.325529	0.007892	3340	1.332867	0.002300
3600	1.325772	0.009227	3330	1.332919	0.002500
3598	1.326452	0.010952	3320	1.332727	0.002100
3596	1.327602	0.012285	3310	1.332696	0.002600
3594	1.329047	0.013277	3300	1.332831	0.002600
3592	1.330403	0.013926	3290	1.332893	0.002300
3590	1.332020	0.014685	3280	1.332902	0.002700
3588	1.333899	0.015116	3270	1.333053	0.002200
3586	1.336056	0.014956	3260	1.332915	0.002300
3584	1.338145	0.014403	3250	1.332833	0.002100
3582	1.339980	0.012925	3240	1.332813	0.002300
3580	1.341374	0.011528	3230	1.332705	0.002000
3578	1.342312	0.009423	3220	1.332644	0.002300
3576	1.342361	0.007368	3210	1.332786	0.002300
3574	1.341952	0.005996	3200	1.332809	0.002000
3572	1.341612	0.005037	3190	1.332641	0.002000
3570	1.341418	0.004033	3180	1.332563	0.002000
3568	1.341026	0.002908	3170	1.332476	0.002000
3566	1.340240	0.001819	3160	1.332481	0.002100

Table 2. Continued.

ν, cm^{-1}	n	k	ν, cm^{-1}	n	k
3150	1.332584	0.002100	2710	1.329236	0.001200
3140	1.332527	0.001800	2700	1.329112	0.001100
3130	1.332416	0.001900	2690	1.328945	0.001100
3120	1.332339	0.001800	2680	1.328744	0.001100
3110	1.332296	0.001800	2670	1.328629	0.001200
3100	1.332238	0.001800	2660	1.328545	0.001200
3090	1.332127	0.001600	2650	1.328382	0.001100
3080	1.331988	0.001800	2640	1.328190	0.001200
3070	1.331962	0.001700	2630	1.328163	0.001300
3060	1.331931	0.001800	2620	1.328074	0.001100
3050	1.331807	0.001600	2610	1.327781	0.001000
3040	1.331706	0.001800	2600	1.327552	0.001200
3030	1.331707	0.001800	2590	1.327445	0.001200
3020	1.331653	0.001700	2580	1.327233	0.001200
3010	1.331559	0.001800	2570	1.327136	0.001400
3000	1.331575	0.001800	2560	1.327156	0.001400
2990	1.331510	0.001700	2550	1.326978	0.001100
2980	1.331378	0.001700	2540	1.326671	0.001200
2970	1.331307	0.001800	2530	1.326513	0.001300
2960	1.331289	0.001800	2520	1.326358	0.001200
2950	1.331253	0.001800	2500	1.326000	0.001200
2940	1.331198	0.001800	2480	1.325486	0.001200
2930	1.331134	0.001800	2470	1.325284	0.001300
2920	1.331141	0.001900	2460	1.325107	0.001300
2910	1.331150	0.001800	2450	1.324846	0.001200
2900	1.331144	0.001800	2440	1.324522	0.001300
2890	1.331116	0.001700	2430	1.324343	0.001400
2880	1.331052	0.001600	2420	1.324060	0.001300
2870	1.330839	0.001500	2410	1.323806	0.001400
2860	1.330794	0.001700	2400	1.323467	0.001400
2850	1.330892	0.001700	2390	1.323235	0.001400
2840	1.330801	0.001300	2380	1.322701	0.001400
2830	1.330633	0.001500	2370	1.322370	0.001500
2820	1.330545	0.001300	2360	1.321434	0.001700
2810	1.330385	0.001300	2350	1.320825	0.002400
2800	1.330304	0.001400	2340	1.322460	0.005400
2790	1.330213	0.001200	2330	1.323512	0.001500
2780	1.330076	0.001300	2320	1.322225	0.001400
2770	1.329962	0.001200	2310	1.321166	0.001500
2760	1.329835	0.001200	2300	1.320768	0.001400
2750	1.329670	0.001200	2290	1.319851	0.001400
2740	1.329561	0.001200	2280	1.319206	0.001600
2730	1.329488	0.001300	2270	1.318376	0.001600
2720	1.329392	0.001100	2260	1.316792	0.001300

Table 2. Continued.

ν, cm^{-1}	n	k	ν, cm^{-1}	n	k
2250	1.311999	0.001300	1930	1.275524	0.001600
2248	1.311404	0.002355	1920	1.269404	0.001300
2246	1.309511	0.002866	1910	1.261443	0.001400
2244	1.307456	0.004190	1900	1.251075	0.001900
2242	1.304455	0.007468	1898	1.248659	0.002041
2240	1.303358	0.013122	1896	1.246112	0.002090
2238	1.304968	0.020421	1894	1.243260	0.001886
2236	1.311385	0.026868	1892	1.239920	0.001697
2234	1.320449	0.029013	1890	1.236127	0.001500
2232	1.329485	0.025860	1888	1.231809	0.001400
2230	1.334764	0.018817	1886	1.226907	0.001200
2228	1.335824	0.011557	1884	1.221036	0.001000
2226	1.333793	0.006380	1882	1.214068	0.000900
2224	1.331040	0.003567	1880	1.205431	0.001000
2222	1.328472	0.002453	1878	1.194804	0.001500
2220	1.326864	0.002173	1876	1.180902	0.002800
2210	1.322937	0.001300	1874	1.161792	0.005400
2200	1.320975	0.001300	1872	1.133454	0.013500
2190	1.319663	0.001300	1870	1.097507	0.037200
2180	1.318780	0.001300	1868	1.062098	0.087700
2170	1.317850	0.001200	1866	1.047285	0.168600
2160	1.316960	0.001100	1864	1.091311	0.280800
2150	1.315953	0.001200	1862	1.200341	0.347100
2140	1.315212	0.001400	1860	1.324528	0.333000
2130	1.314544	0.001500	1858	1.412364	0.263880
2120	1.313932	0.001300	1856	1.449249	0.175650
2110	1.312957	0.001000	1854	1.442743	0.100010
2100	1.311796	0.000900	1852	1.413993	0.050199
2090	1.310666	0.001100	1850	1.380711	0.025078
2080	1.309651	0.001100	1848	1.354176	0.015619
2070	1.308513	0.001100	1846	1.335188	0.011769
2060	1.307150	0.001000	1844	1.321785	0.009526
2050	1.305518	0.001200	1842	1.310613	0.007423
2040	1.304473	0.002100	1840	1.301011	0.005586
2030	1.303802	0.002000	1838	1.291794	0.004508
2020	1.302346	0.000900	1836	1.283823	0.003962
2010	1.300052	0.000800	1834	1.276096	0.003634
2000	1.297716	0.000800	1832	1.269312	0.003676
1990	1.295278	0.001100	1830	1.262559	0.003720
1980	1.292861	0.001500	1828	1.256456	0.003766
1970	1.290383	0.001800	1826	1.250024	0.003843
1960	1.287573	0.001800	1824	1.244092	0.003912
1950	1.284194	0.001800	1822	1.237554	0.003826
1940	1.280288	0.001800	1820	1.231225	0.003867

Table 2. Continued.

ν, cm^{-1}	n	k	ν, cm^{-1}	n	k
1818	1.224206	0.004031	1730	1.616826	0.009801
1816	1.217541	0.004273	1728	1.598379	0.008226
1814	1.210044	0.004358	1726	1.582771	0.006829
1812	1.202616	0.004424	1724	1.568510	0.005540
1810	1.193974	0.004415	1722	1.556221	0.004753
1808	1.185237	0.004539	1720	1.544935	0.004037
1806	1.175101	0.004694	1718	1.535180	0.003447
1804	1.164591	0.004743	1716	1.525955	0.002928
1802	1.152181	0.005110	1714	1.517812	0.002435
1800	1.139271	0.005519	1712	1.509992	0.002272
1798	1.123666	0.005745	1710	1.503209	0.002141
1796	1.106643	0.006405	1708	1.496741	0.002199
1794	1.085834	0.007280	1706	1.491242	0.002221
1792	1.062159	0.008320	1704	1.485814	0.002060
1790	1.031390	0.010236	1702	1.481101	0.002053
1788	0.993344	0.014407	1700	1.476390	0.001989
1786	0.941710	0.025246	1690	1.457532	0.001100
1784	0.879458	0.051134	1680	1.442854	0.001000
1782	0.800603	0.100290	1670	1.431898	0.001300
1780	0.727419	0.197000	1660	1.423040	0.000900
1778	0.709327	0.356000	1650	1.415620	0.000800
1776	0.743904	0.467040	1640	1.409339	0.000900
1774	0.792981	0.570210	1630	1.404176	0.000900
1772	0.857765	0.665800	1620	1.399250	0.000800
1770	0.939898	0.742400	1610	1.395521	0.001800
1768	1.030268	0.804940	1600	1.392920	0.002200
1766	1.132500	0.856500	1590	1.390556	0.001200
1764	1.239722	0.883180	1580	1.387561	0.000700
1762	1.352432	0.902560	1570	1.384882	0.000600
1760	1.471070	0.899700	1560	1.382488	0.000700
1758	1.593234	0.875350	1550	1.380453	0.000600
1756	1.711891	0.826070	1540	1.378551	0.000800
1754	1.822158	0.748450	1530	1.376922	0.000700
1752	1.911700	0.644500	1520	1.375350	0.000800
1750	1.970389	0.518460	1510	1.374028	0.000800
1748	1.990810	0.387820	1500	1.372681	0.000700
1746	1.976163	0.265140	1490	1.371447	0.000700
1744	1.929781	0.159680	1480	1.370263	0.000700
1742	1.865616	0.088225	1470	1.369148	0.000600
1740	1.799687	0.046005	1460	1.368122	0.000800
1738	1.743252	0.025667	1450	1.367169	0.000600
1736	1.698506	0.017550	1440	1.366134	0.000700
1734	1.665024	0.013651	1430	1.365332	0.000900
1732	1.638205	0.011470	1420	1.364576	0.000800

Table 2. Concluded.

ν, cm^{-1}	n	k	ν, cm^{-1}	n	k
1410	1.363703	0.000800	970	1.350230	0.001900
1400	1.363004	0.001100	960	1.349928	0.001900
1390	1.362525	0.001100	950	1.349703	0.001900
1380	1.361934	0.000900	940	1.349336	0.001700
1370	1.361177	0.000800	930	1.348797	0.001600
1360	1.360394	0.000800	920	1.348173	0.001700
1350	1.359631	0.000900	910	1.347397	0.001700
1340	1.359021	0.001100	900	1.346803	0.002300
1330	1.358300	0.001000	890	1.345657	0.002100
1320	1.357335	0.001100	880	1.344027	0.003100
1310	1.355070	0.001200	870	1.342411	0.005700
1300	1.354493	0.005100	860	1.343291	0.009500
1290	1.358570	0.009000	850	1.347572	0.013300
1280	1.361501	0.003200	840	1.350498	0.008500
1270	1.359799	0.001100	830	1.350773	0.008700
1260	1.357940	0.001300	820	1.349960	0.006500
1250	1.357455	0.001300	810	1.349553	0.007400
1240	1.356712	0.001100	800	1.349769	0.008300
1230	1.356237	0.001300	790	1.349646	0.006400
1220	1.355709	0.001300	780	1.348520	0.008800
1210	1.355420	0.001400	770	1.349721	0.010200
1200	1.354975	0.001400	760	1.352011	0.011300
1190	1.354690	0.001400	750	1.354223	0.009700
1180	1.354124	0.001400	740	1.355155	0.008000
1170	1.353735	0.001600	730	1.354924	0.006000
1160	1.353542	0.002100	720	1.353752	0.004900
1150	1.353458	0.001800	710	1.352462	0.005100
1140	1.353035	0.002000	700		0.006400
1130	1.352838	0.002200			
1120	1.352749	0.002400			
1110	1.352634	0.002300			
1100	1.352339	0.002400			
1090	1.352263	0.002700			
1080	1.352386	0.002800			
1070	1.352398	0.002500			
1060	1.352169	0.002400			
1050	1.351987	0.002400			
1040	1.351774	0.002300			
1030	1.351615	0.002400			
1020	1.351603	0.002400			
1010	1.351513	0.002100			
1000	1.351102	0.001800			
990	1.350749	0.002000			
980	1.350508	0.001900			

Table 3. Solid HCl Optical Properties at 20 K

ν, cm^{-1}	n	k	ν, cm^{-1}	n	k
3700		0.000400	3250	1.259844	0.000900
3690	1.265753	0.000900	3240	1.259820	0.000600
3680	1.265962	0.000200	3230	1.259321	0.000300
3670	1.265671	0.000100	3220	1.258873	0.000500
3660	1.265437	0.000100	3210	1.258412	0.000400
3650	1.265320	0.000100	3200	1.258053	0.000700
3640	1.265186	0.000100	3190	1.257671	0.000700
3630	1.265044	0.000100	3180	1.257463	0.001000
3620	1.264858	0.000100	3170	1.257232	0.000900
3610	1.264852	0.000400	3160	1.256902	0.000800
3600	1.264753	0.000100	3150	1.256145	0.000600
3590	1.264795	0.000500	3140	1.255784	0.001300
3580	1.264751	0.000100	3130	1.255432	0.001100
3570	1.264598	0.000100	3120	1.255017	0.001200
3560	1.264397	0.000200	3110	1.254535	0.001500
3550	1.264391	0.000100	3100	1.254229	0.001300
3540	1.264144	0.000100	3090	1.253529	0.001400
3530	1.264017	0.000100	3080	1.252932	0.001400
3520	1.263873	0.000300	3070	1.252197	0.001700
3510	1.263930	0.000200	3060	1.251502	0.001700
3500	1.263664	0.000100	3050	1.250747	0.002300
3490	1.263396	0.000100	3040	1.250297	0.002500
3480	1.263446	0.000700	3030	1.249798	0.002800
3470	1.263542	0.000100	3020	1.249054	0.002500
3460	1.263104	0.000100	3010	1.248011	0.002900
3450	1.263038	0.000500	3000	1.247120	0.003200
3440	1.263036	0.000300	2990	1.246317	0.003700
3430	1.262829	0.000100	2980	1.245462	0.003800
3420	1.262555	0.000400	2970	1.244632	0.004300
3410	1.262324	0.000100	2960	1.243554	0.004100
3400	1.262246	0.000800	2950	1.242305	0.004500
3390	1.262265	0.000300	2940	1.241076	0.004800
3380	1.261909	0.000400	2930	1.239681	0.004700
3370	1.261785	0.000700	2920	1.238257	0.005200
3360	1.261843	0.000700	2910	1.236680	0.004600
3350	1.261670	0.000400	2900	1.234362	0.004000
3340	1.261567	0.000700	2898	1.233710	0.003828
3330	1.261290	0.000100	2896	1.233078	0.003631
3320	1.260507	0.000200	2894	1.232252	0.003574
3310	1.260280	0.001100	2892	1.231543	0.003617
3300	1.260654	0.001400	2890	1.230846	0.003725
3290	1.260566	0.000700	2888	1.230389	0.003812
3280	1.260579	0.001500	2886	1.229721	0.003501
3270	1.260567	0.000600	2884	1.228995	0.003452
3260	1.260105	0.000600			

Table 3. Continued.

ν, cm^{-1}	n	k	ν, cm^{-1}	n	k
2882	1.228205	0.003374	2794	1.056245	0.087846
2880	1.227443	0.003160	2792	1.044799	0.112090
2878	1.226473	0.003072	2790	1.037685	0.142480
2876	1.225575	0.002992	2788	1.039050	0.177750
2874	1.224605	0.002953	2786	1.051558	0.214960
2872	1.223642	0.002798	2784	1.074748	0.244800
2870	1.222428	0.002661	2782	1.102825	0.266640
2868	1.221300	0.002810	2780	1.131508	0.278790
2866	1.220169	0.002813	2778	1.158956	0.287640
2864	1.219073	0.002807	2776	1.185656	0.290180
2862	1.217772	0.002728	2774	1.208512	0.288460
2860	1.216512	0.002781	2772	1.227525	0.285330
2858	1.215056	0.002718	2770	1.246853	0.285680
2856	1.213632	0.002819	2768	1.264992	0.277950
2854	1.212129	0.002948	2766	1.278733	0.272200
2852	1.210648	0.002892	2764	1.291280	0.268460
2850	1.208861	0.002929	2762	1.305935	0.265590
2848	1.207084	0.003067	2760	1.320425	0.258810
2846	1.205175	0.003296	2758	1.333410	0.251690
2844	1.203430	0.003540	2756	1.345324	0.244360
2842	1.201460	0.003560	2754	1.357573	0.236680
2840	1.199136	0.003426	2752	1.368471	0.226260
2838	1.196674	0.003892	2750	1.377657	0.216060
2836	1.194302	0.004135	2748	1.384797	0.205210
2834	1.191521	0.004288	2746	1.391975	0.196290
2832	1.188595	0.004812	2744	1.398073	0.185090
2830	1.185636	0.005465	2742	1.402396	0.174090
2828	1.182518	0.005770	2740	1.405865	0.165590
2826	1.178844	0.006298	2738	1.409944	0.155700
2824	1.175097	0.007230	2736	1.412460	0.145730
2822	1.171004	0.007920	2734	1.414030	0.136320
2820	1.166505	0.008885	2732	1.415526	0.128500
2818	1.161337	0.010044	2730	1.417200	0.119410
2816	1.155898	0.011848	2728	1.417580	0.110500
2814	1.149790	0.013834	2726	1.417366	0.102430
2812	1.143459	0.016777	2724	1.417200	0.095194
2810	1.136724	0.020221	2722	1.416926	0.087237
2808	1.129878	0.024131	2720	1.416089	0.079971
2806	1.122378	0.028696	2718	1.414979	0.072628
2804	1.114355	0.033595	2716	1.413501	0.065631
2802	1.104929	0.039555	2714	1.411820	0.058861
2800	1.094457	0.047059	2712	1.409633	0.051878
2798	1.082527	0.056994	2710	1.406938	0.045487
2796	1.069764	0.070038	2708	1.403703	0.039247

Table 3. Continued.

ν, cm^{-1}	n	k	ν, cm^{-1}	n	k
2706	1.400164	0.033739	2618	1.311762	0.000100
2704	1.396330	0.028671	2616	1.310992	0.000100
2702	1.392390	0.024053	2614	1.310583	0.000100
2700	1.388313	0.020087	2612	1.309846	0.000100
2698	1.384155	0.016243	2610	1.309472	0.000100
2696	1.379756	0.013154	2608	1.308766	0.000100
2694	1.375578	0.010705	2606	1.308424	0.000100
2692	1.371483	0.008465	2604	1.307745	0.000100
2690	1.367596	0.006820	2602	1.307432	0.000100
2688	1.363967	0.005460	2600	1.306778	0.000100
2686	1.360534	0.004128	2590	1.304754	0.000100
2684	1.357077	0.003188	2580	1.302613	0.000100
2682	1.353942	0.002657	2570	1.301064	0.000100
2680	1.351196	0.002183	2560	1.299275	0.000100
2678	1.348639	0.001734	2550	1.298005	0.000100
2676	1.346265	0.001272	2540	1.296548	0.000300
2674	1.343975	0.000861	2530	1.295677	0.000200
2672	1.341703	0.000723	2520	1.294365	0.000200
2670	1.339849	0.000516	2510	1.293492	0.000100
2668	1.337800	0.000205	2500	1.292372	0.000400
2666	1.336030	0.000100	2490	1.291690	0.000100
2664	1.334108	0.000100	2480	1.290676	0.000500
2662	1.332665	0.000100	2470	1.290265	0.000300
2660	1.331011	0.000100	2460	1.289299	0.000200
2658	1.329765	0.000100	2450	1.288680	0.000100
2656	1.328277	0.000100	2440	1.287572	0.000100
2654	1.327179	0.000100	2430	1.287119	0.000300
2652	1.325823	0.000100	2420	1.286054	0.000100
2650	1.324845	0.000100	2410	1.285489	0.000200
2648	1.323597	0.000100	2400	1.284050	0.000100
2646	1.322722	0.000100	2390	1.283206	0.000300
2644	1.321565	0.000100	2380	1.281275	0.000500
2642	1.320776	0.000100	2370	1.278810	0.000500
2640	1.319699	0.000100	2360	1.269465	0.001800
2638	1.318945	0.000100	2350	1.272125	0.022300
2636	1.317976	0.000100	2340	1.294787	0.035200
2634	1.317328	0.000100	2330	1.305005	0.001000
2632	1.316379	0.000100	2320	1.294910	0.000100
2630	1.315790	0.000100	2310	1.289769	0.000100
2628	1.314894	0.000100	2300	1.289320	0.000100
2626	1.314357	0.000100	2290	1.287411	0.000100
2624	1.313507	0.000100	2280	1.287242	0.000200
2622	1.313017	0.000100	2270	1.286149	0.000100
2620	1.312210	0.000100	2260	1.285981	0.000100

Table 3. Continued.

ν, cm^{-1}	n	k	ν, cm^{-1}	n	k
2250	1.285169	0.000100	1810	1.278650	0.000100
2240	1.285047	0.000100	1800	1.278593	0.000100
2230	1.284424	0.000100	1790	1.278519	0.000100
2220	1.284312	0.000100	1780	1.278463	0.000100
2210	1.283807	0.000100	1770	1.278394	0.000100
2200	1.283697	0.000100	1760	1.278339	0.000100
2190	1.283274	0.000100	1750	1.278275	0.000100
2180	1.283162	0.000100	1740	1.278221	0.000100
2170	1.282800	0.000100	1730	1.278162	0.000100
2160	1.282670	0.000100	1720	1.278108	0.000100
2150	1.282306	0.000100	1700	1.278000	0.000100
2140	1.282287	0.000300	1680	1.277896	0.000100
2130	1.282065	0.000100	1670	1.277846	0.000100
2120	1.281861	0.000100	1660	1.277797	0.000100
2110	1.281624	0.000300	1650	1.277748	0.000100
2100	1.281697	0.000300	1640	1.277702	0.000100
2090	1.281507	0.000100	1630	1.277655	0.000100
2080	1.281328	0.000100	1620	1.277610	0.000100
2070	1.281076	0.000100	1610	1.277565	0.000100
2060	1.280994	0.000200	1600	1.277522	0.000100
2050	1.280792	0.000100	1590	1.277478	0.000100
2040	1.280743	0.000300	1580	1.277437	0.000100
2030	1.280544	0.000100	1570	1.277395	0.000100
2020	1.280549	0.000400	1560	1.277356	0.000100
2010	1.280487	0.000200	1550	1.277315	0.000100
2000	1.280398	0.000100	1540	1.277278	0.000100
1990	1.280187	0.000200	1530	1.277238	0.000100
1980	1.280146	0.000100	1520	1.277202	0.000100
1970	1.280001	0.000200	1510	1.277164	0.000100
1960	1.279968	0.000100	1500	1.277129	0.000100
1950	1.279806	0.000100	1490	1.277092	0.000100
1940	1.279726	0.000100	1480	1.277059	0.000100
1930	1.279600	0.000100	1470	1.277022	0.000100
1920	1.279532	0.000100	1460	1.276991	0.000100
1910	1.279416	0.000100	1450	1.276956	0.000100
1900	1.279352	0.000100	1440	1.276926	0.000100
1890	1.279245	0.000100	1430	1.276891	0.000100
1880	1.279183	0.000100	1420	1.276862	0.000100
1870	1.279084	0.000100	1410	1.276828	0.000100
1860	1.279024	0.000100	1400	1.276801	0.000100
1850	1.278932	0.000100	1390	1.276768	0.000100
1840	1.278873	0.000100	1380	1.276742	0.000100
1830	1.278787	0.000100	1370	1.276709	0.000100
1820	1.278729	0.000100	1360	1.276684	0.000100

Table 3. Concluded.

ν, cm^{-1}	n	k	ν, cm^{-1}	n	k
1350	1.276652	0.000100	910	1.275513	0.000100
1340	1.276629	0.000100	900	1.275576	0.000100
1330	1.276597	0.000100	890	1.275373	0.000100
1320	1.276575	0.000100	880	1.275468	0.000100
1310	1.276543	0.000100	870	1.275124	0.000100
1300	1.276523	0.000100	860	1.275280	0.000100
1290	1.276491	0.000100	850	1.274399	0.000100
1280	1.276472	0.000100	840	1.273199	0.000100
1270	1.276441	0.000100	830	1.275646	0.006000
1260	1.276423	0.000100	820	1.278005	0.000100
1250	1.276391	0.000100	810	1.276948	0.000100
1240	1.276375	0.000100	800	1.275863	0.000100
1230	1.276343	0.000100	790	1.276187	0.000100
1220	1.276328	0.000100	780	1.275596	0.000100
1210	1.276296	0.000100	770	1.275857	0.000100
1200	1.276283	0.000100	760	1.275295	0.000100
1190	1.276250	0.000100	750	1.275489	0.000100
1180	1.276238	0.000100	740	1.274280	0.000100
1170	1.276205	0.000100	730	1.273809	0.001100
1160	1.276195	0.000100	720	1.276317	0.005400
1150	1.276160	0.000100	710	1.278358	0.000100
1140	1.276152	0.000100	700		0.000100
1130	1.276116	0.000100			
1120	1.276110	0.000100			
1110	1.276073	0.000100			
1100	1.276068	0.000100			
1090	1.276029	0.000100			
1080	1.276027	0.000100			
1070	1.275986	0.000100			
1060	1.275986	0.000100			
1050	1.275941	0.000100			
1040	1.275945	0.000100			
1030	1.275896	0.000100			
1020	1.275903	0.000100			
1010	1.275849	0.000100			
1000	1.275860	0.000100			
990	1.275799	0.000100			
980	1.275815	0.000100			
970	1.275744	0.000100			
960	1.275767	0.000100			
950	1.275682	0.000100			
940	1.275714	0.000100			
930	1.275608	0.000100			
920	1.275653	0.000100			

Table 4. Solid CH_4 Optical Properties at 20 K

ν, cm^{-1}	n	k	ν, cm^{-1}	n	k
3700		0.000700	3250	1.321456	0.001200
3690	1.325826	0.000100	3240	1.323505	0.001300
3680	1.326640	0.001000	3230	1.320867	0.001300
3670	1.325596	0.000700	3220	1.323092	0.001400
3660	1.326823	0.001200	3210	1.320152	0.001200
3650	1.325582	0.000800	3200	1.322226	0.001200
3640	1.326634	0.001200	3190	1.318920	0.001500
3630	1.325632	0.001500	3180	1.321340	0.001500
3620	1.327079	0.001300	3170	1.317678	0.001700
3610	1.325883	0.001200	3160	1.320181	0.001800
3600	1.327305	0.001300	3150	1.316113	0.002200
3590	1.325685	0.000400	3140	1.318826	0.002200
3580	1.326596	0.001200	3130	1.314073	0.002800
3570	1.325595	0.001400	3120	1.317099	0.003000
3560	1.326885	0.000800	3110	1.311470	0.003600
3550	1.325161	0.001100	3100	1.314802	0.004100
3540	1.326639	0.001600	3090	1.307709	0.004800
3530	1.325618	0.001400	3080	1.311389	0.005900
3520	1.327052	0.001200	3070	1.301817	0.007200
3510	1.325297	0.000800	3060	1.307225	0.009700
3500	1.326598	0.001400	3050	1.293432	0.010100
3490	1.325460	0.001400	3040	1.295719	0.010300
3480	1.326885	0.000800	3030	1.248243	0.016100
3470	1.325087	0.001000	3020	1.225148	0.065500
3460	1.326393	0.000900	3010	1.352787	0.268400
3450	1.324898	0.001300	3000	1.455705	0.018800
3440	1.326404	0.001000	2990	1.402273	0.003900
3430	1.325009	0.001300	2980	1.360557	0.003500
3420	1.326405	0.000700	2970	1.364828	0.002100
3410	1.324410	0.000700	2960	1.349217	0.001600
3400	1.325852	0.001300	2950	1.352604	0.001700
3390	1.324467	0.001100	2940	1.343653	0.001700
3380	1.326054	0.001000	2930	1.346683	0.001600
3370	1.324110	0.000700	2920	1.340410	0.001600
3360	1.325481	0.000900	2910	1.343084	0.001900
3350	1.323702	0.001100	2900	1.338557	0.001700
3340	1.325303	0.000900	2890	1.340763	0.001700
3330	1.323293	0.001100	2880	1.337007	0.001700
3320	1.325261	0.001400	2870	1.338843	0.001700
3310	1.323226	0.000700	2860	1.335690	0.001900
3300	1.324759	0.001000	2850	1.337432	0.002100
3290	1.322541	0.001000	2840	1.334354	0.002000
3280	1.324357	0.001000	2830	1.335234	0.003100
3270	1.322028	0.001200	2820	1.335190	0.006400
3260	1.323991	0.001100			

Table 4. Continued.

ν, cm^{-1}	n	k	ν, cm^{-1}	n	k
2810	1.339396	0.004100	2370	1.330979	0.000700
2800	1.337529	0.001200	2360	1.330537	0.000600
2790	1.337366	0.001000	2350	1.330396	0.000800
2780	1.335327	0.001000	2340	1.330880	0.002000
2770	1.336134	0.000900	2330	1.331486	0.000600
2760	1.334545	0.000900	2320	1.331080	0.000600
2750	1.335258	0.000800	2310	1.330987	0.000600
2740	1.333921	0.001000	2300	1.330914	0.000400
2730	1.334697	0.000900	2290	1.330803	0.000400
2720	1.333588	0.001000	2280	1.330644	0.000300
2710	1.334311	0.000900	2270	1.330616	0.000400
2700	1.333231	0.000800	2260	1.330551	0.000300
2690	1.333815	0.000900	2250	1.330463	0.000200
2680	1.332838	0.000800	2240	1.330356	0.000300
2670	1.333304	0.000900	2230	1.330359	0.000200
2660	1.332617	0.001200	2220	1.330235	0.000100
2650	1.333231	0.000900	2200	1.330000	0.000100
2640	1.332452	0.001000	2180	1.329830	0.000100
2630	1.332956	0.001000	2170	1.329798	0.000100
2620	1.332354	0.000900	2160	1.329674	0.000100
2610	1.332490	0.000700	2150	1.329679	0.000100
2600	1.331714	0.001100	2140	1.329524	0.000100
2590	1.332514	0.001700	2130	1.329567	0.000100
2580	1.332311	0.001000	2120	1.329377	0.000100
2570	1.332560	0.001000	2110	1.329458	0.000100
2560	1.331978	0.000900	2100	1.329232	0.000100
2550	1.332295	0.000900	2090	1.329353	0.000100
2540	1.331815	0.000900	2080	1.329087	0.000100
2530	1.332086	0.000800	2070	1.329248	0.000100
2520	1.331639	0.000900	2060	1.328941	0.000100
2510	1.331887	0.000800	2050	1.329144	0.000100
2500	1.331498	0.000900	2040	1.328792	0.000100
2490	1.331806	0.000900	2030	1.329040	0.000100
2480	1.331501	0.000800	2020	1.328640	0.000100
2470	1.331646	0.000700	2010	1.328935	0.000100
2460	1.331269	0.000800	2000	1.328484	0.000100
2450	1.331536	0.000800	1990	1.328828	0.000100
2440	1.331210	0.000700	1980	1.328324	0.000100
2430	1.331333	0.000700	1970	1.328720	0.000100
2420	1.331058	0.000800	1960	1.328157	0.000100
2410	1.331261	0.000700	1950	1.328609	0.000100
2400	1.330954	0.000700	1940	1.327985	0.000100
2390	1.331090	0.000700	1930	1.328494	0.000100
2380	1.330817	0.000700	1920	1.327804	0.000100

Table 4. Continued.

ν, cm^{-1}	n	k	ν, cm^{-1}	n	k
1910	1.328376	0.000100	1470	1.320657	0.000100
1900	1.327615	0.000100	1460	1.313335	0.000100
1890	1.328254	0.000100	1450	1.319241	0.000100
1880	1.327417	0.000100	1440	1.310533	0.000100
1870	1.328126	0.000100	1430	1.317290	0.000100
1860	1.327207	0.000100	1420	1.306617	0.000200
1850	1.327991	0.000100	1410	1.314596	0.000500
1840	1.326985	0.000100	1400	1.301419	0.000700
1830	1.327850	0.000100	1390	1.310921	0.001000
1820	1.326748	0.000100	1380	1.293698	0.001700
1810	1.327701	0.000100	1370	1.306052	0.002600
1800	1.326496	0.000100	1360	1.281983	0.002900
1790	1.327542	0.000100	1350	1.298100	0.003800
1780	1.326225	0.000100	1340	1.258790	0.004500
1770	1.327373	0.000100	1330	1.280646	0.004300
1760	1.325933	0.000100	1320	1.176730	0.005700
1750	1.327192	0.000100	1310	1.062026	0.026800
1740	1.325617	0.000100	1300	1.337602	0.655900
1730	1.326996	0.000100	1290	1.609447	0.014300
1720	1.325273	0.000100	1280	1.488196	0.000100
1710	1.326784	0.000100	1270	1.380653	0.000100
1700	1.324898	0.000100	1260	1.405556	0.000100
1690	1.326553	0.000100	1250	1.361936	0.000100
1680	1.324486	0.000100	1240	1.380803	0.000100
1670	1.326299	0.000100	1230	1.353215	0.000100
1660	1.324030	0.000100	1220	1.368413	0.000100
1650	1.326019	0.000100	1210	1.348235	0.000100
1640	1.323522	0.000100	1200	1.361108	0.000100
1630	1.325707	0.000100	1190	1.344970	0.000100
1620	1.322953	0.000100	1180	1.356214	0.000100
1610	1.325358	0.000100	1170	1.342691	0.000100
1600	1.322311	0.000100	1160	1.352698	0.000100
1590	1.324962	0.000100	1150	1.341001	0.000100
1580	1.321578	0.000100	1140	1.350043	0.000100
1570	1.324510	0.000100	1130	1.339693	0.000100
1560	1.320735	0.000100	1120	1.347960	0.000100
1550	1.323987	0.000100	1110	1.338643	0.000100
1540	1.319751	0.000100	1100	1.346275	0.000100
1530	1.323374	0.000100	1090	1.337776	0.000100
1520	1.318590	0.000100	1080	1.344875	0.000100
1510	1.322644	0.000100	1070	1.337041	0.000100
1500	1.317195	0.000100	1060	1.343686	0.000100
1490	1.321759	0.000100	1050	1.336402	0.000100
1480	1.315485	0.000100	1040	1.342653	0.000100

Table 3. Concluded.

ν, cm^{-1}	n	k
1030	1.335832	0.000100
1020	1.341734	0.000100
1010	1.335310	0.000100
1000	1.340898	0.000100
990	1.334817	0.000100
980	1.340112	0.000100
970	1.334332	0.000100
960	1.339345	0.000100
950	1.333829	0.000100
940	1.338553	0.000100
930	1.333265	0.000100
920	1.337654	0.000100
910	1.332549	0.000100
900	1.336456	0.000100
890	1.331388	0.000100
880	1.333635	0.000100
870	1.326841	0.001800
860	1.333873	0.010500
850	1.334102	0.005600
840	1.339266	0.005900
830	1.334214	0.002400
820	1.338443	0.005200
810	1.333761	0.001900
800	1.338450	0.005200
790	1.333358	0.001300
780	1.336823	0.004600
770	1.332961	0.005000
760	1.339097	0.006000
750	1.336123	0.004900
740	1.341499	0.003700
730	1.335831	0.000600
720	1.338948	0.002400
710	1.334077	0.001700
700		0.003000

Table 5. Solid O_2 Optical Properties at 20 K

ν, cm^{-1}	n	k	ν, cm^{-1}	n	k
3700		0.000001	3260	1.264426	0.000001
3690	1.264436	0.000001	3250	1.264426	0.000001
3680	1.264435	0.000001	3240	1.264425	0.000001
3670	1.264435	0.000001	3230	1.264425	0.000001
3660	1.264435	0.000001	3220	1.264425	0.000001
3650	1.264435	0.000001	3210	1.264425	0.000001
3640	1.264435	0.000001	3200	1.264424	0.000001
3630	1.264435	0.000001	3190	1.264424	0.000001
3620	1.264434	0.000001	3180	1.264424	0.000001
3610	1.264434	0.000001	3170	1.264423	0.000001
3600	1.264434	0.000001	3160	1.264423	0.000001
3590	1.264434	0.000001	3150	1.264423	0.000001
3580	1.264434	0.000001	3140	1.264422	0.000001
3570	1.264433	0.000001	3130	1.264422	0.000001
3560	1.264433	0.000001	3120	1.264421	0.000001
3550	1.264433	0.000001	3110	1.264421	0.000001
3540	1.264433	0.000001	3100	1.264421	0.000001
3530	1.264433	0.000001	3090	1.264420	0.000001
3520	1.264432	0.000001	3080	1.264420	0.000001
3510	1.264432	0.000001	3070	1.264419	0.000001
3500	1.264432	0.000001	3060	1.264419	0.000001
3490	1.264432	0.000001	3050	1.264419	0.000001
3480	1.264432	0.000001	3040	1.264418	0.000001
3470	1.264431	0.000001	3030	1.264418	0.000001
3460	1.264431	0.000001	3020	1.264417	0.000001
3450	1.264431	0.000001	3010	1.264417	0.000001
3440	1.264431	0.000001	3000	1.264416	0.000001
3430	1.264431	0.000001	2990	1.264416	0.000001
3420	1.264430	0.000001	2980	1.264415	0.000001
3410	1.264430	0.000001	2970	1.264415	0.000001
3400	1.264430	0.000001	2960	1.264414	0.000001
3390	1.264430	0.000001	2950	1.264414	0.000001
3380	1.264429	0.000001	2940	1.264413	0.000001
3370	1.264429	0.000001	2930	1.264413	0.000001
3360	1.264429	0.000001	2920	1.264412	0.000001
3350	1.264429	0.000001	2910	1.264412	0.000001
3340	1.264428	0.000001	2900	1.264411	0.000001
3330	1.264428	0.000001	2890	1.264410	0.000001
3320	1.264428	0.000001	2880	1.264410	0.000001
3310	1.264428	0.000001	2870	1.264409	0.000001
3300	1.264427	0.000001	2860	1.264409	0.000001
3290	1.264427	0.000001	2850	1.264408	0.000001
3280	1.264427	0.000001	2840	1.264407	0.000001
3270	1.264426	0.000001	2830	1.264407	0.000001

Table 5. Continued.

ν, cm^{-1}	n	k	ν, cm^{-1}	n	k
2820	1.264406	0.000001	2380	1.264318	0.000001
2810	1.264405	0.000001	2370	1.264318	0.000001
2800	1.264404	0.000001	2360	1.264296	0.000001
2790	1.264404	0.000001	2350	1.264273	0.000001
2780	1.264403	0.000001	2340	1.264305	0.000100
2770	1.264402	0.000001	2330	1.264341	0.000001
2760	1.264401	0.000001	2320	1.264313	0.000001
2750	1.264400	0.000001	2310	1.264290	0.000001
2740	1.264399	0.000001	2300	1.264283	0.000001
2730	1.264398	0.000001	2290	1.264267	0.000001
2720	1.264398	0.000001	2280	1.264255	0.000001
2710	1.264397	0.000001	2270	1.264238	0.000001
2700	1.264396	0.000001	2260	1.264222	0.000001
2690	1.264395	0.000001	2250	1.264201	0.000001
2680	1.264393	0.000001	2240	1.264177	0.000001
2670	1.264392	0.000001	2230	1.264147	0.000001
2660	1.264391	0.000001	2220	1.264110	0.000001
2650	1.264390	0.000001	2200	1.264000	0.000001
2640	1.264389	0.000001	2180	1.263777	0.000001
2630	1.264387	0.000001	2170	1.263810	0.000001
2620	1.264386	0.000001	2160	1.263065	0.000001
2610	1.264385	0.000001	2150	1.261701	0.000001
2600	1.264383	0.000001	2140	1.264419	0.006100
2590	1.264382	0.000001	2130	1.266731	0.000001
2580	1.264380	0.000001	2120	1.265797	0.000001
2570	1.264379	0.000001	2110	1.264610	0.000001
2560	1.264377	0.000001	2100	1.265084	0.000001
2550	1.264375	0.000001	2090	1.264583	0.000001
2540	1.264373	0.000001	2080	1.264862	0.000001
2530	1.264371	0.000001	2070	1.264697	0.000001
2520	1.264369	0.000001	2060	1.264751	0.000001
2510	1.264367	0.000001	2050	1.264715	0.000001
2500	1.264365	0.000001	2040	1.264685	0.000001
2490	1.264363	0.000001	2030	1.264661	0.000001
2480	1.264360	0.000001	2020	1.264641	0.000001
2470	1.264359	0.000001	2010	1.264624	0.000001
2460	1.264354	0.000001	2000	1.264609	0.000001
2450	1.264354	0.000001	1990	1.264596	0.000001
2440	1.264347	0.000001	1980	1.264584	0.000001
2430	1.264347	0.000001	1970	1.264575	0.000001
2420	1.264340	0.000001	1960	1.264565	0.000001
2410	1.264340	0.000001	1950	1.264558	0.000001
2400	1.264330	0.000001	1940	1.264550	0.000001
2390	1.264330	0.000001	1930	1.264543	0.000001

Table 5. Continued.

ν, cm^{-1}	n	k	ν, cm^{-1}	n	k
1920	1.264537	0.000001	1480	1.264412	0.000001
1910	1.264531	0.000001	1470	1.264412	0.000001
1900	1.264526	0.000001	1460	1.264407	0.000001
1890	1.264521	0.000001	1450	1.264407	0.000001
1880	1.264516	0.000001	1440	1.264402	0.000001
1870	1.264512	0.000001	1430	1.264402	0.000001
1860	1.264508	0.000001	1420	1.264396	0.000001
1850	1.264504	0.000001	1410	1.264397	0.000001
1840	1.264500	0.000001	1400	1.264391	0.000001
1830	1.264497	0.000001	1390	1.264391	0.000001
1820	1.264493	0.000001	1380	1.264385	0.000001
1810	1.264491	0.000001	1370	1.264385	0.000001
1800	1.264487	0.000001	1360	1.264379	0.000001
1790	1.264485	0.000001	1350	1.264379	0.000001
1780	1.264481	0.000001	1340	1.264372	0.000001
1770	1.264479	0.000001	1330	1.264373	0.000001
1760	1.264475	0.000001	1320	1.264365	0.000001
1750	1.264474	0.000001	1310	1.264366	0.000001
1740	1.264470	0.000001	1300	1.264358	0.000001
1730	1.264469	0.000001	1290	1.264358	0.000001
1720	1.264465	0.000001	1280	1.264350	0.000001
1710	1.264464	0.000001	1270	1.264350	0.000001
1700	1.264461	0.000001	1260	1.264341	0.000001
1690	1.264460	0.000001	1250	1.264341	0.000001
1680	1.264456	0.000001	1240	1.264331	0.000001
1670	1.264455	0.000001	1230	1.264332	0.000001
1660	1.264452	0.000001	1220	1.264321	0.000001
1650	1.264451	0.000001	1210	1.264321	0.000001
1640	1.264447	0.000001	1200	1.264310	0.000001
1630	1.264447	0.000001	1190	1.264310	0.000001
1620	1.264443	0.000001	1180	1.264297	0.000001
1610	1.264442	0.000001	1170	1.264297	0.000001
1600	1.264439	0.000001	1160	1.264283	0.000001
1590	1.264438	0.000001	1150	1.264283	0.000001
1580	1.264434	0.000001	1140	1.264267	0.000001
1570	1.264434	0.000001	1130	1.264267	0.000001
1560	1.264430	0.000001	1120	1.264250	0.000001
1550	1.264430	0.000001	1110	1.264249	0.000001
1540	1.264425	0.000001	1100	1.264229	0.000001
1530	1.264425	0.000001	1090	1.264228	0.000001
1520	1.264421	0.000001	1080	1.264206	0.000001
1510	1.264421	0.000001	1070	1.264204	0.000001
1500	1.264416	0.000001	1060	1.264179	0.000001
1490	1.264416	0.000001	1050	1.264176	0.000001

Table 5. Concluded.

ν, cm^{-1}	n	k
1040	1.264147	0.000001
1030	1.264142	0.000001
1020	1.264108	0.000001
1010	1.264102	0.000001
1000	1.264060	0.000001
990	1.264051	0.000001
980	1.264000	0.000001
970	1.263965	0.000001
960	1.263921	0.000001
950	1.263898	0.000001
940	1.263812	0.000001
930	1.263774	0.000001
920	1.263650	0.000001
910	1.263580	0.000001
900	1.263374	0.000001
890	1.263226	0.000001
880	1.262733	0.000001
870	1.261535	0.000001
860	1.261124	0.002700
850	1.263579	0.004900
840	1.265960	0.003000
830	1.265508	0.000400
820	1.264604	0.001500
810	1.264782	0.001100
800	1.264771	0.000900
790	1.264091	0.000500
780	1.263234	0.001100
770	1.263398	0.003000
760	1.265247	0.004000
750	1.266967	0.002800
740	1.267394	0.001200
730	1.266696	0.000001
720	1.265994	0.000001
710	1.265601	0.000001
700		0.000100

Table 6. Solid N_2 Optical Properties at 20 K

ν, cm^{-1}	n	k	ν, cm^{-1}	n	k
3700		0.000800	3260	1.228483	0.000700
3690	1.228940	0.000300	3250	1.228532	0.000700
3680	1.228952	0.000300	3240	1.228317	0.000800
3670	1.228521	0.001000	3230	1.228464	0.000700
3660	1.228853	0.000800	3220	1.227950	0.000700
3650	1.228566	0.000300	3210	1.228223	0.001000
3640	1.228610	0.001200	3200	1.227405	0.000900
3630	1.228937	0.000800	3190	1.226301	0.000900
3620	1.228872	0.000400	3180	1.228775	0.000900
3610	1.228648	0.000800	3170	1.231316	0.000900
3600	1.228623	0.000400	3160	1.230141	0.000800
3590	1.228630	0.001100	3150	1.229190	0.000900
3580	1.228754	0.000500	3140	1.229489	0.000900
3570	1.228775	0.001000	3130	1.229125	0.000800
3560	1.228679	0.000400	3120	1.229233	0.000800
3550	1.228792	0.001100	3110	1.228955	0.000800
3540	1.228731	0.000400	3100	1.229082	0.000900
3530	1.228746	0.000900	3090	1.228981	0.000900
3520	1.228775	0.000700	3080	1.229170	0.000900
3510	1.228849	0.000600	3070	1.229014	0.000700
3500	1.228485	0.000500	3060	1.228957	0.000700
3490	1.228741	0.001100	3050	1.228741	0.000800
3480	1.228908	0.000700	3040	1.228899	0.001000
3470	1.228951	0.000500	3030	1.228881	0.000900
3460	1.228558	0.000400	3020	1.228962	0.000900
3450	1.228598	0.000700	3010	1.228844	0.000900
3440	1.228530	0.000700	3000	1.228898	0.000900
3430	1.228786	0.000800	2990	1.228812	0.001000
3420	1.228543	0.000500	2980	1.228946	0.001000
3410	1.228644	0.000800	2970	1.228900	0.001000
3400	1.228570	0.000800	2960	1.228904	0.000900
3390	1.228708	0.000600	2950	1.228807	0.001100
3380	1.228643	0.001000	2940	1.228919	0.001100
3370	1.228789	0.000400	2930	1.228939	0.001200
3360	1.228550	0.000800	2920	1.229115	0.001200
3350	1.228625	0.000500	2910	1.229126	0.001100
3340	1.228378	0.000700	2900	1.229238	0.001100
3330	1.228471	0.000800	2890	1.229234	0.001000
3320	1.228559	0.001000	2880	1.229217	0.000800
3310	1.228648	0.000600	2870	1.229005	0.000900
3300	1.228355	0.000800	2860	1.229057	0.001000
3290	1.228534	0.001000	2850	1.229203	0.001200
3280	1.228633	0.001000	2840	1.229322	0.000800
3270	1.228774	0.000700	2830	1.229191	0.000900

Table 6. Continued.

ν, cm^{-1}	n	k	ν, cm^{-1}	n	k
2820	1.229181	0.000800	2380	1.229162	0.000500
2810	1.229150	0.000900	2370	1.229061	0.000400
2800	1.229160	0.000800	2360	1.229016	0.000600
2790	1.229145	0.000900	2350	1.229187	0.000800
2780	1.229183	0.000800	2340	1.229309	0.000500
2770	1.229109	0.000800	2330	1.229220	0.000500
2760	1.229056	0.000800	2320	1.229179	0.000500
2750	1.229141	0.001000	2310	1.229151	0.000500
2740	1.229140	0.000700	2300	1.229230	0.000600
2730	1.229059	0.000900	2290	1.229217	0.000400
2720	1.229083	0.000900	2280	1.229113	0.000400
2710	1.229106	0.000900	2270	1.229125	0.000600
2700	1.229152	0.001000	2260	1.229168	0.000400
2690	1.229220	0.000900	2250	1.229103	0.000500
2680	1.229238	0.000900	2240	1.229128	0.000500
2670	1.229176	0.000800	2230	1.229168	0.000500
2660	1.229141	0.000900	2220	1.229155	0.000400
2650	1.229200	0.001000	2200	1.229000	0.000400
2640	1.229299	0.000900	2180	1.229078	0.000400
2630	1.229292	0.000900	2170	1.229029	0.000500
2620	1.229262	0.000800	2160	1.229035	0.000500
2610	1.229305	0.001000	2150	1.229050	0.000500
2600	1.229368	0.000800	2140	1.229055	0.000500
2590	1.229419	0.000900	2130	1.229092	0.000500
2580	1.229419	0.000700	2120	1.229064	0.000400
2570	1.229373	0.000700	2110	1.228953	0.000400
2560	1.229293	0.000700	2100	1.228951	0.000500
2550	1.229405	0.000800	2090	1.228990	0.000500
2540	1.229375	0.000600	2080	1.228982	0.000500
2530	1.229300	0.000600	2070	1.228973	0.000500
2520	1.229309	0.000800	2060	1.229038	0.000600
2510	1.229418	0.000600	2050	1.229027	0.000400
2500	1.229331	0.000600	2040	1.228981	0.000500
2490	1.229338	0.000600	2030	1.228984	0.000500
2480	1.229329	0.000600	2020	1.228939	0.000400
2470	1.229312	0.000500	2010	1.228926	0.000600
2460	1.229262	0.000600	2000	1.228987	0.000500
2450	1.229246	0.000500	1990	1.228976	0.000500
2440	1.229284	0.000700	1980	1.228950	0.000500
2430	1.229356	0.000500	1970	1.228956	0.000500
2420	1.229323	0.000500	1960	1.228936	0.000500
2410	1.229248	0.000400	1950	1.228940	0.000500
2400	1.229221	0.000500	1940	1.228917	0.000500
2390	1.229179	0.000400	1930	1.228921	0.000500

Table 6. Continued.

ν, cm^{-1}	n	k	ν, cm^{-1}	n	k
1920	1.228880	0.000500	1480	1.228928	0.001000
1910	1.228838	0.000500	1470	1.228999	0.001100
1900	1.228911	0.000700	1460	1.229140	0.001100
1890	1.228987	0.000500	1450	1.229190	0.000900
1880	1.228952	0.000500	1440	1.229144	0.000900
1870	1.228950	0.000500	1430	1.229082	0.000800
1860	1.228812	0.000300	1420	1.229056	0.000900
1850	1.228738	0.000600	1410	1.228969	0.000800
1840	1.228828	0.000600	1400	1.228936	0.001000
1830	1.228864	0.000500	1390	1.229156	0.001200
1820	1.228750	0.000500	1380	1.229255	0.000800
1810	1.228764	0.000600	1370	1.229106	0.000800
1800	1.228783	0.000600	1360	1.229039	0.000900
1790	1.228764	0.000500	1350	1.229101	0.000900
1780	1.228670	0.000600	1340	1.229110	0.000900
1770	1.228657	0.000600	1330	1.229085	0.000800
1760	1.228594	0.000700	1320	1.229017	0.000900
1750	1.228640	0.000800	1310	1.228998	0.000900
1740	1.228722	0.000900	1300	1.229101	0.001100
1730	1.228828	0.000800	1290	1.229318	0.001000
1720	1.228815	0.000800	1280	1.229201	0.000600
1710	1.228798	0.000700	1270	1.229008	0.000800
1700	1.228718	0.000800	1260	1.228964	0.000900
1690	1.228754	0.000800	1250	1.229131	0.001000
1680	1.228777	0.000900	1240	1.229173	0.000900
1670	1.228746	0.000700	1230	1.229117	0.000700
1660	1.228719	0.001000	1220	1.229051	0.001000
1650	1.228749	0.000800	1210	1.229165	0.000800
1640	1.228699	0.001000	1200	1.229150	0.000900
1630	1.228725	0.001000	1190	1.229127	0.000700
1620	1.228845	0.001200	1180	1.229130	0.000900
1610	1.228884	0.001000	1170	1.229214	0.000700
1600	1.229067	0.001300	1160	1.228981	0.000500
1590	1.229168	0.000900	1150	1.228851	0.000800
1580	1.229042	0.000800	1140	1.228998	0.001000
1570	1.228959	0.001000	1130	1.229120	0.000700
1560	1.229024	0.000900	1120	1.229032	0.000800
1550	1.229053	0.001000	1110	1.229110	0.000700
1540	1.229119	0.000900	1100	1.229036	0.000600
1530	1.229097	0.000800	1090	1.228822	0.000400
1520	1.229038	0.000800	1080	1.228642	0.000800
1510	1.228916	0.000700	1070	1.228875	0.000900
1500	1.228828	0.000900	1060	1.228867	0.000700
1490	1.228880	0.001000	1050	1.228833	0.000700

Table 6. Concluded.

ν, cm^{-1}	n	k
1040	1.228979	0.001000
1030	1.229109	0.000300
1020	1.228670	0.000300
1010	1.228400	0.000300
1000	1.228607	0.001000
990	1.228666	0.000001
980	1.228286	0.000300
970	1.227948	0.000100
960	1.227687	0.000400
950	1.227667	0.000700
940	1.227615	0.000500
930	1.227381	0.000400
920	1.227007	0.000500
910	1.226795	0.000600
900	1.226080	0.000300
890	1.224965	0.000600
880	1.223589	0.001900
870	1.222762	0.003800
860	1.224218	0.008000
850	1.227429	0.008200
840	1.229531	0.007100
830	1.230359	0.005800
820	1.230077	0.004400
810	1.229189	0.004300
800	1.229259	0.005600
790	1.230390	0.005600
780	1.229455	0.004000
770	1.229318	0.006800
760	1.232634	0.009300
750	1.234729	0.003800
740	1.233305	0.003700
730	1.232322	0.003000
720	1.233573	0.005300
710	1.234532	0.002300
700		0.001300

Table 7. Solid Argon Optical Properties at 20 K

ν, cm^{-1}	n	k	ν, cm^{-1}	n	k
3700		0.000001	3260	1.225012	0.000001
3690	1.225014	0.000001	3250	1.225012	0.000001
3680	1.225014	0.000001	3240	1.225012	0.000001
3670	1.225014	0.000001	3230	1.225012	0.000001
3660	1.225014	0.000001	3220	1.225012	0.000001
3650	1.225014	0.000001	3210	1.225012	0.000001
3640	1.225014	0.000001	3200	1.225012	0.000001
3630	1.225014	0.000001	3190	1.225012	0.000001
3620	1.225014	0.000001	3180	1.225012	0.000001
3610	1.225014	0.000001	3170	1.225012	0.000001
3600	1.225014	0.000001	3160	1.225012	0.000001
3590	1.225014	0.000001	3150	1.225012	0.000001
3580	1.225014	0.000001	3140	1.225012	0.000001
3570	1.225014	0.000001	3130	1.225012	0.000001
3560	1.225014	0.000001	3120	1.225011	0.000001
3550	1.225014	0.000001	3110	1.225011	0.000001
3540	1.225014	0.000001	3100	1.225011	0.000001
3530	1.225014	0.000001	3090	1.225011	0.000001
3520	1.225014	0.000001	3080	1.225011	0.000001
3510	1.225014	0.000001	3070	1.225011	0.000001
3500	1.225014	0.000001	3060	1.225011	0.000001
3490	1.225014	0.000001	3050	1.225011	0.000001
3480	1.225013	0.000001	3040	1.225011	0.000001
3470	1.225013	0.000001	3030	1.225011	0.000001
3460	1.225013	0.000001	3020	1.225011	0.000001
3450	1.225013	0.000001	3010	1.225011	0.000001
3440	1.225013	0.000001	3000	1.225011	0.000001
3430	1.225013	0.000001	2990	1.225011	0.000001
3420	1.225013	0.000001	2980	1.225010	0.000001
3410	1.225013	0.000001	2970	1.225010	0.000001
3400	1.225013	0.000001	2960	1.225010	0.000001
3390	1.225013	0.000001	2950	1.225010	0.000001
3380	1.225013	0.000001	2940	1.225010	0.000001
3370	1.225013	0.000001	2930	1.225010	0.000001
3360	1.225013	0.000001	2920	1.225010	0.000001
3350	1.225013	0.000001	2910	1.225010	0.000001
3340	1.225013	0.000001	2900	1.225010	0.000001
3330	1.225013	0.000001	2890	1.225010	0.000001
3320	1.225013	0.000001	2880	1.225010	0.000001
3310	1.225013	0.000001	2870	1.225010	0.000001
3300	1.225013	0.000001	2860	1.225009	0.000001
3290	1.225013	0.000001	2850	1.225009	0.000001
3280	1.225012	0.000001	2840	1.225009	0.000001
3270	1.225012	0.000001	2830	1.225009	0.000001

Table 7. Continued.

ν, cm^{-1}	n	k	ν, cm^{-1}	n	k
2820	1.225009	0.000001	2380	1.225004	0.000001
2810	1.225009	0.000001	2370	1.225003	0.000001
2800	1.225009	0.000001	2360	1.225001	0.000001
2790	1.225009	0.000001	2350	1.225003	0.000001
2780	1.225009	0.000001	2340	1.225003	0.000001
2770	1.225009	0.000001	2330	1.225003	0.000001
2760	1.225009	0.000001	2320	1.225002	0.000001
2750	1.225008	0.000001	2310	1.225002	0.000001
2740	1.225008	0.000001	2300	1.225002	0.000001
2730	1.225008	0.000001	2290	1.225002	0.000001
2720	1.225008	0.000001	2280	1.225002	0.000001
2710	1.225008	0.000001	2270	1.225001	0.000001
2700	1.225008	0.000001	2260	1.225001	0.000001
2690	1.225008	0.000001	2250	1.225001	0.000001
2680	1.225008	0.000001	2240	1.225001	0.000001
2670	1.225008	0.000001	2230	1.225001	0.000001
2660	1.225007	0.000001	2220	1.225000	0.000001
2650	1.225007	0.000001	2200	1.225000	0.000001
2640	1.225007	0.000001	2180	1.225000	0.000001
2630	1.225007	0.000001	2170	1.224999	0.000001
2620	1.225007	0.000001	2160	1.224999	0.000001
2610	1.225007	0.000001	2150	1.224999	0.000001
2600	1.225007	0.000001	2140	1.224999	0.000001
2590	1.225007	0.000001	2130	1.224998	0.000001
2580	1.225006	0.000001	2120	1.224998	0.000001
2570	1.225006	0.000001	2110	1.224998	0.000001
2560	1.225006	0.000001	2100	1.224998	0.000001
2550	1.225006	0.000001	2090	1.224997	0.000001
2540	1.225006	0.000001	2080	1.224997	0.000001
2530	1.225006	0.000001	2070	1.224997	0.000001
2520	1.225006	0.000001	2060	1.224996	0.000001
2510	1.225006	0.000001	2050	1.224996	0.000001
2500	1.225005	0.000001	2040	1.224996	0.000001
2490	1.225005	0.000001	2030	1.224995	0.000001
2480	1.225005	0.000001	2020	1.224995	0.000001
2470	1.225005	0.000001	2010	1.224995	0.000001
2460	1.225005	0.000001	2000	1.224995	0.000001
2450	1.225005	0.000001	1990	1.224994	0.000001
2440	1.225005	0.000001	1980	1.224994	0.000001
2430	1.225004	0.000001	1970	1.224993	0.000001
2420	1.225004	0.000001	1960	1.224993	0.000001
2410	1.225004	0.000001	1950	1.224993	0.000001
2400	1.225004	0.000001	1940	1.224993	0.000001
2390	1.225004	0.000001	1930	1.224992	0.000001

Table 7. Continued.

ν, cm^{-1}	n	k	ν, cm^{-1}	n	k
1920	1.224992	0.000001	1480	1.224963	0.000001
1910	1.224991	0.000001	1470	1.224960	0.000001
1900	1.224991	0.000001	1460	1.224960	0.000001
1890	1.224990	0.000001	1450	1.224958	0.000001
1880	1.224990	0.000001	1440	1.224958	0.000001
1870	1.224989	0.000001	1430	1.224955	0.000001
1860	1.224989	0.000001	1420	1.224955	0.000001
1850	1.224989	0.000001	1410	1.224952	0.000001
1840	1.224988	0.000001	1400	1.224952	0.000001
1830	1.224988	0.000001	1390	1.224949	0.000001
1820	1.224988	0.000001	1380	1.224949	0.000001
1810	1.224987	0.000001	1370	1.224946	0.000001
1800	1.224987	0.000001	1360	1.224946	0.000001
1790	1.224986	0.000001	1350	1.224942	0.000001
1780	1.224986	0.000001	1340	1.224942	0.000001
1770	1.224985	0.000001	1330	1.224938	0.000001
1760	1.224985	0.000001	1320	1.224938	0.000001
1750	1.224984	0.000001	1310	1.224934	0.000001
1740	1.224983	0.000001	1300	1.224934	0.000001
1730	1.224982	0.000001	1290	1.224929	0.000001
1720	1.224982	0.000001	1280	1.224929	0.000001
1710	1.224981	0.000001	1270	1.224924	0.000001
1700	1.224981	0.000001	1260	1.224924	0.000001
1690	1.224980	0.000001	1250	1.224919	0.000001
1680	1.225008	0.000001	1240	1.224918	0.000001
1670	1.224979	0.000001	1230	1.224912	0.000001
1660	1.224979	0.000001	1220	1.224912	0.000001
1650	1.224977	0.000001	1210	1.224906	0.000001
1640	1.224977	0.000001	1200	1.224905	0.000001
1630	1.224976	0.000001	1190	1.224898	0.000001
1620	1.224976	0.000001	1180	1.224898	0.000001
1610	1.224974	0.000001	1170	1.224890	0.000001
1600	1.224974	0.000001	1160	1.224889	0.000001
1590	1.224972	0.000001	1150	1.224880	0.000001
1580	1.224972	0.000001	1140	1.224879	0.000001
1570	1.224971	0.000001	1130	1.224870	0.000001
1560	1.224971	0.000001	1120	1.224868	0.000001
1550	1.224969	0.000001	1110	1.224858	0.000001
1540	1.224969	0.000001	1100	1.224856	0.000001
1530	1.224967	0.000001	1090	1.224844	0.000001
1520	1.224967	0.000001	1080	1.224841	0.000001
1510	1.224965	0.000001	1070	1.224827	0.000001
1500	1.224965	0.000001	1060	1.224824	0.000001
1490	1.224962	0.000001	1050	1.224808	0.000001

Table 7. Concluded.

ν, cm^{-1}	n	k
1040	1.224803	0.000001
1030	1.224785	0.000001
1020	1.224779	0.000001
1010	1.224756	0.000001
1000	1.224748	0.000001
990	1.224720	0.000001
980	1.224709	0.000001
970	1.224674	0.000001
960	1.224657	0.000001
950	1.224611	0.000001
940	1.224584	0.000001
930	1.224521	0.000001
920	1.224473	0.000001
910	1.224376	0.000001
900	1.224280	0.000001
890	1.224103	0.000001
880	1.223805	0.000001
870	1.222706	0.000001
860	1.222485	0.002263
850	1.224870	0.004519
840	1.226980	0.001766
830	1.226511	0.000179
820	1.225560	0.000001
810	1.225163	0.000001
800	1.224819	0.000001
790	1.224263	0.000001
780	1.223414	0.000509
770	1.223752	0.002606
760	1.225417	0.003187
750	1.226875	0.002205
740	1.227158	0.000981
730	1.226712	0.000001
720	1.226120	0.000001
710	1.225901	0.000001
700		0.000001